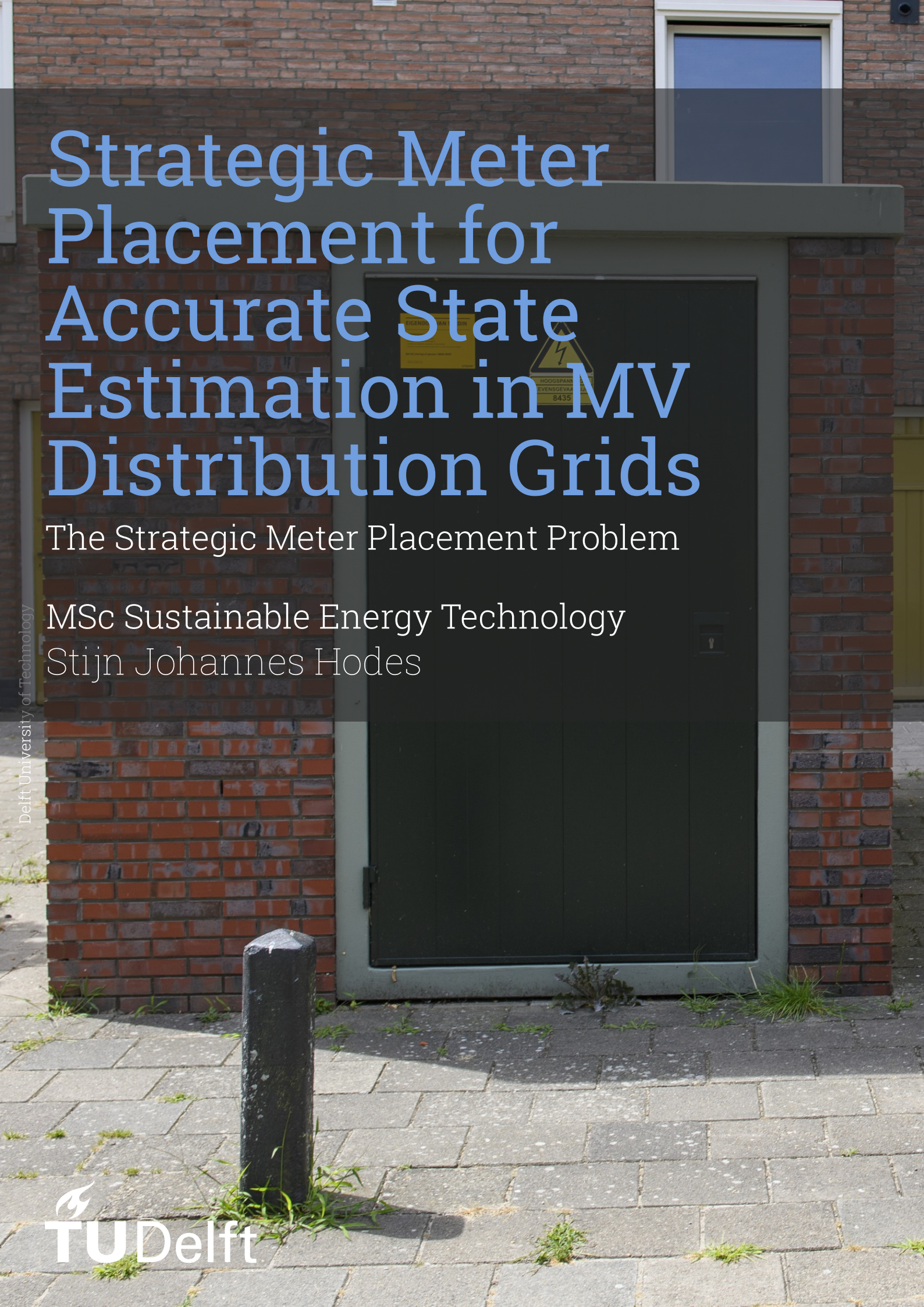

Strategic Meter Placement for Accurate State Estimation in MV Distribution Grids

The Strategic Meter Placement Problem

MSc Sustainable Energy Technology

Stijn Johannes Hodes

Delft University of Technology

TU Delft

Strategic Meter Placement for Accurate State Estimation in MV Distribution Grids

The Strategic Meter Placement Problem

by

Stijn Johannes Hodes

to obtain the degree of Master of Science
at the Delft University of Technology,
to be defended publicly on 28 May, 2025

Student number:	4960750
Project duration:	September, 2024 – May, 2025
Faculty:	Faculty of Electrical Engineering, Mathematics & Computer Science
Thesis committee:	Dr. P.P. Vergara Barrios, TU Delft, Supervisor, IEPG
	Dr. M. Cvetkovic, TU Delft, Committee Chair, IEPG
	Dr. J. Dong, TU Delft, External Member, DCE&S
	Dr. N. Cihangir Martin, Stedin Group, Supervisor

Cover: Stedin (Modified)

An electronic version of this thesis is available at `http://repository.tudelft.nl/`.

TU Delft

STEDIN.NET

Preface

This thesis rounds up my MSc programme in Sustainable Energy Technology. It was an exciting programme after my BSc in Mechanical Engineering, where I could delve into multiple new subjects and technologies. This has expanded my interest and motivated me to advance in the energy industry. I hope that I will be able to contribute more to this world regarding the energy transition in the future.

I want to extend my sincere gratitude to both my supervisors, Dr. Pedro P. Vergara and Dr. Nuran Cihangir Martin, for their unwavering support and guidance throughout this research project. Their academic expertise has been instrumental to my understanding and the project's progression. Company insights from Stedin have also contributed to defining the problem. I am grateful for all the company experts who took the time to talk to me and explain their point of view on the relevant subjects.

I also want to thank my parents for their love and support throughout my studies. It has not always been smooth sailing, and their support, sometimes with harsh words of motivation, has ensured that we will all be able to reflect on this with satisfaction.

The subject of this thesis was entirely new to me, which made it quite challenging at times. However, each moment of understanding brought a sense of joy that motivated me. Working on this thesis has significantly enhanced my analytical skills, and I am satisfied with the results obtained.

I look forward to the next steps in my professional career and hope to continue to surprise and challenge myself.

Stijn Johannes Hodes
Delft, May 2025

Abstract

This thesis explores how accurate state estimation can support Distribution System Operators (DSO) in managing MV grids. As the energy transition drives increasing complexity in electricity networks, more precise and reliable data is necessary for planning and operational decisions. Although state estimation offers a way to enhance data, DSOs struggle to implement it. The main objective of this thesis is to develop a general strategy for placing measurements to achieve accurate state estimation using as few measurements as possible.

Multiple cases were designed to assess the impact of specific measurement placement. A reference "perfect case" network load scenario was created, and the values were corrupted using normally distributed noise, with standard deviations reflecting the expected accuracy of each measurement type. These noisy measurements were fed into the PandaPower Weighted Least Squares (WLS) state estimation algorithm, implemented in Python. The resulting state estimates were compared to the perfect case values to evaluate the state estimator's accuracy and the placement strategy's effect.

The results show that Power Injection Measurements (PIMs) primarily improve accuracy at the node where they are placed. In contrast, Medium Voltage Measurement Units (MVMUs) offer broader improvements across the entire feeder where they are installed. One strategic measurement location was identified based on financial grounds. Results also indicate that improving the accuracy of an inaccurate node is possible without improving its measurement, but requires widespread deployment elsewhere, which is rarely justifiable economically. Retrofitting stations solely for measurement purposes is generally not considered worthwhile.

The main focus should be on identifying the substations with the poorest measurement accuracy, typically pseudo-measurements. As a consequence, overall pseudo-measurement accuracy will also improve. This makes it more likely that the state estimates will fall within predetermined limits. The number of measurements that need to be placed depends on this predetermined limit.

Contents

Nomenclature

Abbreviations

Abbreviation	Definition
AC	Alternating Current
DC	Direct Current
DER	Distributed Energy Resources
DG	Distributed Generation
DSO	Distribution System Operator
HV	High Voltage
HRMP	Heuristic for Remote Terminal Unit and Measurement Planning
LV	Low Voltage
MCS	Monte Carlo Simulation
MILP	Mixed-Integer Linear Programming
MV	Medium Voltage
MVMU	Medium Voltage Measurement Unit
PMU	Phasor Measurement Unit
PIM	Power Injection Measurement
RES	Renewable Energy Sources
RTU	Remote Terminal Unit
SCADA	Supervisory Control and Data Acquisition
SM	Smart Meter
TNF	Technically Not Feasible
TSO	Transmission System Operator
WLS	Weighted Least Squares

Symbols

Symbol	Definition	Unit
P	Active Power	[MW]
Q	Reactive Power	[MVar]
V	Voltage	[V]
ϵ	Error	[%]
θ	Voltage Phase	[Degrees]

1 Introduction

The first chapter contains the motivation and background behind the research, a brief historical introduction to state estimation and the objective and research questions. It ends with a rough outline of the thesis.

1.1. Motivation

The Netherlands is undergoing an electrical energy revolution. Renewable energy solutions like wind and solar replace traditional power plants like coal to reduce emissions [1]. This significant development is expected to strengthen over the coming years due to the ambitious climate goals set by the Netherlands [2] and, in a broader sense, the European Union [3]. However, these advancements will have implications for the electricity networks.

In the past, systems were designed and operated assuming they were passive. This has shifted with integrating distributed energy resources such as solar panels and electric cars, which exhibit volatile and irregular behaviour [4], [5]. Factors such as sizing and location are beyond the control of all Distribution System Operators (DSO), as individuals can independently decide to install solar panels on their roofs and connect them to the grid, creating implications that all DSOs must address. This uncontrolled integration can result in decreased voltage stability, increased harmonics and reverse power flow, possibly damaging the network's equipment and growing losses in the system [6], [7]. The problems that generally characterise distributed generation are stability and power quality [8].

In addition to these developments, there is an increasing demand for electricity as many processes in daily life and industrial operations are gradually being electrified [9]. The dynamic profile of the emerging Renewable Energy Sources (RES) and the rising electricity demand can increase pressure on the electricity grid.

As the pressure on the electricity system increases, it becomes crucial for distribution operators to gather comprehensive data about their grids [10]. This data can inform critical decisions, such as disconnecting RES or implementing load curtailment and, in the worst case, load shedding during periods of congestion in specific areas. Additionally, it can provide insights into whether maintenance is needed sooner, particularly in the case of persistent overloads.

This data also enables effective congestion mapping and facilitates timely planning for network expansion. Since installing measuring equipment at every station to gather data incurs significant costs, this is generally avoided until the economics can be justified. State estimation calculates all states in the network without requiring direct measurements at all points. Under states fall parameters such as power, voltage, current and voltage phase. Real-world data is utilised to determine the missing states through a state estimation algorithm while considering the accuracy of the measurement data. A system is considered observable if sufficient measurements are available to perform state estimation effectively. This approach bridges the gap between the theoretical framework, where systems are assumed to function flawlessly and the real-world scenario, where data is often imperfect or incomplete. It also filters the

raw data before being used in potential use cases like control and protection. This is done by detecting corrupted data in the measurement sets.

1.2. State Estimation

State estimation for power systems originated in the late 1960s. This development was driven by the rise of digital computers and advancements in state estimation within the aerospace field, particularly for military purposes. Fred C. Schweppe is widely regarded as the founder of state estimation for power systems. In addition to his scientific contributions [11],[12],[13], he also collaborated with American Electric Power, an American electric utility company, on the first successful real-time power system state estimator.

Currently, state estimation is widely used by Transmission System Operators (TSOs) to calculate the real-time status of the power grid. Due to the high demand for redundancy, the transmission system is well-measured (observable), enabling state estimation. DSOs, however, do not have this luxury. Historically, there was no need for a well-measured distribution system, as the system was more straightforward with one-directional flow and less strain, making it easier to predict. Hence, the distribution networks mostly have little to no real-time measurement capability. As a result, the system tends to be unobservable, making state estimation impossible.

1.3. Objective and Research Questions

This research aims to develop a workflow for analysing existing medium-voltage (MV) networks operated by DSOs to acquire observability. The process will then identify strategic locations within the network where measurement equipment can be placed, prioritising placements from the most to the least strategic, building the network to achieve a certain accuracy. The main objective focuses on the fundamental requirements for achieving basic observability and accurate state estimation. It is formulated as follows: *What is the minimum of actual measurements required to achieve observability and adequate state estimation?* Answering this question should provide a clear understanding of how DSOs can achieve network observability by implementing minimum measurements in their networks while keeping technical and practical perspectives in mind. This thesis could serve as a guide for DSOs during the design phase of their measurement equipment deployment.

Different aspects should be taken into account to reach a well-considered conclusion. One key aspect is evaluating how the placement of additional measurements affects the accuracy of state estimation and whether associated costs would be justified. Since these measurements can be carried out using different devices, such as Remote Terminal Units (RTU) or Phase Measurement Units (PMU), it becomes essential to evaluate whether investing in specific devices yields better results. This includes determining whether power flow direction is a vital piece of information for DSOs in some regions of the network. Another aspect to explore is strategic locations for placing measurement equipment in the networks. As the research is conducted in collaboration with Stedin, it will mainly focus on Stedin's specific priorities regarding measurement placement. At the same time, the findings will be generalised to address the needs of other DSOs, ensuring the broader applicability of the results. This translates into the following research questions.

Research Question 1: *What are the minimum conditions to create an observable network?*

At first, the basic conditions for an observable network must be defined without looking at certain difficulties that may complicate the situation, such as existing equipment or Technically Not Feasible (TNF) substations due to complications like physical characteristics of the substation or deployed location. The minimum number of measurements and their placement will be discussed in this question.

Research Question 2: *What is the effect of placing more than the minimum amount of measurements?*

If the minimum amount of measurements is placed, a company could choose to place more measurements, but it would have to be worth it. So, it is interesting to see what effect additional measurements have on accuracy and if their location is important to the accuracy of the system's state.

Research Question 3: *Is the type of measurement taken of great importance to the accuracy of the system's state?*

Different types of measurement equipment are available on the market at different prices. For example, simple measurements give just P and Q and their direction (negative or positive). More sophisticated measurements may also provide the voltage magnitude. Measurements can also be distinguished into power injection and line measurements. Both carry different advantages. Phase Measurement Units (PMU) are also available but tend to be expensive, as they measure power, voltage magnitude, and phasor at an exact time. Obtaining greater accuracy can be achieved with more expensive equipment, but it might also be possible to solve it with less expensive options.

Research Question 4: *Which strategic substations would benefit the most from the placement of a measurement?*

As substations differ in a technical and non-technical sense, some substations could be more influential in obtaining better results or lower costs. Identifying these differences is important so that DSOs can make the best choices for their networks.

1.4. Outline

This thesis is structured as follows: Chapter 2 provides a comprehensive background on state estimation and network observability. Chapter 3 presents a literature review focused on measurement placement. In Chapter 4, a method is proposed to address the main research question. This method is applied to two network scenarios. An empty network is analysed in Chapter 5 to isolate the impact of specific measurements. In Chapter 6, an operational network utilising its existing equipment is analysed, representing a real-world DSO scenario. Both chapters present the results and discuss the method's effectiveness and limitations. Finally, conclusions and recommendations are provided in Chapter 7.

2

Theoretical Background

This chapter provides the background and context necessary to understand the decisions made throughout the thesis. It also presents various methods relevant to the research that may complement the method designed in chapter 4. The chapter explains the Dutch MV grid and its operation. Next, the concept of weighted least squares state estimation is introduced. Following this, a deeper understanding of the two forms of observability is provided.

2.1. Dutch Medium Voltage Distribution System

The Dutch electricity grid is divided into two layers. The transmission system and the distribution system. Their difference is the voltage levels at which they operate High Voltage (HV) (50-380 kV) and MV (3-25 kV) or Low Voltage (LV) (0,4 kV), respectively [14]. Figure 2.1 illustrates the different voltage levels in the Dutch electricity network.

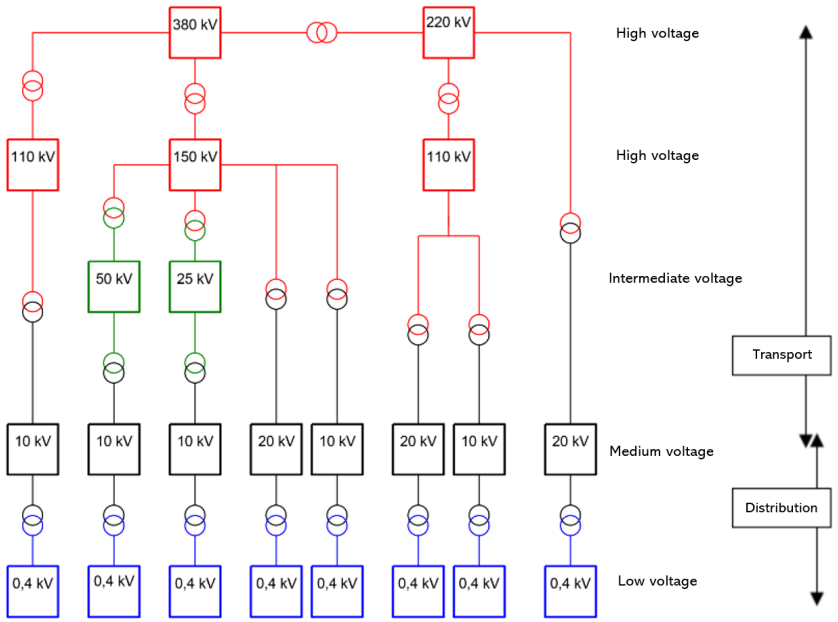

Figure 2.1: Voltage levels for transport and distribution levels[14].

This study will focus on the MV level of 10 kV, mainly used to distribute electricity from the transmission network into the LV network or to feed larger customers. A characteristic of the distribution network is that it has many more stations than the transmission network, while the measurement density is severely lower [15], [16]. This results in a poorly observed distribution network where historical records

usually predict its states. Important to note is that while distribution grids may have a mesh or a ring structure, they are operated in a radial configuration for better control and operation [14], [17].

The MV distribution system was initially designed for a one-sided power flow where energy is generated in large power plants and gradually fed to consumers at the end of the MV or LV grid. With the introduction of RES and sustainable energy technology, the dynamics of the distribution grid will change. Power generation shifts from one-sided to two-sided due to solar power on the roofs of consumers or car batteries that may be discharged at certain times. RES also come with peak generation, which can cause voltage violations and power congestion, leading to equipment damage, shorter lifespan, losses and even outages [18]. Therefore, the system needs to be monitored better to prevent it from violating its boundaries. A popular way is state estimation.

2.2. State Estimation

State estimation for power systems is a procedure for obtaining all the states of nodes/buses in a given network. The states are estimated using available measurements in the network and possibly pseudo-measurements to complement the available measurements where necessary. For state estimation, it is assumed that the network topology and parameters are perfectly known. The power system is considered to be operating in a steady state under balanced conditions. This means all branch power flows and bus loads are three-phase and balanced, all transmission lines are fully transposed, and the series and shunt devices are symmetrical in all three phases. These assumptions allow using a single-phase positive sequence equivalent circuit for modelling the power system [19]. Loads and generators will be modelled as power injections, thereby not affecting the network model.

State estimation will be explained primarily based on the work of M. Brown [20] and secondarily on the works of Abdur et al. and Monticelli [19],[21]. A standard measurement problem equation can be defined as in Equation 2.1. Here, the z is the measurement, the x is the actual value, and v is the error in the measurement.
Throughout this MSc thesis, consider the following: lowercase and uppercase italicised boldface letters denote column vectors and matrices, respectively. Superscript t indicates a vector or matrix transpose.

$$z = x + v \tag{2.1}$$

When multiple measurements are available, it results in a matrix form called the SE measurement model, which is seen in Equation 2.2.

$$\boldsymbol{z} = \boldsymbol{H}x + \boldsymbol{v} \tag{2.2}$$

If combined with the least squares method developed by Gauss, the objective function of this problem can be written as:

$$J(x) = (\boldsymbol{z}_1 - \boldsymbol{H}_1 x)^2 + \cdots + (\boldsymbol{z}_m - \boldsymbol{H}_m x)^2 \tag{2.3}$$

The objective function equals the error in Equation 2.2. To minimise the error, the first-order derivative of $J(x)$ should be taken and set equal to zero. In this way, $\hat{x}$ is computed. The $\boldsymbol{H}$ values are all 1 in this problem.

$$\left.\frac{\partial J}{\partial x}\right|_{\boldsymbol{x}=\hat{\boldsymbol{x}}} = 0 \rightarrow \hat{x} = \frac{\boldsymbol{H}_1 z_1 + \cdots + \boldsymbol{H}_m z_m}{\boldsymbol{H}_1^2 + \cdots + \boldsymbol{H}_m^2} \rightarrow \hat{x} = \frac{z_1 + \cdots + z_m}{m} \tag{2.4}$$

As illustrated by the results, this represents the most intuitive solution. Gauss also acknowledged this and reasoned that measurement accuracy should be considered. This consideration resulted in the formulation of the Weighted Least Squares (WLS) method with an alternate objective function from Equation 2.3.

$$J(x) = w_1(\boldsymbol{z}_1 - \boldsymbol{H}_1 x)^2 + \cdots + w_m(\boldsymbol{z}_m - \boldsymbol{H}_m x)^2 \tag{2.5}$$

2.2.1. Linear WLS state estimation

Linear state estimation, also known as Direct Current (DC) state estimation, is a simplified form of state estimation. While its simplicity reduces accuracy compared to non-linear state estimation, it remains valuable for multiple applications, including pricing calculations, analysis techniques for network security, transmission planning, transfer analysis, contingency screening, and transmission loading relief. The simplification assumes that all bus voltages are set to 1 p.u. and neglects network branches' series resistances and shunt admittances.

As power networks deal with multiple measurements of multiple states Equation 2.5 can be rewritten in matrix form.

$$\boldsymbol{J}(\boldsymbol{x}) = (\boldsymbol{z} - \boldsymbol{H}\boldsymbol{x})^t \boldsymbol{R}^{-1} (\boldsymbol{z} - \boldsymbol{H}\boldsymbol{x}) \tag{2.6}$$

With $\boldsymbol{R} = E(\boldsymbol{v}\boldsymbol{v}^t) = diag[\sigma_1^2, \ldots, \sigma_m^2]$ where $E(\boldsymbol{v}_1^2) = \sigma_i^2$. The linear state estimation solution can be computed by $\frac{\partial \boldsymbol{J}(\boldsymbol{x})}{\partial \boldsymbol{x}}\Big|_{\boldsymbol{x}=\hat{\boldsymbol{x}}} = \boldsymbol{0}^t$, obtaining:

$$\boldsymbol{H}^t \boldsymbol{R}^{-1} (\boldsymbol{z} - \boldsymbol{H}\hat{\boldsymbol{x}}) = \boldsymbol{0} \rightarrow \boldsymbol{H}^t \boldsymbol{R}^{-1} \boldsymbol{z} - \boldsymbol{H}^t \boldsymbol{R}^{-1} \boldsymbol{H}\hat{\boldsymbol{x}} = \boldsymbol{0} \rightarrow \boldsymbol{H}^t \boldsymbol{R}^{-1} \boldsymbol{H}\hat{\boldsymbol{x}} = \boldsymbol{H}^t \boldsymbol{R}^{-1} \boldsymbol{z} \tag{2.7a}$$

$$\boldsymbol{G} = (\boldsymbol{H}^t \boldsymbol{R}^{-1} \boldsymbol{H}) \tag{2.7b}$$

$$\boldsymbol{G}\hat{\boldsymbol{x}} = \boldsymbol{H}^t \boldsymbol{R}^{-1} \boldsymbol{z} \tag{2.7c}$$

$$\hat{\boldsymbol{x}} = \boldsymbol{G}^{-1} \boldsymbol{H}^t \boldsymbol{R}^{-1} \boldsymbol{z} \tag{2.7d}$$

$$\hat{\boldsymbol{x}} = (\boldsymbol{H}^t \boldsymbol{R}^{-1} \boldsymbol{H})^{-1} \boldsymbol{H}^t \boldsymbol{R}^{-1} \boldsymbol{z} \tag{2.7e}$$

Where $\boldsymbol{G}$ is the *gain* matrix (symmetric) and $\boldsymbol{0}$ is the *zero* vector. The *gain* matrix can be used to calculate the covariance matrix of the estimation error of the state.

$$\boldsymbol{G}^{-1} = \boldsymbol{\Sigma} = cov(\boldsymbol{x} - \hat{\boldsymbol{x}}) = E[(\boldsymbol{x} - \hat{\boldsymbol{x}})(\boldsymbol{x} - \hat{\boldsymbol{x}})^t] \tag{2.8}$$

2.2.2. Non-linear WLS state estimation

The relationship between measurements and state variables in physical power systems is often nonlinear. The simplified linear version will not suffice to accurately estimate the states of a distribution system. This is due to a high reactance to resistance ratio (X/R ratio) needed for the DC power flow model [20], which is low for distribution systems [22], [23]. Therefore, the measurement model and the following WLS objective function should be expressed as:

$$\boldsymbol{z} = \boldsymbol{h}(\boldsymbol{x}) + \boldsymbol{v} \tag{2.9a}$$

$$\boldsymbol{J}(\boldsymbol{x}) = [\boldsymbol{z} - \boldsymbol{h}(\boldsymbol{x})]^t \boldsymbol{R}^{-1} [\boldsymbol{z} - \boldsymbol{h}(\boldsymbol{x})] \tag{2.9b}$$

The same steps as those for the linear process are followed, where the gradient of $\boldsymbol{J(x)}$ must be set to zero, i.e. $\frac{\partial J}{\partial x}\big|_{\boldsymbol{x}=\hat{\boldsymbol{x}}} = 0^t$. This results after a transpose operation in:

$$\boldsymbol{H}^t \boldsymbol{R}^{-1} [\boldsymbol{z} - \boldsymbol{h}(\boldsymbol{x})] = \boldsymbol{0} \; or \; \boldsymbol{f}(\boldsymbol{x}) = \boldsymbol{0} \tag{2.10}$$

Where $\boldsymbol{H}(\hat{\boldsymbol{x}}) = \frac{\partial \boldsymbol{h}(\boldsymbol{x})}{\partial \boldsymbol{x}}\Big|_{\boldsymbol{x}=\hat{\boldsymbol{x}}}$ is the *Jacobian* matrix. Since Equation 2.10 represents a system of non-linear equations, it must be solved through an iterative process, such as the **Newton** method, as follows:

$$\frac{\partial \boldsymbol{f}(\boldsymbol{x})}{\partial \boldsymbol{x}}\Big|_{\boldsymbol{x}=\boldsymbol{x}^{(k)}} \Delta \boldsymbol{x}^{(k)} = -\boldsymbol{f}(\boldsymbol{x}^{(k)}) \tag{2.11}$$

$$\frac{\partial \boldsymbol{f}(\boldsymbol{x})}{\partial \boldsymbol{x}}\Big|_{\boldsymbol{x}=\boldsymbol{x}^{(k)}} = \frac{\partial}{\partial \boldsymbol{x}} \boldsymbol{H}^t \boldsymbol{R}^{-1} [\boldsymbol{z} - \boldsymbol{h}(\boldsymbol{x})]\Big|_{\boldsymbol{x}=\boldsymbol{x}^{(k)}} \Rightarrow \frac{\partial \boldsymbol{f}(\boldsymbol{x})}{\partial \boldsymbol{x}}\Big|_{\boldsymbol{x}=\boldsymbol{x}^{(k)}} = (-\boldsymbol{H}^t \boldsymbol{R}^{-1} \boldsymbol{H} + \boldsymbol{\mathcal{H}})\big|_{\boldsymbol{x}=\boldsymbol{x}^{(k)}} \tag{2.12a}$$

where (k) is the iteration index, $\Delta \boldsymbol{x}^{(k)} = \boldsymbol{x}^{(k+1)} - \boldsymbol{x}^{(k)}$ and $\boldsymbol{\mathcal{H}}$ an $(m \; x \; m)$ matrix. The matrix elements, typically denoted as (p, q), depend on the second derivatives of $\boldsymbol{h}_\ell(\boldsymbol{x})$, the covariance matrix $\boldsymbol{R}_{\ell\ell}^{-1}$ and the corresponding measurement residuals for any set of ℓ measurements, as illustrated in Equation 2.12b.

$$\mathcal{H}_{pq} = \sum_{\ell=1}^{m} \frac{\partial^2 \boldsymbol{h}_\ell(\boldsymbol{x})}{\partial \boldsymbol{x}_p \partial \boldsymbol{x}_q} \boldsymbol{R}_{\ell\ell}^{-1} \left[\boldsymbol{z}_\ell - \boldsymbol{h}_\ell(\boldsymbol{x})\right] \tag{2.12b}$$

As the matrix $\boldsymbol{\mathcal{H}}$ is expensive to compute its contribution in Equation 2.12a and Equation 2.12b is typically neglected. Therefore, the solution of $\hat{\boldsymbol{x}}$ can be obtained through the convergence of the iterative process known as the **Gauss-Newton** method:

$$\boldsymbol{G}^{(k)} \Delta \boldsymbol{x}^{(k)} = [\boldsymbol{H}^{(k)}]^t \boldsymbol{R}^{-1} [\boldsymbol{z} - \boldsymbol{h}(\boldsymbol{x}^{(k)})] \tag{2.13a}$$

$$\boldsymbol{G}^{(k)} = [\boldsymbol{H}^{(k)}]^t \boldsymbol{R}^{-1} \boldsymbol{H}^{(k)} \tag{2.13b}$$

Where *Jacobian* matrix $\boldsymbol{H}^{(k)} = \frac{\partial \boldsymbol{h}(\boldsymbol{x})}{\partial \boldsymbol{x}}$ is evaluated for $\boldsymbol{x} = \boldsymbol{x}^{(k)}$. If the system is observable, the gain matrix $\boldsymbol{G}^{(k)}$ is symmetric, sparse and positive definite. The iteration process continues with $\boldsymbol{x}^{(k+1)} = \boldsymbol{x}^{(k)} + \Delta \boldsymbol{x}^{(k)}$ until absolute value of $\Delta \boldsymbol{x}^{(k)}$ becomes smaller than a specified tolerance.

2.2.3. Non-linear state estimation for power systems

Active and reactive power flow measurements are most commonly used in power system state estimation. The voltage magnitude and angle, important states in power systems, can be derived from these measurements. The power flow measurements can be divided into two types. The power injection measurements and the line flow measurements. The formulas for injection into a bus and power flow in a branch, respectively, are shown in Equation 2.14, [20]:

Power injections into a bus

$$\boldsymbol{P}_i = |\boldsymbol{V}_i| \sum_{l=1}^{n} |\boldsymbol{V}_l| \left(\boldsymbol{G}_{il} \cos \boldsymbol{\theta}_{il} + \boldsymbol{B}_{il} \sin \boldsymbol{\theta}_{il}\right) \tag{2.14a}$$

$$\boldsymbol{Q}_i = |\boldsymbol{V}_i| \sum_{l=1}^{n} |\boldsymbol{V}_l| \left(\boldsymbol{G}_{il} \cos \boldsymbol{\theta}_{il} - \boldsymbol{B}_{il} \sin \boldsymbol{\theta}_{il}\right) \tag{2.14b}$$

Power flow in a branch

$$\boldsymbol{P}_{i-k} = |\boldsymbol{V}_i|^2 (g_{i-k} + g_i^{sh}) - |\boldsymbol{V}_i||\boldsymbol{V}_k| (g_{i-k} \cos \boldsymbol{\theta}_{ik} + b_{i-k} \sin \boldsymbol{\theta}_{ik}) \tag{2.14c}$$

$$\boldsymbol{Q}_{i-k} = -|\boldsymbol{V}_i|^2 (b_{i-k} + b_i^{sh}) - |\boldsymbol{V}_i||\boldsymbol{V}_k| (g_{i-k} \sin \boldsymbol{\theta}_{ik} - b_{i-k} \cos \boldsymbol{\theta}_{ik}) \tag{2.14d}$$

It is assumed that the parameters $\boldsymbol{G}_{il}, \boldsymbol{B}_{il}, g_{i-k}, g_i^{sh}, b_{i-k}$ and b_i^{sh} are known. The *Jacobian* matrix $\boldsymbol{H}$ can be formed from here. First we start with $\boldsymbol{h}(\boldsymbol{x}^{(k)})$ and apply $\boldsymbol{H}(\hat{\boldsymbol{x}}) = \left.\frac{\partial \boldsymbol{h}(\boldsymbol{x})}{\partial \boldsymbol{x}}\right|_{\boldsymbol{x}=\hat{\boldsymbol{x}}}$ where $\boldsymbol{x}$ will consist of the desired states. Table 2.1 exemplifies how this could look.

The derivatives corresponding to the power flows and injections and voltage magnitudes mentioned above in the *Jacobian* matrix are further detailed in the Equations (A.1)(A.2)(A.3)(A.4)(A.5) which are found in Appendix A.

The iteration process itself usually begins with a flat start for power systems, i.e.:

$$\boldsymbol{x}^{(0)} = \begin{bmatrix} \boldsymbol{\theta}_1^{(0)} \\ \vdots \\ \boldsymbol{\theta}_n^{(0)} \\ |\boldsymbol{V}_1^{(0)}| \\ \vdots \\ |\boldsymbol{V}_n^{(0)}| \end{bmatrix} = \begin{bmatrix} 0 \\ \vdots \\ 0 \\ 1 \\ \vdots \\ 1 \end{bmatrix}$$

where $\boldsymbol{V}_n$ is in p.u. and $\boldsymbol{\theta}$ in degrees.

$\boldsymbol{h}(\boldsymbol{x}^{(k)}) =$	...	$\boldsymbol{P}_{i-k}^{(k)}$	...	$\boldsymbol{P}_{i}^{(k)}$	...	$\boldsymbol{Q}_{i-k}^{(k)}$	...	$\boldsymbol{Q}_{i}^{(k)}$	...	$\lvert\boldsymbol{V}_{i}^{(k)}\rvert$	...

$\boldsymbol{H}$	...	$\partial/\partial\theta_i$	...	$\partial/\partial\theta_k$	...	$\partial/\partial\lvert\boldsymbol{V}_i\rvert$	...	$\partial/\partial\lvert\boldsymbol{V}_k\rvert$	...
		⋮		⋮		⋮		⋮	
$\boldsymbol{P}_{i-k}^{(k)}$	...	$\partial P_{i-k}^{(k)}/\partial\theta_i$	...	$\partial P_{i-k}^{(k)}/\partial\theta_k$	...	$\partial P_{i-k}^{(k)}/\partial\lvert\boldsymbol{V}_i\rvert$	...	$\partial P_{i-k}^{(k)}/\partial\lvert\boldsymbol{V}_k\rvert$	...
		⋮		⋮		⋮		⋮	
$\boldsymbol{P}_{i}^{(k)}$	...	$\partial P_{i}^{(k)}/\partial\theta_i$	...	$\partial P_{i}^{(k)}/\partial\theta_k$	...	$\partial P_{i}^{(k)}/\partial\lvert\boldsymbol{V}_i\rvert$	...	$\partial P_{i}^{(k)}/\partial\lvert\boldsymbol{V}_k\rvert$	...
		⋮		⋮		⋮		⋮	
$\boldsymbol{Q}_{i-k}^{(k)}$	...	$\partial Q_{i-k}^{(k)}/\partial\theta_i$	...	$\partial Q_{i-k}^{(k)}/\partial\theta_k$	...	$\partial Q_{i-k}^{(k)}/\partial\lvert\boldsymbol{V}_i\rvert$	...	$\partial Q_{i-k}^{(k)}/\partial\lvert\boldsymbol{V}_k\rvert$	...
		⋮		⋮		⋮		⋮	
$\boldsymbol{Q}_{i}^{(k)}$	...	$\partial Q_{i}^{(k)}/\partial\theta_i$	...	$\partial Q_{i}^{(k)}/\partial\theta_k$	...	$\partial Q_{i}^{(k)}/\partial\lvert\boldsymbol{V}_i\rvert$	...	$\partial Q_{i}^{(k)}/\partial\lvert\boldsymbol{V}_k\rvert$	...
		⋮		⋮		⋮		⋮	
$\lvert\boldsymbol{V}_{i}^{(k)}\rvert$	...	0	...	0	...	1	...	0	...

Table 2.1: Partial derivatives in the power system analysis.

2.3. Observability Analysis

Observability refers to the ability to calculate the system's state. A commonly used formula that provides a simple and quick approach to assess observability is given in Equation 2.15.

$$m \geq 2n - 1 \tag{2.15}$$

Here, m represents the number of measurements, and n denotes the number of buses in the network. This value is used because each node has two unknown states: the voltage magnitude and the phase angle. One less measurement is required since one phase angle is set to zero as the reference bus. The number of measurements is chosen to construct a *Jacobian* matrix with a rank equal to the number of unknown states. The number of $m \approx 4n$ is taken for reasonable performance in practical situations [24].

This represents the minimum requirement for system observability. However, having sufficient measurements does not guarantee the system will be observable. For instance, if all measurements are concentrated in a small network section, the system might still pass the observability test of Equation 2.15 but remain unobservable. More advanced methods have been developed to address such cases, categorised into numerical and topological observability, involving manipulation of *Jacobian*, *Gain* and *Gram* matrices and graph-based theory.

2.3.1. Numerical Observability

According to [20], numerical observability can be checked using the linear decoupled/DC model. This entails a few assumptions: all power measurements are in pairs (active/reactive), and the system is simplified to a state where branch parameters do not influence observability. Shunt resistances to the ground are ignored. Equation 2.16 describes the linear decoupled model:

$$\boldsymbol{z}_a = \boldsymbol{H}_a\boldsymbol{\theta} + \boldsymbol{v}_a \tag{2.16a}$$

$$\boldsymbol{G}\hat{\boldsymbol{\theta}} = \boldsymbol{H}^t\boldsymbol{z}_a \tag{2.16b}$$

$$\boldsymbol{G} = \boldsymbol{H}^t\boldsymbol{H} \tag{2.16c}$$

In this model, $\boldsymbol{H}$ is filled with the relations between measurements and their surrounding buses and will take on the following form.

$\boldsymbol{H}_a$	...	$\boldsymbol{\theta}_i$	...	$\boldsymbol{\theta}_j$	...	$\boldsymbol{\theta}_k$	...
⋮		⋮		⋮		⋮	
$\boldsymbol{P}_{i-k}$		1		0		-1	
$\boldsymbol{P}_i$		nb_i		-1		-1	
⋮		⋮		⋮		⋮	
$\boldsymbol{\theta}_i$		1		0		0	
$\boldsymbol{I}a_{i-k}$		1		0		-1	
⋮		⋮		⋮		⋮	

Here nb_i is the number of buses connected to b_i, and $\boldsymbol{I}a_{i-k}$ is a current measurement on a branch. Now observability can be checked via the $\boldsymbol{G}$ matrix. If observable, the $\boldsymbol{G}$ matrix is non-singular, i.e. it has no zero pivots after Gauss elimination.

Unobservable branches and nodes can also be identified. Various ways are given by [19], [25] and [26]. They each manipulate the *Gain* matrix with triangular decomposition. Their methods can take several iterations to expose the numeral unobservable parts of the network.

The *Gram* matrix method from [27] is an alternative to the *Gain* matrix method used above. Instead of creating a matrix corresponding to the nodes in the system as in Equation 2.16c, this matrix is coupled to the measurements by:

$$\boldsymbol{A} = \boldsymbol{H}\boldsymbol{H}^t \tag{2.17}$$

It can identify non-redundant measurements through triangular decomposition, where zero pivots correspond to non-redundant measurements. Furthermore, a method for identifying observable islands is given by using the minimum norm formulation:

$$\boldsymbol{\theta} = \boldsymbol{H}_{nr}^t \boldsymbol{A}_{nr}^{-1} \boldsymbol{z} \tag{2.18}$$

Where $\boldsymbol{H}_{nr}^t$ is the DC-model *Jacobian* matrix with an added phase angle pseudo measurement at the node where an island may be detected, the vector $\boldsymbol{z}$ contains all zeros except at the position of the pseudo measurement and $\boldsymbol{\theta}$ is a matrix that contains ones for nodes belonging to the observable island and zeros for nodes that are not part of the observable island.

2.3.2. Topological Observability

Topological observability uses graph theory to obtain the network status [20]. Graph theory makes use of the relationship between objects. These objects are nodes or buses for power systems, and edges imply a relationship between them. Graphs can be modelled in specific ways, with undirected, directed and coloured edges and as simple and multi-edged graphs as shown in Figure 2.2. The simple graph's edge indicates a relationship between two nodes, whereas a directed graph suggests the direction of the relation. A multi-graph is used when there are multiple relations between nodes.

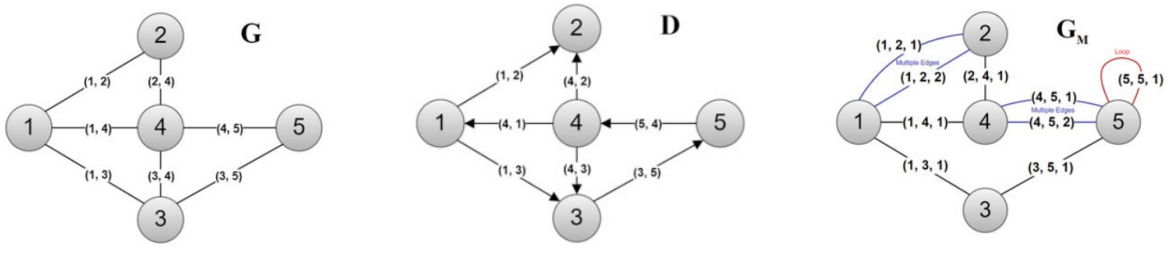

(a) Simple graph. **(b)** Directed graph. **(c)** Multigraph.

Figure 2.2: Basic graphs [20].

For the observability test in power systems, it is assumed that the measurements come in pairs; i.e., if there is an active power measurement, there is also a reactive power measurement. A distinction is

made between power injection measurements and power flow measurements. Power flow measurements are associated with a specific edge. In contrast, a power injection measurement at a node can become an edge to one of all neighbouring nodes, i.e. a node linked by a line to the node with the power injection. An example given in [20] shows all possibilities of a given network illustrated in Figure 2.3

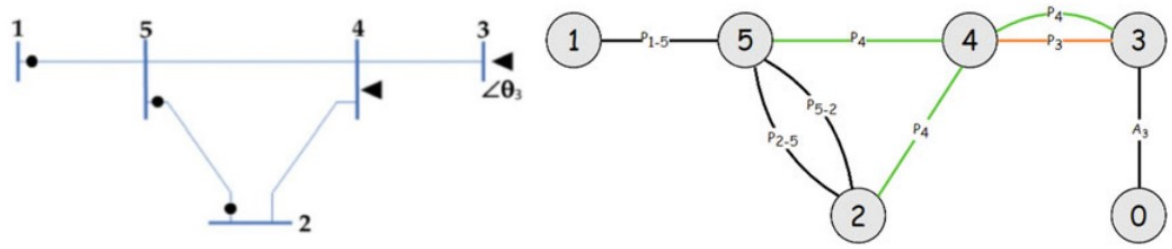

(a) Five bus network [20]. **(b)** Five bus multi graph [20].

Figure 2.3: Representation of a normal network into a graph network.

The method discussed in [20] firstly created a multi-graph Z_m containing all nodes. Next, it processes all flow measurements into T_f, a sub-graph containing all flow edges, while ensuring no double lines exist between nodes to avoid creating loops in the graph. For example, in Figure 2.3b, there are two measurements between nodes 5 and 2. This method selects only one measurement to be added to T_f. Now, power injection measurements are added. Important to note is that all measurements will be given a distinct colour, as P_4 in Figure 2.3b has three options. All these edges have the same colour. This way, a colour constraint can be implemented so that one colour will not occur twice in the multi-graph. So, a colour and a loop constraint are needed to add injection measurements. Depending on the order in which the power injection measurements are added, the spanning tree may not be created in one iteration. To combat this a *bipartite* graph is needed which saves existing edges and remembers which constraints are active. If a path with more than edges in the *bipartite* graph than the current path is found, the path should be replaced with the found path. This process is shown in Figure 2.4 with the completed spanning tree of the five bus network from Figure 2.3a in the bottom left and the *bipartite* graphs on the right. Once all steps of the method are completed, the optimal spanning tree for a given network is constructed. If spanning tree T encompasses the whole network, i.e. it is of full rank [28], the network is deemed observable.

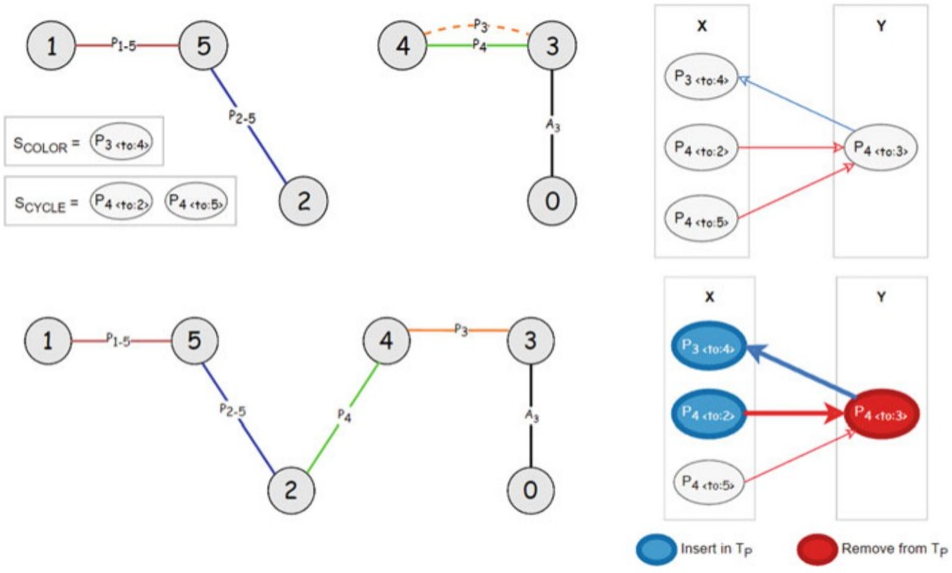

Figure 2.4: Creation of rainbow spanning tree [20].

The method is validated in [19]. Earlier implementations can be found in [28] and [29]. The same

procedure is applied universally. All flow measurements are assigned to their respective edges for a given network of nodes, ensuring no loops are created. Subsequently, all injection measurements should be assigned edges. This process iterates through all injection measurements until the optimal spanning tree is identified. If the spanning tree does not achieve full rank, the network is deemed unobservable and consists of multiple sub-graphs called forests.

2.3.3. Hybrid Methods for Observability

The methods mentioned in subsection 2.3.1 and subsection 2.3.2 can also be combined, creating a hybrid method. In [30], a topological method based on three rules is employed to check for observability. Some observable islands may be overlooked as these rules state adequate but not mandatory conditions. Therefore, the simplified network is analysed using a numerical method to determine its observability. Due to the simplification of the network by the topological part, the computational time for the numerical part is significantly reduced. This time reduction makes the hybrid method faster than just the numerical method.

The methods used in [31] and [32] have more in common with a numerical method. It also simplifies the network through a topological process that merges parts of the network. Subsequently, it performs observability analysis using the echelon form of the reduced network matrix. The method in [31] relies exclusively on 0, +1 and -1 entries, making it resistant to rounding errors, which can occur in the traditional numerical methods involving triangular decomposition of the *gain* matrix.

2.3.4. Used Method for Observability

For this thesis, the PandaPower State Estimation code will be used for running the state estimation [33]. The first observability check in this code assesses the number of available measurements. If the number of measurements does not exceed or is equal to $2n - 1$, where n is the number of nodes, the estimation will not proceed. The second check follows the numerical method, where the networks *Gain* matrix is checked for singularity.

3

Literature Review

This chapter explores various approaches to the meter placement problem, ranging from straightforward reasoning and strategic location selection to complex optimisation methods considering multiple types of measurements. Based on the reviewed literature, a decision will be made regarding the most suitable approach to achieving observability with actual measurements for DSOs, with a particular focus on Stedin.

3.1. Strategic locations

In [34], a categorisation of the importance of network capabilities is presented, with substation automation ranked as the highest priority and load management as the lowest. Under substation automation fall services like fault location and isolation, service restoration, power factor control and transformer load balancing. Load management concerns load control, surveys and remote meter readings. With this in mind, the main focus of measurement placement is around switches, as accurate estimation at these points plays a significant role in network control. In addition, it is recommended that the loads between the measuring point on lines be as balanced as possible. This balance creates a more uniform state estimation with similar accuracy for those nodes. This balance is achieved by prioritising the measurement of outlier nodes with higher loads.

The cost of placing measurement equipment can be significant. The research in [35] suggests that all nodes with more than two flow branches should be fully measured. Figure 3.1 shows such a node in orange. Beware that the blue nodes are also substations and not loads. This approach prioritises minimising the number of locations that require measurement equipment rather than the total number of measurements. The rationale is that the primary expense lies not in the measurement devices but in their installation, revision and maintenance. Therefore, maximising the number of devices placed at a single station during these operations is practical. The branch voltage phasor and complex power flow and failure rate were chosen as a criterion for further placement. The paper stopping conditions for voltage regulations, switching consequence assessment and loss estimation are met when 20% of the point of connection stations are measured. The obtained voltage requirements do not indicate a high accuracy for the other systems states. While the method is effective for the predefined requirements, its adaptability should be assessed if these constraints change. Expanding the requirements increases computational complexity, potentially necessitating a more efficient selection process or alternative methodologies.

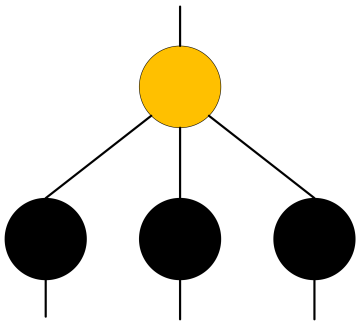

Figure 3.1: Stategic location of splitting point feeder displayed as orange node.

Today, many distribution networks are without actual measurements and use pseudo-measurements, often inadequate for an accurate state estimation. Work [36] suggests a method to place actual measurements based on the uncertainty level of the pseudo-measurements. It classifies networks as observable if the estimated states are confidently accurate enough so that the possible actual states would be inside the physical constraints of the system. If this is not the case, it looks at where placing an actual measurement would make it so that the states of most pseudo-measurement nodes will be within these uncertainty boundaries. It does this one measurement at a time. Due to this, the best solution might not be found if multiple measurements are placed in the network.

If only a few parameters are of concern, observability can be achieved using pseudo-measurements. In [37], an initial selection of measurements is made at locations considered of high importance, and pseudo-measurements are then used to supplement the network to achieve observability. When the calculated network states do not meet the desired accuracy range, additional actual measurements are incorporated until the required accuracy is achieved. This technique prioritises certain buses over others, which is advantageous for a DSO who knows the importance of specific bus parameters. However, if such information is unavailable, the method would require a random starting point, potentially leading to unnecessary costs.

3.2. Criteria for accuracy

Identifying the impact of measurement placement and type of measurement on the accuracy of various states and reliability of the SE is the focus of [38]. The study primarily relies on pseudo-measurements, supplemented by actual measurements, to achieve the desired accuracy or meet a predefined measurement quantity. It suggests that achieving observability solely through actual measurements is not economically feasible. The paper also emphasises the increasing importance of effective voltage control in the presence of higher levels of distributed generation. Additional criteria considered include bad data detection and redundancy. To address these issues, measurements should be strategically placed at critical locations to maximise redundancy, enabling data comparison to filter out erroneous data and enhance system stability during faults. Directly monitoring switches provides better insight into network topology, while directional measurements are crucial in the case of uncertain flow direction, as non-directional measurements can lead to convergence issues. These criteria are satisfied by focusing on the accuracy of critical states, utilising directional measurements, directly metering large distributed generation units and metering switches.

An example of the extensive use of pseudo measurements is presented in [39]. The study demonstrates that a network can be observable primarily through pseudo measurements, supplemented by a few actual measurements at the primary busbars. However, the state estimator frequently failed to converge, and the resulting estimates were inaccurate due to contradictions between the measurements. The constant failing of the state estimation shows the necessity of incorporating actual or more precise pseudo-measurements to ensure reliable state estimation.

3.3. Location Selection

The work [40] addresses network observability by identifying unobservable branches and selecting buses for power injection measurements to resolve unobservability. This is achieved by manipulating the gain

matrix and randomly selecting buses adjacent to an observable island. However, the method can be inefficient, as choosing a second adjacent bus could enable placing two line measurements in a single operation and achieve observability while significantly reducing operational costs. Notably, these must be actual measurements, as pseudo measurements for line power flow are unavailable.

3.3.1. Heuristic for RTUs and Measurements Planning Algorithm

Creating a radial network while minimising costs, ensuring observability, and eliminating critical measurements and sets is the main objective in [41]. Only assuming radial networks is a simplification, as distribution networks can also have ring or meshed topologies. The Heuristic for RTU and Measurement Planning (HRMP) algorithm is proposed to meet the minimum observability requirements, based on the graph theory of [42]. RTUs collect data from all surrounding measurements, i.e. power flow and injection measurements. The paper demonstrates that HRMP is more cost- and time-efficient than a genetic algorithm. The tests are conducted on different networks under three scenarios: achieving observability, eliminating critical measurements and eliminating essential sets.

However, the study only considers the failure of individual measurements when evaluating criticality. If an RTU fails, all its associated measurements become unavailable, meaning that only a network without critical sets would retain full observability in such a case.

3.3.2. Singular Value Decomposition Algorithm

In [43], a list of potential measurement locations is generated using the singular value decomposition algorithm. The method is also used in [44] for harmonic state estimation. The candidate locations are then evaluated through a Monte Carlo Simulation (MCS) to assess their accuracy. If the resulting accuracy does not meet the predefined requirements, the singular value decomposition algorithm is rerun to generate a new set of potential locations, and the process is repeated until the target accuracy is achieved. The computational time is very high for large networks, as it has to evaluate all potential locations. The proposed algorithm tries to prevent this by shortlisting high-potential candidates. However, this approach may not always find the optimal solution, as the best location may not be included in a given candidate list that meets the accuracy threshold. Additionally, the method relies heavily on pseudo measurements, as achieving full observability with actual measurements is deemed economically unfeasible.

3.4. Optimization Techniques

3.4.1. Mixed Integer Linear Programming

Mixed-Integer Linear Programming (MILP) is used in several meter placement problems [45], [46], [47]. The work in [46] builds on the MILP formulation of [45] to review multiple scenarios. It determines the optimal meter placement for a radial nine-bus system, considering scenarios with and without Distributed Generation (DG). The approach provides a solution for both scenarios, ensuring optimal placement even when DERs are not generating power. MILP based on error minimisation is employed to identify the best placement. It is a mixed integer problem as the decision variable of placement can be 0 or 1, where other variables are not bound to be integers—the load, for example.

As elements in state estimation like the *Gain* matrix are nonlinear, linearising is necessary to use them in an MILP format. Which comes with extra effort. Linear problems are easier to solve than non-linear problems. However, linearization introduces additional constraints to the problem, which may lead to over-constraining while increasing complexity. This added complexity results in higher computational effort and longer solution times. The issue becomes even more prominent for more extensive networks. This challenge arises quickly since DSOs operate networks with numerous potential placement locations. The solution's reliability is connected to the scenarios tested. A good scenario sample is crucial for a good result, so if not correctly chosen, the result is unreliable. As DER penetration increases, network volatility leads to higher error levels. The study highlights that error indices can vary significantly across different scenarios, emphasising the importance of running multiple scenarios to ensure a robust and reliable solution.

3.4.2. Optimal Experimental Design Algorithms

The goal in [48] is to minimise the maximum error covariance error by selecting the optimal subset of measurements to achieve an observable network. Their approach is based on the state error covariance matrix, which adapts the gain matrix. This method serves as a measurement planning tool, allowing DSOs to incorporate their preferences regarding economic, geographical and technological factors. It is flexible in adjusting the desired number of measurements and is applicable to both observable and unobservable networks. The method utilises the gain matrix $\boldsymbol{G}(\boldsymbol{x})$ to formulate an M-optimal experimental design task, focusing on the minimisation of the maximum variance of the worst states, which is then transformed into a mixed-integer semidefinite programming (SDP) model. Their findings indicate that a combined placement of power flow and voltage magnitude measurements is the most effective approach. However, if a single type of measurement is preferred, power flow measurements are recommended due to their ability to provide information on both state variables (θ and V).

Optimal experimental design is also employed in [49], specifically in D-optimality, to create a Boolean-convex optimisation model. The D-optimal method maximises the determinant of the system Fisher information matrix by selecting a predefined number of new measurements from a given candidate set. The study highlights that the combined placement of power flow and voltage meters yields the highest accuracy.

The method in [50] works along the same line as [48], using the state error covariance matrix and formulating the problem as a mixed integer semidefinite programming problem. It uses four optimal design methods to minimise a distinct part of the error covariance matrix. A disadvantage is the longer run time that comes with these methods. However, this is not a significant obstacle, as the methods are intended for the design phase, which is not subject to time constraints. The comparison between the branch and bound method and the proposed method is made where the proposed method works faster but will only find local optima. The faster runtime is preferred when specific parameters like budget or uncertainty levels still need to be fine-tuned.

These algorithms require significant computational time as system complexity and size increase, which is particularly relevant for MV grids. Additionally, they are sensitive to the assumptions about the problem they aim to solve. Inaccuracies in these assumptions, such as variations in network topology or measurement noise, can lead to suboptimal solutions. Given that such discrepancies are likely to occur, designing meter placement using this algorithm becomes challenging.

3.4.3. Binary Particle Swarm Algorithm

The study presented in [51] focuses on optimising state estimation accuracy under specific constraints. The optimisation problem is addressed using a binary particle swarm algorithm, which has also been used successfully in [52] but then for LV networks. To reduce computational time, the authors employ an analytical approach instead of the traditional MCS method to determine the accuracy of the state estimation. The work prioritises uncorrelated measurements, considers multiple load levels, and addresses the high computational costs associated with MCS. The study concludes that allocating measurements based on the probability of exceeding the maximum risk is an effective metric for improving state estimation accuracy. Additionally, it identifies a correlation between active and reactive power measurements, suggesting that their accuracy should be coupled. The analytical approach demonstrated in the paper proves to be significantly less computationally intensive.

The binary particle swarm optimisation algorithm differs from the standard one because it operates in a binary search space. Particles navigate this space based on three key vectors: their current direction, personal best position, and the swarm's best-known position. These vectors are updated iteratively to guide the search process. The algorithm can converge to a suboptimal solution if the balance between these vectors is not well-maintained. In the context of measurement placement in MV grids, the problem can become complex due to the numerous factors influencing placement, such as network topology, load variability, and DG. As a result, the search space can grow large, increasing computational demands and convergence time.

3.4.4. Simulated Annealing Algorithm

The simulated annealing algorithm uses a temperature gradient and an acceptance probability. It starts with a high initial temperature, where the acceptance probability is high, allowing the algorithm

to accept worse solutions. This helps it escape local minima. The acceptance probability decreases as the temperature decreases following a set pattern over time. Consequently, the algorithm will only accept lower-cost solutions as the temperature and acceptance probability decrease.

The works [53], [54], [55], [56] focus on creating an observable and reliable network with the simulated annealing algorithm at the lowest possible cost. [56] analyses three cases distinguished by the presence of critical measurements or critical sets. These scenarios range from a network composed entirely of critical measurements to one dominated by critical sets and finally to a network with no criticality. This approach is achieved at a relatively low cost. However, as the network studied is highly meshed, it raises questions about whether the relative price of achieving redundancy remains similarly low in other networks.

The simulated annealing algorithm selects measurements based on even distribution, monetary cost, and the inclusion of critical measurements and sets. The measurements considered include active and reactive power and voltage magnitude. The computation time is extensive for larger networks due to the vast search space and iteration process. This could be brought back by 'cooling down' faster, but the most optimal solution may not be found then. The solution is based primarily on the cost of specific properties, making the algorithm very selective.

3.4.5. Genetic Algorithm

Genetic algorithms used in [57], [58], [59], [60] mimic natural evolution through the principle of survival of the fittest. The process begins with an initial population of possible solutions. The fittest individuals from this population are selected as parents for the next generation. Some offspring are exact copies of their parents, while others are created through crossover between two parents or mutation. This process continues over many generations, allowing the algorithm to converge on an optimal solution. The algorithm can be stopped after several generations or when specific thresholds are met.

PMUs provide more detailed data than conventional measurement devices, as they precisely capture the voltage phase. In [59], the authors analyse the accuracy of different measurement types, reporting a range of 1% for substation and PMU measurements, 10% for Smart Metering (SM), and 50% for pseudo-measurements. Substation measurements are excluded from the optimisation process since they are limited to slack buses. The study concludes that combining measurement types is optimal for achieving predefined accuracy at the lowest cost. The optimisation accounts for multiple grid configurations, acknowledging that dynamic grid topology changes will become an inevitable feature of future active distribution grids.

In [60], the work of [59] is expanded to address the lack of information about the distribution grid. The study considers the possibility of non-Gaussian distributions for DG and the impact of data loss and degradation. The proposed method successfully meets the N-1 objective for robustness and data integrity. The approach relies solely on PMUs and smart metering devices. According to [60], "*the term smart meter is used to identify either single metering devices or data concentrators, which collect and process active and reactive power measurements provided by the aggregated loads at the distribution feeders or secondary substations.*" This definition suggests that the smart meters considered in the study primarily measure power flow entering or exiting the MV grid but do not capture line power flow through substations. As a result, the study overlooks MV power flow measurements on lines that could potentially enhance cost-effective grid observability. The sampling frequency of such smart metering is also not stated, so it might not be helpful or accurate for operating a real-time distribution management system.

3.4.6. Tabu Search Algorithm

The Tabu Search Algorithm is a heuristic algorithm similar to simulated annealing and the genetic algorithm, but some regard it as superior due to its flexible memory [61],[62]. Tabu Search can use its flexible memory to prevent getting stuck in local optima and cycling through previously attempted configurations. It starts with a feasible solution, exploring the 'neighbourhood' for better solutions. In this way, it can escape local optima. A list is created to store all visited solutions to prevent revisiting them. For large networks, significant memory storage is needed for the tabu list. After a certain amount of movement, it moves to the best solution from the tabu list. From here, it will begin the search for better solutions again, only stopping after a maximum number of iterations if satisfactory results are

found.

PMU placement based on redundancy and observability is discussed in [61]. The method begins by placing PMUs at nodes with the highest number of incident branches, as these nodes contribute the most to network observability. Each step decreases the number of incident branches until the network becomes fully observable. However, this approach may result in more PMUs than necessary. To address this issue, the Tabu Search algorithm optimises placement and eliminates redundant PMUs. According to the authors, the typical ratio of buses equipped with PMUs is approximately one-third to one-fourth of the total number of buses in the system. This relatively low ratio is attributed to the meshed nature of the grids studied and the presence of zero-injection buses. In contrast, networks operated by Stedin, which are more radial, would likely require a higher number of PMUs to achieve full observability. The focus on PMUs may also be unnecessary. This type of equipment is expensive, and the problem could be addressed through alternative solutions.

3.4.7. Sub-modular Saturation Algorithm

Sub-modular saturation algorithms start with an empty data set that can be filled with possibilities from another set, in this case, measuring points, based on the marginal profit these measuring points provide. The marginal profit diminishes as the set grows. The algorithm stops when certain conditions are met, such as when the network's state estimation is accurate enough. It can also stop after a predefined number of iterations. For sub-modular saturation algorithms to work, the marginal gain of each option must be calculated. This results in high computation times for large networks. Heuristic algorithms may be faster by not evaluating every option.

Due to the dynamic changes in topology within active distribution systems, the meter placement problem could call for a more robust formulation. In [63], a robust algorithm called sub-modular saturation is proposed, which surpasses greedy and genetic algorithms in most cases and competes with them in others. The algorithm optimises the worst-case total estimation variance, which could be an outlier from a faulty measurement. Therefore, it may be more beneficial to assess the overall variance rather than focusing solely on the worst case. Furthermore, the algorithm relies only on voltage magnitude meters and PMUs, meaning additional costs can be minimised by opting for more cost-effective measurements.

3.4.8. Adaptive Step Multidimensional Fruit Fly Algorithm

The Adaptive Step Multidimensional Fruit Fly Algorithm adapts the standard fruit fly optimisation algorithm. The standard algorithm starts at a specific location and has a fixed population size. The number of iterations is chosen beforehand. Each fruit fly is sent to a random location from the original location, and their distance is calculated. The smell concentration judgment is made based on this distance. This is, in turn, used to determine the smell of the location. The best smell will determine the new location of the fruit flies. This process is repeated while keeping track of the best smell so far. The algorithm will stop if no new location is found within a given amount of iterations. Adding an adaptive step allows the algorithm to dynamically adjust the search area under certain conditions, improving convergence speed and preventing the algorithm from getting stuck in local optima. Multidimensional means that the algorithm can process three or more variables to optimise. It is, in a way, quite similar to the tabu search algorithm that also explores the 'neighbourhood' for potential solutions.

In [64], the most critical network nodes are identified for PMU placement to achieve network observability. Subsequently, the fruit fly optimisation algorithm is applied to minimise the number of PMUs required to observe the network. This algorithm seeks the global optimum by exploring alternatives to an existing solution and iteratively converging on the best placement scheme. The method demonstrates accelerated convergence and generates placement schemes within smaller solution spaces compared to earlier approaches. However, the study focuses only on PMU placement and does not account for other types of measurement devices that could achieve the same goal at a lower cost.

3.5. Critics on available literature

The science of state estimation has been established for approximately 55 years. Over time, it has evolved into a mature and well-developed method, although ongoing advances continue to refine the approach. It has been used widely by TSOs, but the technology has yet to see widespread adaptation among DSOs.

The covered literature addresses various aspects of meter placement. However, all the studies presented above focus on algorithms for measurement allocation in new or 'empty' networks. A significant challenge in achieving observability is the high cost of deploying sufficient actual measurements. Surprisingly, none of the discussed algorithms consider existing meter placements. Leveraging already installed measurements could significantly reduce placement costs. While existing measurements can be incorporated with minimal effort, it is an aspect that requires deliberate consideration.

Additionally, the literature does not account for the practical constraints of real-world networks. Construction limitations or ageing infrastructure may prevent meter installations at theoretically optimal locations. Most algorithms require significant computational resources, data storage, and processing time. These resources incur costs that DSOs preferably avoid. While computational time may not be an immediate issue during the design phase, it increases exponentially with network size, eventually exceeding what DSOs can feasibly manage.

Most studies propose tailored solutions optimised for specific conditions, such as a fixed topology and predefined load scenarios. However, these solutions become ineffective when network conditions change significantly due to topological modifications or highly variable load patterns, which are increasingly relevant with the rise of DG. Furthermore, minimising errors for certain network states does not ensure accuracy across all conditions. As a result, existing approaches are often too specialised and complex to implement in practice. There is a clear need for DSOs to adopt more general, intuitive solutions that can adapt to changing network conditions.

This thesis aims to bridge these gaps by providing a workflow for DSOs to redesign or enhance their existing networks while addressing their practical challenges. Rather than seeking a specialised solution, the workflow focuses on a broader approach to ensure a generally reliable state estimation, even as network conditions change. Additionally, it is designed to be practical and feasible for DSOs to implement in real-world scenarios.

4

Accurate State Estimation in Distribution Networks

This chapter introduces the preparatory steps for measurement placement and outlines a workflow for determining how measurements should be placed within an existing or yet-to-be-built network.

4.1. Network Conditions

Some assumptions were made during this research to simplify the analysis. First, the network operates under balanced conditions and in a steady state. MV networks operate from a nominal 10 kV to 30 kV, and the measurement equipment used should be capable of handling these conditions. MV networks consist of a primary station and substations. The primary station will be called a slack bus, and substations will be called nodes. The primary station is the connection to the HV grid, where substations connect to customers or LV grids.

The nodes in the Figures 4.2 to 4.4, 5.2 and 6.1 represent locations with connected loads, though these loads are not explicitly drawn. These loads can vary from residential and industrial consumers to generation units. Slack buses will have no load. For the state estimation, all nodes will have a load directly connected to them without a transformer in between the node and the load.

All active and reactive power measurements are taken in pairs. According to Stedin's policy, the primary substation behind the HV/MV transformer is always fully equipped with measurements. These are line power flow measurements.

Stedin aims to operate its MV networks in a radial configuration. For simplicity, this research assumes that all networks are operated in this manner. A node is considered "measured" only if all active MV network lines connected to it are measured.

4.2. Measurement Types

Multiple types of measurement placements are possible. A brief overview of the available types, along with an explanation of their consequences, will be given in this section. This analysis considers only active and reactive power measurement pairs and voltage measurements. The Figure 4.1 is used to illustrate the placement of the measurements. For simplicity, this research assumes fixed accuracy values across each type of measurement, ensuring consistency in analysis and comparison.

4.2.1. MV Measurements

The red circles in Figure 4.1 indicate possible locations for MV-side measurements, which include P, Q and V magnitude values. The top two are line measurements and can only represent their respective lines. However, the measurement between the transformer and MV node functions as a node power injection measurement (PIM). This measurement represents a load or generation on a node. According

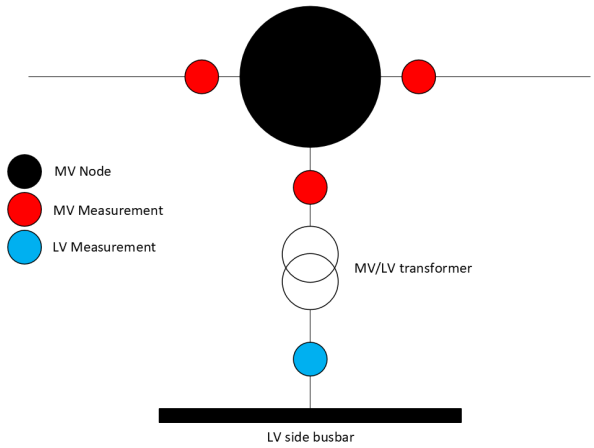

Figure 4.1: Possible locations for MV and LV measurements.

to subsection 2.3.2, PIMs can represent one of the outgoing lines. This measurement will not be included in further cases since Stedin's current Medium Voltage Measurement Units (MVMU) do not support it.

The accuracy of the measurement is essential as it influences the error of the state estimator. In subsection 4.5.4, the process from accuracy to an accompanying standard deviation will be explained. The same relative standard deviation must be applied to a measurement pair in simulations, as both values originate from the same instrument.

Stedin has implemented the ComPass B 2.0 for the MV side, a directional short-circuit and earth fault indicator with high-precision monitoring capabilities [65]. This device integrates with SCADA and provides current, voltage, and power measurements. Current measurement errors range between 0.5% and 5%, while voltage measurements maintain a maximum error of 0.5% if the voltage remains within 80–120% of V_{nom}. A generalised accuracy of 5% for P and Q and 0.5% for V magnitude is assumed for the MVMU to ensure robustness while reflecting worst-case conditions.

Due to outdated equipment, MVMUs are not feasible in all substations. Therefore, measurement devices should be installed immediately whenever a substation is revised, built or upgraded to up-to-date equipment, as the additional cost is relatively low.

4.2.2. LV Measurements

The blue circle in Figure 4.1 indicates the LV side measurement, which provides P, Q and voltage magnitude values. While P and Q are reliable, the voltage magnitude requires a conversion step. Accurate MV-side voltage values depend on knowing the transformer's tap position. However, tap positions are often not accurately recorded in practice, making the voltage measurement unreliable. This research generalises this limitation to all cases.

LV side measurements are less costly as they require less specialist equipment due to their operation at a lower voltage level. They can be used as bus PIMs, offering the same advantages as those described in subsection 4.2.1.

The importance of accuracy applies here, just as it does for MV measurements. The same relative standard deviation must be applied to a measurement pair in simulations, as both values originate from the same instrument. Stedin plans to adapt the so-called DA3-box to perform LV-side measurements. The device for processing these measurements is the Mikronika MEM-102 [66]. In-house testing has shown that its accuracy ranges between 3% and 5%. For this research, the maximum error of actual LV-side PIMs is assumed to be 5%.

4.2.3. Pseudo Measurements

Pseudo-measurements contribute to observability in the same way as LV measurements. However, since they are essentially estimates or approximations, they tend to be less accurate, potentially reducing the overall accuracy of the state estimation. Their main advantage is their low cost, as they do not require

physical measurement equipment, making them a preferred option in case of budget constraints.

In DSO terminology, pseudo-measurements are referred to as profiles. Due to privacy restrictions, DSOs usually cannot access detailed individual consumption data. Therefore, they create profiles to estimate electricity usage at a given historical moment. These profiles are created based on variables such as solar panels or electric cars. The aggregated consumption can be divided over this profile to get the load. This allows the load on an MV/LV transformer to be estimated by aggregating the consumption of all customers connected to it. While the aggregated load tends not to shift significantly from year to year, it can change noticeably over more extended periods [67].

While most profiles are reasonably accurate, errors can arise due to outdated network topologies or incorrect data allocation. These inaccuracies make it difficult to determine for which nodes larger errors occur. Consequently, all pseudo-measurements will be considered uniform, with a maximum error of 50% at first, based on [36], [59].

Stedin profiles can differ widely in accuracy. Their accuracy is verified by comparing the profiles with temporary measurement data of the identical network element. Of this research, 48% of the profiles fell in a ±10% margin [68]. However, which network elements are associated with the inaccurate profiles remains uncertain if untested.

4.3. Standards for Placement

Following Stedin's standard, the main substation will always be fully measured. To ensure only single-line non-measured radial feeders occur, every node with more than one outgoing line should also be fully measured. This process is illustrated in Figure 4.2. The next step is to make these single-line unmeasured radial feeders observable by implementing measurements. All lines in the network must be measured for full observability, thereby creating a spanning tree of full rank, as explained in subsection 2.3.2. As discussed in section 4.2, three measurements can be implemented to achieve this goal: MV, LV and pseudo measurements.

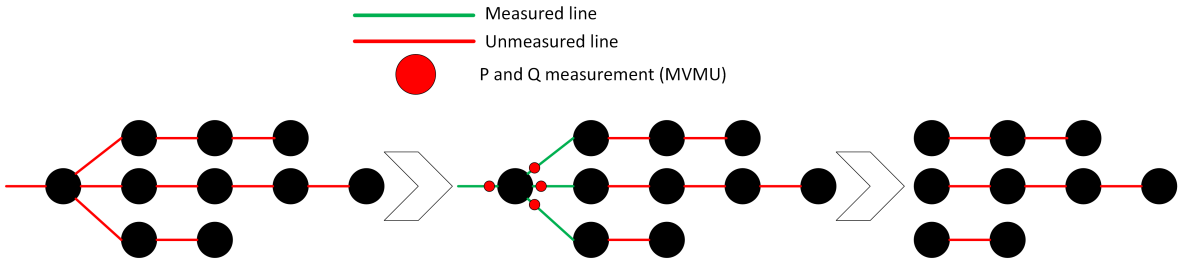

Figure 4.2: Transformation of a network into single-line non-measured radial feeders through the addition of MVMUs.

4.3.1. Power Injection Measurement Implementation

To illustrate the possibilities of PIM placement, an example uses a four-node unmeasured radial MV feeder, of which the loads are not drawn, shown in Figure 4.3. As discussed in subsection 2.3.2, PIMs, which are taken at the LV side, can serve as line measurements for one of the lines on the MV side connected to the bus of the PIM. For instance, a PIM measurement at node 1 can only be used as a line 1-2 measurement, whereas an LV measurement at node 2 can provide data for lines 1-2 or 2-3.

Following this logic, placing PIMs at nodes 1, 2, and 3 would ensure an observable network. However, alternative configurations are possible. Table Figure 4.1 outlines all valid measurement placement options for this example. As shown, leaving one node in the feeder unmeasured is possible while maintaining network observability. If more than one node cannot be measured due to technical constraints, MVMUs must be added to ensure observability.

4.3.2. Medium Voltage Measurement Unit Implementation

MVMUs should be placed at nodes with the most unmeasured lines available for the most efficient deployment. For a radial feeder without branches, this excludes the two outermost nodes. A single PIM is required to minimise the number of measurements in unmeasured radial feeders with an even number

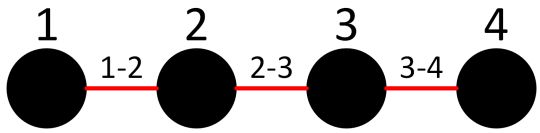

Figure 4.3: Four-node unmeasured radial MV feeder.

PIM Measurement Placement
1, 2, 3
1, 2, 4
1, 3, 4
2, 3, 4

Table 4.1: Possibilities with PIM measurements.

of nodes. Otherwise, an MVMU must be placed, resulting in one line receiving double measurements, which is inefficient and more expensive.

The possible measurement configurations for Figure 4.3 are summarised in Table 4.2. Observability is achieved most efficiently for unmeasured radial feeders with an odd number of nodes by placing measurements at every other node, beginning at the second node. For example, in Figure 4.4, the most strategic placement is at the second and fourth nodes. This setup ensures that lines 1-2, 2-3, 3-4, and 4-5 are measured, achieving network observability with minimal measurement deployment.

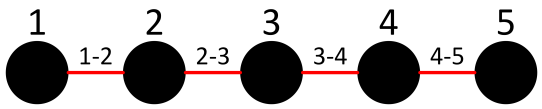

Figure 4.4: Five-node unmeasured radial MV feeder.

	MVMU Placement
4 node feeder	MVMU: 2 PIM: 3
	MVMU: 2 PIM: 4
	MVMU: 3 PIM: 1
	MVMU: 3 PIM: 2
5 node feeder	MVMU: 2, 4

Table 4.2: Possibilities with MVMUs.

4.4. Network Changes

Network topologies can change due to risks such as cable and transformer overloading. To mitigate this, DSOs adjust the network topology to distribute the load more efficiently. When placing measurements, these potential topology changes should be considered to ensure the network remains observable even after adjustments.

If PIMs are used, all nodes connected to a line with a switch or breaker should be measured to maintain observability. The logic described in subsection 4.3.1 for minimum observability no longer holds. One of the nodes in the radial feeders that did not require measurements now has to be measured to retain observability during a topology change. The leftover unmeasured node cannot be connected to a line with a switch or breaker. Instead, it must be connected only to lines that will always remain online.

For MVMUs, the most effective approach is to consider offline lines as if they were online. This method creates a larger unmeasured feeder that can be equipped with measurements. The network remains observable even after topology changes if these measurements are placed according to the steps in subsection 4.3.2.

A part of the network deemed 'observable' should be reviewed to verify that it meets the necessary conditions for power injection and MV-side measurement placement, as this may not always be true.

4.5. General Workflow

A general workflow can be followed to test a placement strategy to get an image of what this placement strategy did to improve the accuracy of state estimation. This can be applied to each network, but it should be tailored for its exact purpose. The workflow can be summarised in seven steps, shown in Figure 4.5 where green boxes are choices to be made by the DSO. The steps will be explained in more detail in sections 4.5.1 to 4.5.7.

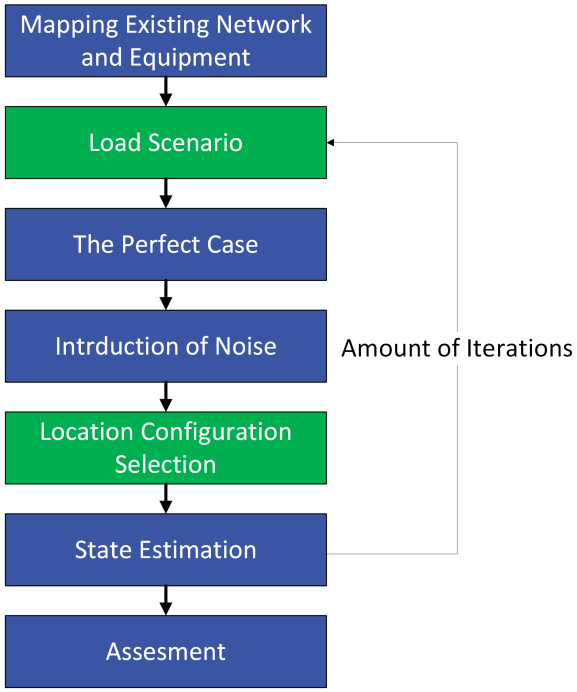

Figure 4.5: General workflow for assessing a placement strategy.

4.5.1. Mapping Existing Network and Equipment

Before designing the measurement placement strategy, it is essential to fully understand the network and its components. DSOs typically use specialised programs to establish the standard network topology for a given area. Once the nodes, lines, and transformers are mapped, the MV network should be prepared to include only MV components by eliminating all unnecessary elements, such as transformers.

Additionally, network components such as switches and existing equipment must be identified. Existing measurement devices are crucial, as they can be integrated into the state estimator, reducing the need for additional equipment. Identifying potential distributed generation sources is also vital. DG can introduce errors in the state estimation process and must be accurately represented. In the next step, DG is modelled as a negative load to ensure proper integration into the network analysis.

For a smooth process, it is advised to realise the network topology in the same programme that will later be used to run the estate estimator. This will minimise the change in conversion errors.

4.5.2. Load Scenario

The realised network topology is taken for the network that will be studied. First, loads need to be designated to their corresponding nodes. These loads can be generated randomly, creating various possible network situations. This choice ensures the network is tested in multiple scenarios, as load is not fixed in real life. The downside is that it introduces another variable, making it harder to find solutions to solve the inaccuracies in a network, and the tests are inconsistent. It can be used to find the general effect of a measurement.

Another option is to create scenarios that reflect situations a DSO may encounter in practice, mirroring real-life conditions. Depending on load levels or measurement placements, these tests provide insights into how specific nodes behave. Ideally, a DSO should base its strategy on a general case representing typical, everyday consumption patterns. The resulting state estimation will likely perform optimally under normal operating conditions by placing measurements according to this representative scenario. Other scenarios can be created to test the measurement placement strategy under more severe conditions.

4.5.3. The Perfect Case

To ensure meaningful comparisons of state estimation results, a reference ”perfect case” must be established, i.e., a scenario in which all actual values are known. To achieve this ”perfect case”, a power flow analysis is conducted, producing the true state values of the network under study. These represent the ”perfect case” network conditions. In practice, however, measurement equipment introduces imperfections, meaning real-world data deviates from these ideal values.

4.5.4. Introduction of Noise

Measurement equipment corrupts the ”perfect case” states, so noise must be applied to simulate real-life Supervisory Control and Data Acquisition (SCADA) results.

As with most equipment, the accuracy is known, not the standard deviation, so the accuracy needs to be converted to a standard deviation to fit in the PandaPower formatting. Measurement errors are expected to follow a Gaussian distribution [69], as illustrated in Figure 4.6. Based on this distribution, 99.7% of all measurements should fall within $\pm 3\sigma$, where σ represents the standard deviation. For simplicity, it is assumed that 100% of measurement errors fall within this range, meaning the maximum error equals three standard deviations. This results in Equation 4.1, where %max.error represents the accuracy of the measurement equipment used in the network. The measurement input for calculating the standard deviation can be P, Q or voltage magnitude.

If the noise for active power is determined by applying a random variation based on the standard deviation, the noise for reactive power is calculated relative to P using Equation 4.2, as both values originate from the same measurement device and are likely to be affected by similar errors. Determining the noise added to the V magnitude measurement goes through the same process as that for P.

This approach ensures that simulated SCADA data accurately reflects real-world measurement variations while maintaining consistency in error modelling.

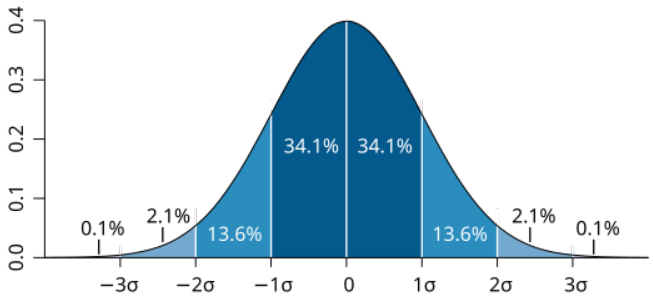

Figure 4.6: Normal distribution [70].

$$\sigma = \frac{\%max.error * Measurement\ input}{3} \tag{4.1}$$

$$noise.Q = real.Q * \frac{noise.P}{real.P} \tag{4.2}$$

4.5.5. Location Configuration Selection

PIMs, MVMUs, and pseudo-measurements are initially produced for all nodes and lines. This setup allows for a selective approach in determining which measurements will be utilised. Measurement selection is done manually, with the location and measurement type chosen from the complete list, which includes added noise. The specific locations selected for study are chosen with deliberate reasoning. Different types of measurements, as outlined in section 4.2, may be used individually or in combination. Since this thesis investigates the effect of measurement placement, multiple configurations will be tested to evaluate their impact. Based on observed effects, assumptions will be formed and incorporated into subsequent configurations. In this iterative manner, the research aims to identify strategic measurement placements that improve state estimation accuracy. If no strategic placement emerges, the study will focus on nodes with the highest estimation error from the initial baseline configuration.

The accuracy of these measurements can vary depending on the equipment used for actual measurements and the algorithms applied to generate pseudo-measurements. If the measurement selection is made correctly, the result should be a functional state estimator. However, additional measurements must be incorporated to achieve observability if the state estimator fails to operate effectively, indicating that the network is unobservable.

4.5.6. State Estimation

The non-linear WLS state estimation is used to obtain results as explained in subsection 2.2.2. This approach is necessary because the relationship between state variables and measurement equations is inherently nonlinear.

In transmission networks, a simplification of a linear model is sometimes possible. However, this is not feasible due to the distribution networks' relatively low X/R ratio. While linear state estimation is often preferred for speed, it is less accurate. Since one of the objectives is to evaluate the accuracy of the state estimator, the non-linear approach is the better choice as it provides more precise results. The additional computational time is not a concern in this case, as the estimation is performed during the design phase, which is not subject to real-time constraints. The non-linear WLS state estimation is run from a flat start, i.e. initial voltage and angles will be set at 1 p.u. and zero degrees, respectively. The state estimator gives all the network's variables, which can be used for multiple applications depending on what the DSO finds essential.

All calculations will be performed using PandaPower in Python, executed within the Spyder IDE [33].

4.5.7. Assessment

After obtaining the state estimation results, the effectiveness of the measurement placement can be evaluated. To assess the state estimation error, Equation 4.3 is used, showing the error percentage for all buses in the network, where X can be any state. These results show how adjustments can be made by adding or replacing measurements. For example, a pseudo measurement could replace an LV measurement if the error is significantly below the threshold. At the same time, pseudo-measurements could be replaced with more accurate alternatives if errors remain too high.

New measurements can be placed purely based on error values, but other factors should also be considered. Additional measurements may not be justified if the error is high at a low-impact load. The most strategic locations for extra measurements are industrial loads and distributed generation sites, which exhibit the most unpredictable load and generation patterns and locations that, on average, experience high loads [71], [72].

$$\epsilon_{i,j\ (SE)}(\%) = \frac{X_{i,j\ (SE)} - X_{j\ (true)}}{X_{j\ (true)}} * 100, \quad \text{where } i = \text{iteration, } j = \text{node} \tag{4.3}$$

Since the results depend on the initial load assignments and numerous load scenarios are possible in a network, two networks will be analysed. The first will have randomised load values for each iteration, analysing the measurement impact without a load preference. The second will work with a standard load scenario and numerous iterations. These results can be more dependent on the reload scenario chosen. The measurement setup from the second network will undergo a sensitivity analysis in two different load scenarios to see the impact of this change. Averaging the percentage errors per node across these iterations, as shown in Equation 4.4, can provide a more comprehensive understanding of the state estimator's overall performance, identifying nodes where performance is consistently firm or weak.

$$absolute\ mean\ \epsilon_j(\%) = \frac{\sum_1^i |\epsilon_{i,j\ (SE)}|}{i}, \quad \text{where } i = \text{iteration, } j = \text{node} \tag{4.4}$$

Outliers can heavily influence the mean, which is acceptable for illustrating the effect of measurements in network 1. For the second network, results will be presented using boxplots, where the median is represented by a line and the mean by a plus symbol (+), providing a more comprehensive overview.

5

Case Study: Network 1

This chapter utilises the simulation methodology designed in chapter 4 to evaluate the accuracy of the state estimation process for a network with a specific measurement placement. All simulations are conducted in the Spyder IDE, utilising Python and the PandaPower package for WLS state estimation. The network has a mean X/R value of 0.82, making linear state estimation inexact. An overview of Network 1 is shown in Figure 5.1.

A generation source is added at node 5 in the network for further simulations. This setup allows for assessing state estimation performance under realistic conditions, considering the impact of distributed generation on the network's observability and accuracy. One of the objectives of this research is to provide recommendations for preparing the network for distributed generation with volatile generation patterns. Ensuring observability will also be addressed in this case.

All existing measurement equipment will be removed from the network, except for the standard measurements present in the primary substation. This creates a "clean slate" that allows for testing the impact of measurements without interference from existing measurements. As a result, observations can be directly attributed to the placed measurements.

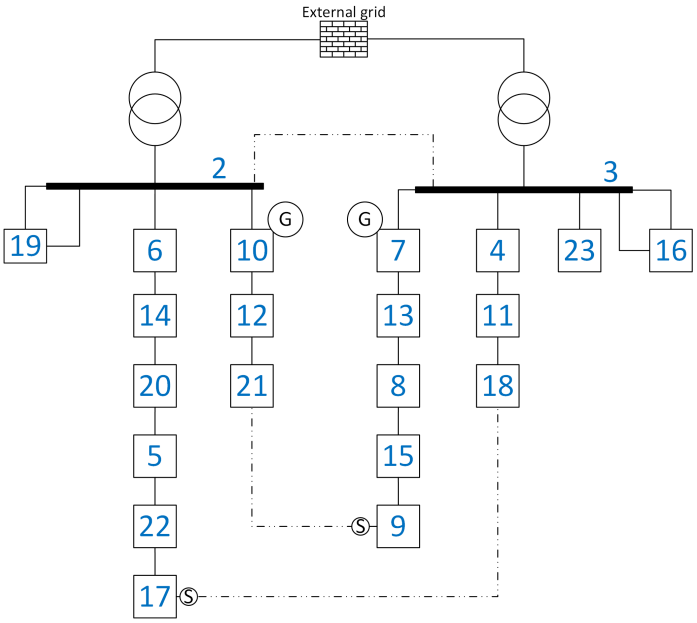

Figure 5.1: Topology formation of network 1.

5.1. Workflow Related to Network 1

The general workflow shown in Figure 4.5 for analysing strategic measurement placement is adapted for use on network 1. The adaptations in the workflow are the following:

1. *Mapping Existing Network and Equipment*

   Initialising network from company files to a PandaPower network. All unnecessary components are removed from the network, leaving only MV components and the transformers connecting to the external grid. Existing measurements are removed except the standard measurements done by Stedin in the primary substation.

2. *Load Scenario*

   The load is generated randomly over 50 iterations for the case study of network 1. In this way, multiple load scenarios are considered, and the load will have less effect on the result. The iteration number was chosen so that there were enough iterations so that a certain iteration did not play a big enough role, and to keep the number of iterations low regarding speed. More iterations will not lead to convergence due to the random generation in each iteration.

5. *Location Configuration Selection*

   The locations are selected purely based on reasoning, as this case study aims to demonstrate the effect of a specific measurement on its corresponding feeder and the wider network. This approach is intended to enhance understanding for future decision making. A more detailed explanation of the reasoning will be provided for each case.

7. *Assessment*

   Once all iterations are completed and the state estimation results are collected, they will be compared to the ”perfect case” values for each respective node. This case study focuses on the absolute mean error, as defined in Equation 4.4. The absolute mean error for each node will be visualised in a bar plot to allow for easy comparison across all feeder nodes.

5.2. Network Conditions

The network must first be constructed to generate perfect values. This research uses Stedin's code to convert BM-GIS files into a PandaPower network. The initial network includes buses, loads, external grids, lines, and transformer elements. It is then refined by removing irrelevant components and retaining only key elements of interest. These include all MV nodes and lines, two HV/MV transformers and two buses that connect the transformers to the external grid to model it as one network. The external grid voltages are set to 1.00 vm_pu.

Next, loads are assigned to all nodes except nodes 0, 1, 2 and 3, as these either represent the external grid or function as slack buses. The assigned loads are randomly generated between 0.5 MW and 5 MW for most nodes. However, for nodes 5, 7 and 11, where generation occurs, the randomly generated loads range from -5 MW to -0.5 MW. The same range, but negative, is chosen for the loads as the error can depend on the magnitude of the load. The power factor for this Stedin distribution system is assumed to be 0.95 [73]. Finally, a power flow analysis is executed to create all baseline voltage and power values within the network, serving as the reference dataset for evaluating state estimation accuracy.

Since nodes 2, 3, 16, 19 and 23 are fully measured, no additional measurements will be placed there. This principle applies to all cases performed for this network.

5.3. Effect State Estimation

Currently, pseudo-measurements are primarily used to predict future loads in the network. However, they can also be integrated with Stedin's standard measurements,i.e. all substations receive a pseudo measurement regarding state estimation. In this case, state estimation could be used for real-time load prediction. As shown in Table 5.1, using active state estimation instead of profiles (pseudo-measurements) improves accuracy, reducing the average error from 11.5% to 8.1%.

Index node	Real active load (MW)	Error of created noise in measurements (%)	Error of state estimation (%)
4	3.835	11.003	0.448
5	−7.807	−26.287	−17.085
6	4.836	8.646	−3.832
7	−3.855	−0.026	4.628
8	1.849	21.037	17.520
9	2.928	−3.837	−7.434
10	−4.800	31.385	5.419
11	1.137	−0.898	−3.420
12	4.993	−7.370	6.133
13	3.562	−6.268	−10.119
14	3.331	−18.913	−23.703
15	2.888	23.507	17.703
16	0.661	1.389	−0.884
17	3.053	−2.388	−8.846
18	1.349	−4.850	−7.661
19	1.803	−33.719	0.589
20	1.174	5.901	3.026
21	1.659	−7.882	−3.440
22	1.959	−15.139	−18.263
23	3.976	1.321	1.867
Absolute total	X	231.766	162.019

Table 5.1: Comparison created measurements with noise before and after state estimation.

5.4. Empty Network Cases

The network's topology from Figure 5.1 was created as a PandaPower network from a BM-GIS file using a Python algorithm developed within Stedin. In these cases, the network will be stripped of all existing measurements except those at the Slack buses, nodes 2 and 3, as those are always present in a Stedin network. This allows for a better analysis of the implications of specific measurement placements, as no other factors interfere with the results once they are removed.

The scanned network is shown in Figure 5.2, where red lines represent unmeasured sections and green lines indicate measured ones. Although the network appears to consist of two separate systems due to the omission of the open switch line in Figure 5.2, it is technically a single network. In practice, however, it operates as two individual networks. Nodes 2 and 3 are slack buses, so they have no loads. According to the theory explained in subsection 2.3.2, the network remains unobservable until all lines or branches are measured. Each case begins with a baseline reference where pseudo measurements are placed at all nodes, except for nodes 2, 3, 16, 19, and 23, as these are already fully measured by the standard measurements on the slack buses at nodes 2 and 3. This baseline configuration is the first configuration in all cases unless stated otherwise.

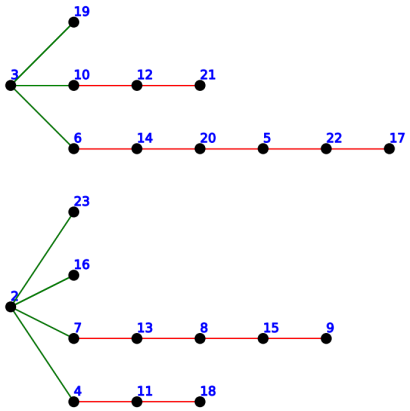

Figure 5.2: Empty network 1 including standard measurements.

5.4.1. Case 1: Only Pseudo Measurements

Pseudo-measurements are the most cost-effective option, as they can be constructed. This case explores whether a minimalistic use of pseudo-measurements, including them only to reach observability, is beneficial. While potentially reducing computational effort, albeit only marginally, it could significantly affect accuracy. This simulation was performed with randomised loads, and the absolute mean error (Equation 4.4) was taken over 50 iterations.

Figure 5.3 illustrates 4 different configurations. The second, third, and fourth configurations minimise the measurements by removing a pseudo measurement from a radial feeder, only at feeders longer than one node. The exact nodes containing pseudo-measurements are displayed in Table 5.2.

Configuration	**Nodes**			
2	10, 12	6, 14, 20, 5, 22	7, 13, 8, 15	4, 11
3	12, 21	14, 20, 5, 22, 17	13, 8, 15, 9	11, 18
4	10, 21	6, 14, 20, 22, 17	7, 13, 15, 9	4, 18

Table 5.2: Nodes with pseudo-measurements per configuration for case 1.

The first configuration has a better state estimation accuracy for all nodes. A key observation is that omitting a pseudo-measurement from a single node significantly worsens state estimator results, even affecting the accuracy of other nodes within the exact radial feeder due to the loss of comparative data. When only the minimum number of measurements required for observability is available, the state estimator lacks the redundancy needed to validate and compare data. As a result, it must assume missing values based solely on the total measured power flow in the feeder, subtracting all available pseudo-measurements. This leads to higher estimation errors.

Since pseudo-measurements are almost always available, they should be placed on all unmeasured nodes when no other measurements exist. This shall ensure the best results for a state estimator based on pseudo measurements and ensure observability.

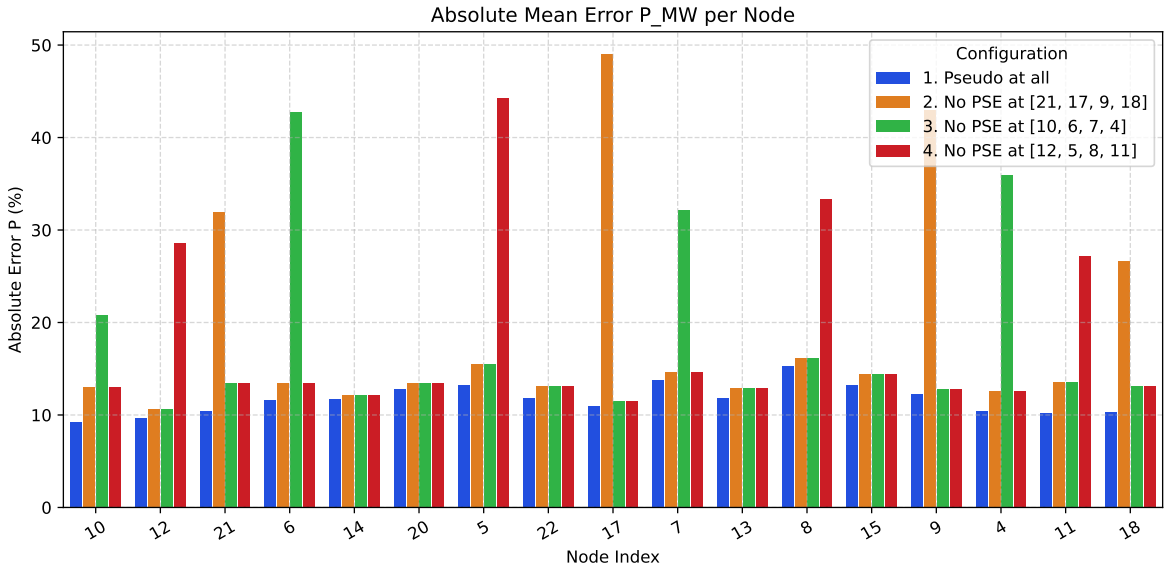

Figure 5.3: Configurations with only pseudo-measurements where one pseudo measurement is taken away per feeder on a different location for configurations 2, 3 and 4.

5.4.2. Case 2: Influence of Power Injection Measurements

Using only pseudo-measurements does not provide an adequately functioning state estimator, as shown in Figure 5.4. PIMs with higher precision are introduced to study the improvements in accuracy. When placing PIMs, pseudo-measurements are removed unless stated otherwise. This simulation was performed with randomised loads, and the absolute mean error was taken over 50 iterations.

Figure 5.4 illustrates four different configurations. In the second configuration, PIMs are placed at the short radial feeders, starting with nodes 10 and 4. This significantly reduces the absolute mean error at those locations, but the influence on nodes outside their respective feeders is negligible. This is likely because the improved accuracy only enhances the estimation of the total power consumption within those specific feeders. For feeders that rely solely on pseudo-measurements, the total power consumed is still determined by other measurements. Although PIMs in one feeder could theoretically improve the accuracy of MVMUs at the beginning of different feeders, this effect is relatively small. The improvement in accuracy becomes further diluted when distributed across all nodes in a feeder.

The third configuration explores placing a single PIM on each long radial feeder, starting at nodes 6 or 7. This placement positively impacts the entire feeder by improving the accuracy for most nodes. Although a slight increase in error may occur infrequently at nodes, the overall effect remains beneficial. The observed improvement is primarily due to the reduction in uncertainty across the entire feeder, which enhances the state estimation along its length.

In the fourth scenario, pseudo-measurements are retained when PIMs are placed to asses whether these measurements would conflict and whether pseudo-measurement, being less accurate, should be removed. Figure 5.4 shows that using both measurements at the same location leads to significant errors. This occurs because PandaPower struggles to process both measurement types correctly. Therefore, pseudo-measurements should be permanently removed when PIMs are placed at a specific location to ensure accurate state estimation.

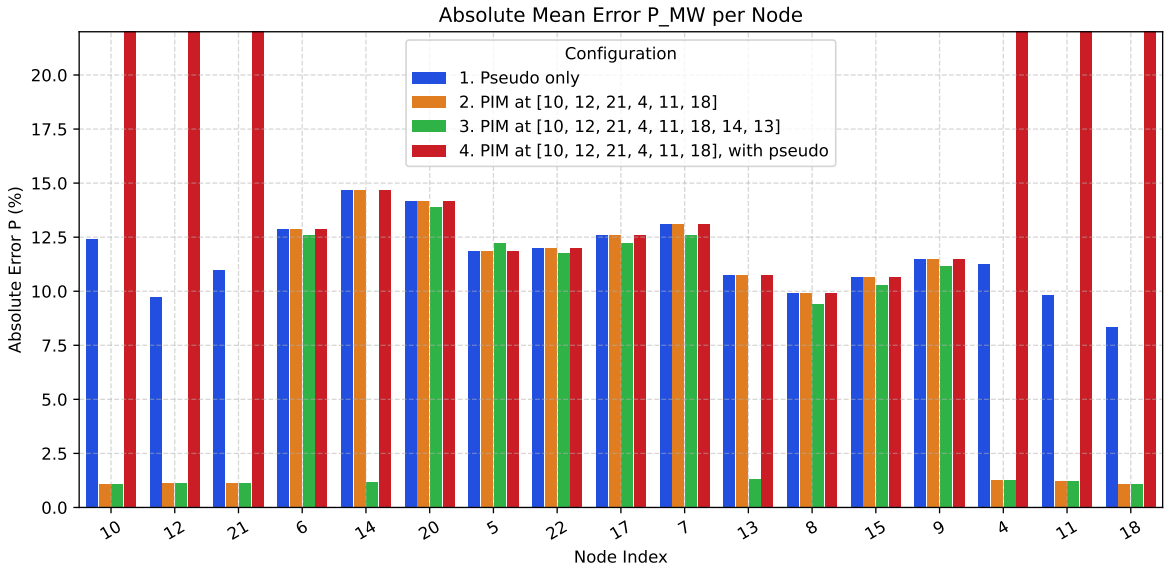

Figure 5.4: Effect PIM measurements on nodes.

5.4.3. Case 3: PIM placement ratio

From subsection 5.4.2, it is evident that PIM measurements only influence the radial feeder they are a part of. Now, it is essential to quantify the effect of the ratio of PIMs against pseudo measurements. This will be done by adjusting the number of measurements per configuration. The focus will be on the feeders, starting with nodes 6, 7, and 4, with six, five, and three unmeasured nodes, respectively. Figure 5.5 illustrates the five different configurations. This simulation was performed with randomised loads, and the absolute mean error was taken over 50 iterations.

The second configuration starts with two PIMs placed from the starting node. Each configuration from here adds one more measurement per configuration. A clear pattern emerges that with the addition of PIM, the overall error decreases. The jump is significant at the spot of the PIM placement as the accuracy of the measurement is much larger, but only slightly for nodes that are measured with pseudo measurements. If state estimation with high accuracy is preferred, only one node can be left unmeasured or multiple if their accuracy is not essential.

The inaccuracy of the nodes with the pseudo measurements comes down to the total uncertainty of that feeder. At the beginning of the unmeasured feeder, the line measurement will give the range in which the sum of all nodes most probable will be. The more accurate measurements are taken, the smaller the range becomes for the remaining nodes with pseudo measurements. As the pseudo measurements (lowest weight in WLS) will be corrected the most, it is better to measure nodes with low loads. This is confirmed in Figure 5.6. For this confirmation, the loads on nodes [4, 11, 18] were 1, 1, and 8 MW, respectively. Three configurations were used, with the pseudo measurement on a different node each time. The second configuration had the pseudo measurement on node 18 with the highest load. The overall error was the lowest for this configuration, even having a mean lower than 2.5% over 50 iterations.

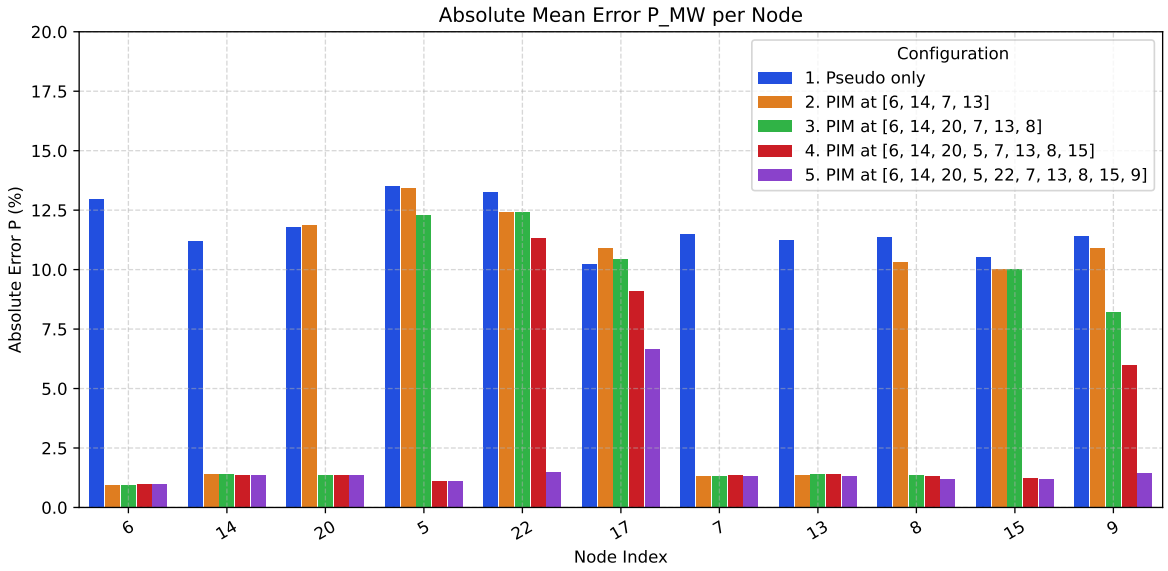

Figure 5.5: Effect of increasing the PIM ratio on accuracy of non measured nodes.

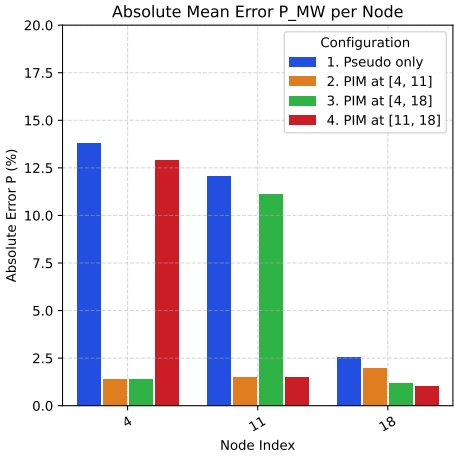

Figure 5.6: Difference in accuracy of unmeasured node with PIM placed on nodes with a high or low load.

5.4.4. Case 4: Influence spacing of PIMs

In literature [34], it was recommended to have loads of equal magnitude between actual measurements, as the state estimator would work best in that case. This drives the question of whether a homogenous spread of PIM would obtain the best results. However, note that as the loads are randomly generated for these configurations, the load will probably never be of equal magnitude. In Figure 5.7, two configurations are illustrated next to the pseudo-only baseline. Both configurations have three measurements for the feeders starting with nodes 6 and 7, and 2 measurements for the feeder starting with node 4. In Configuration 2, the PIMs are all placed at the beginning of the feeder, whereas in Configuration 3, a more homogenous spread is chosen. In all feeders, two nodes are left unmeasured.

The homogeneous distribution of measurements did not lead to significantly different results. Among the comparable nodes, the homogeneous setup yielded better accuracy in two out of three cases, though this may be attributed to randomness in the load scenarios. Additionally, the feeders might be too short to observe the effects of different measurement spreads clearly. If this observation holds more broadly, DSOs would have greater flexibility in choosing measurement locations. They could prioritise nodes based on practical considerations, such as accessibility or cost, without accounting for whether

nearby nodes are already measured. This would simplify the planning process and potentially reduce implementation costs.

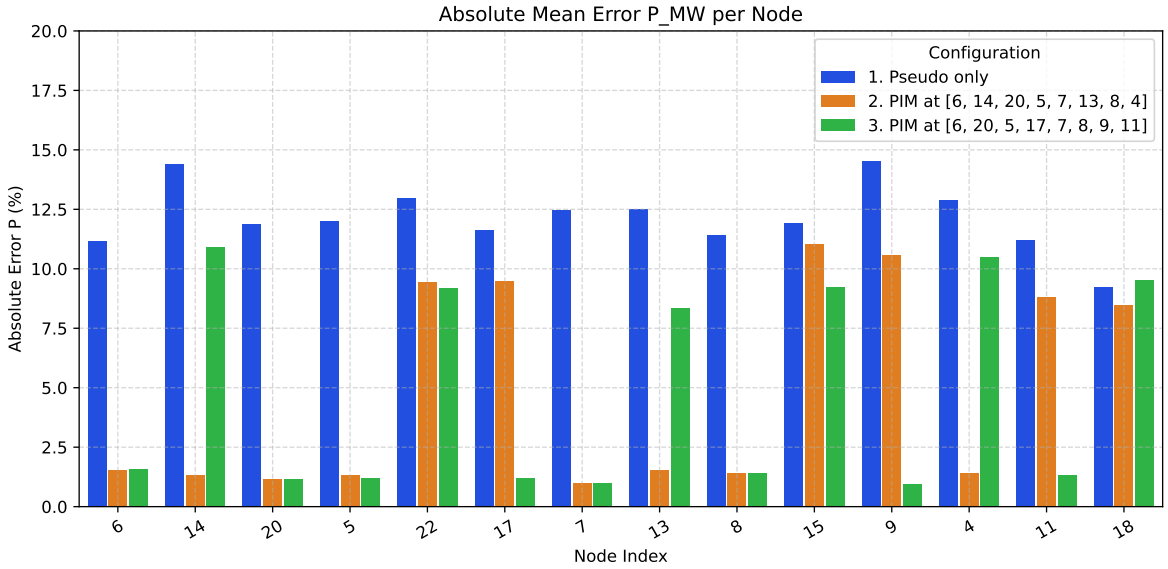

Figure 5.7: Influence of spacing PIMs homogenous throughout the feeder or concentrated at the beginning .

5.4.5. Case 5: Combination of MVMUs with Pseudo Measurements

In subsection 5.4.2, it was shown that PIM and pseudo measurements should not both be fed into a state estimator to achieve the best results. This case compares three approaches: using minimal MVMUs alone, minimal MVMUs with pseudo measurements everywhere except at the nodes where MVMUs are placed, and minimal MVMUs while keeping pseudo measurements at all nodes. These approaches correspond to the second, third, and fourth configurations.

Using pseudo measurements at all nodes resulted in the most accurate state estimation, as shown in Figure 5.8. Still, the difference with pseudo measurements everywhere except at the nodes where MVMUs are placed is minor. Pseudo-measurements should always be used with MVMUs if no PIMs are placed at any nodes, as the result is generally favourable.

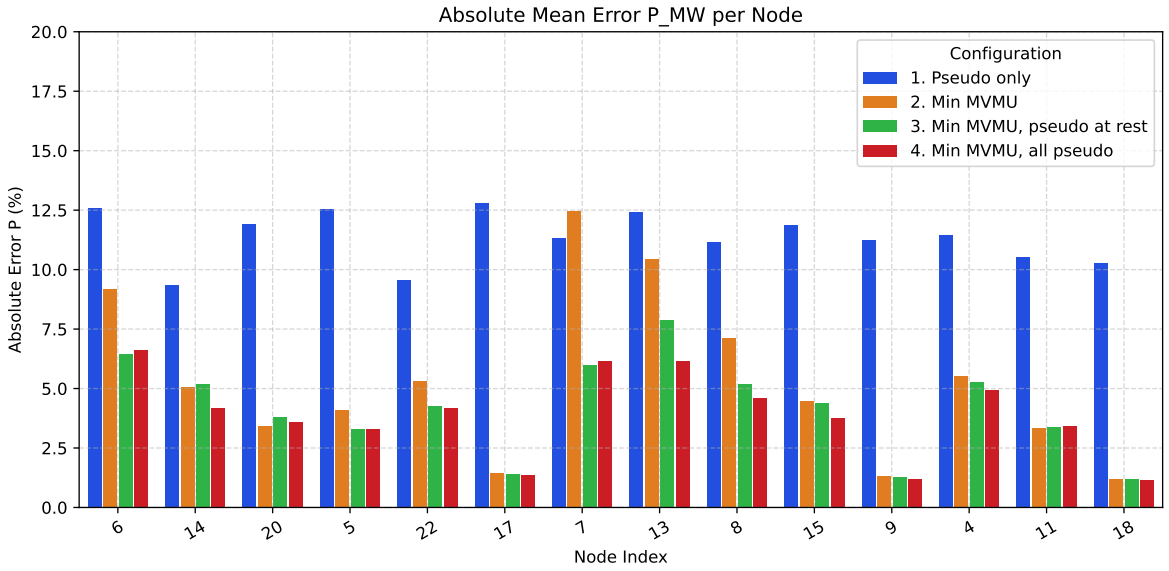

Figure 5.8: Combination of MVMUs and pseudo measurements.

5.4.6. Case 6: Reach of MV Measurement Units

To showcase the reach of an MVMU influence compared to that of a PIM, one MVMU and one PIM shall be placed at nodes 13 and 14 of the feeders, starting with nodes 6 and 7. As the MVMU consists of multiple measurements, it will probably result in a better estimate. This simulation was performed with randomised loads, and the absolute mean error was taken over 50 iterations.

The second scenario contains only PIM, and the third scenario only MVMU. It can be seen in Figure 5.9 that the placement of a PIM results in a better estimate at that specific node. The placement of an MVMU has an excellent effect on the node it is placed on and the node next to it at the end of the unmeasured feeder, nodes 6 and 7 in this case. It does not seem to affect the other nodes of the feeders much. A slight improvement can be observed as the room for error has been decreased by the placement of the MVMU.

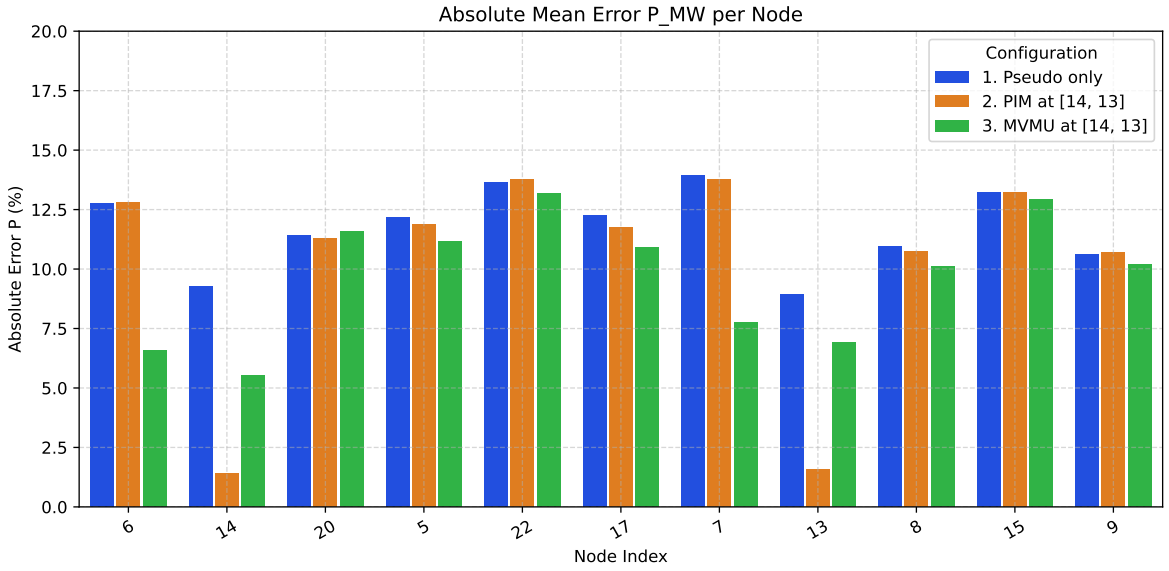

Figure 5.9: The effect of MVMU vs PIM for other nodes in the respective feeder.

5.4.7. Case 7: Influence of MV Measurement Unit placement

In this case, the influence of the MVMU's starting point is considered. The scenarios will take place on the feeder of node six and will each contain two measurements for a fair comparison. This simulation was performed with randomised loads, and the absolute mean error was taken over 50 iterations.

All scenarios in Figure 5.10 start at a different node and skip two subsequent nodes before placing another MVMU. The second configuration starts at node 6, the third at node 14 and the fourth at node 20. The most significant reduction of the absolute mean error concerning the baseline is obtained with the third configuration, as shown in Table 5.3. As discussed in subsection 5.4.2, the influence of measurements is negligible outside of their feeder, so these nodes are not shown. This result complies with the advice in subsection 4.3.2 to start at the second node for the most efficient MVMU placement.

Table 5.4 shows the same case but then performed on the feeder of node seven, and only one node is skipped before placing another MVMU. Again, the third configuration, which starts at the second node, has the best results.

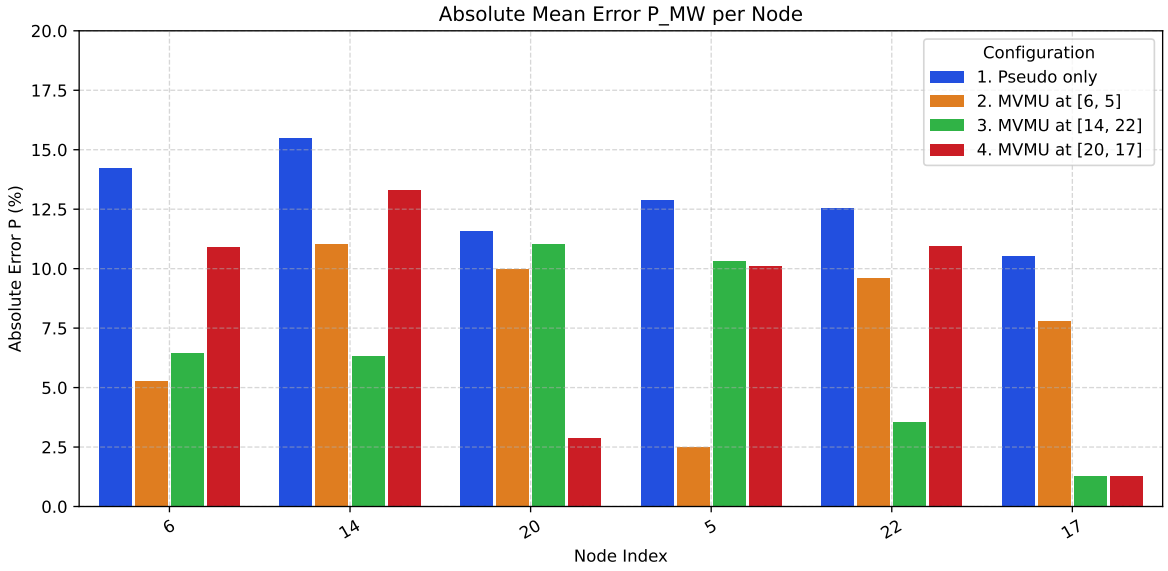

Figure 5.10: MVMUs placed at different locations in the feeder with a spacing of two nodes.

Index	6	14	20	5	22	17	Total
MVMU at [6, 5]	8.95	4.49	1.61	10.37	2.98	2.73	31.13
MVMU at [14, 22]	7.76	9.18	0.56	2.58	9.00	9.27	38.35
MVMU at [20, 17]	3.31	2.22	8.69	2.78	1.64	9.27	27.99

Table 5.3: Improvements of absolute mean error per node towards scenario blue.

Index	7	13	8	15	9	Total
MVMU at [7, 8]	5.68	5.76	6.37	2.90	4.32	25.09
MVMU at [13, 15]	4.75	6.89	6.17	6.99	11.41	36.18
MVMU at [8, 9]	1.27	2.06	6.09	8.30	11.47	29.19

Table 5.4: Improvements in absolute mean error to scenario blue at the feeder of node 7.

5.4.8. Case 8: Spacing of MV Measurement Units

The cases in subsection 5.4.6 and subsection 5.4.7 showed the reach towards PIM and the optimal starting point of MVMUs. This case shall showcase the effect of the spacing between two MVMUs. The starting point will be the second node of the unmeasured feeder as this gave the best results in subsection 5.4.7. From here, the space between MVMUs will be increased by one node in the following configuration, starting at a gap of one node. The fourth configuration showcases the effect of one MVMU on a three-node feeder. This simulation was performed with randomised loads, and the absolute mean error was taken over 50 iterations.

The second and third configurations in Figure 5.11a show one and two nodes spacing, respectively. Introducing one extra space between two MVMUs almost nullifies the effect the MVMUs had on the one node between them. A spacing of two nodes between MVMUs is, therefore, inefficient.

The fourth configuration is seen in Figure 5.11b, which shows that for short unmeasured feeders, one MVMU placement can substantially increase the accuracy for multiple unmeasured nodes. This only applies if one node on either side is without a PIM or MVMU.

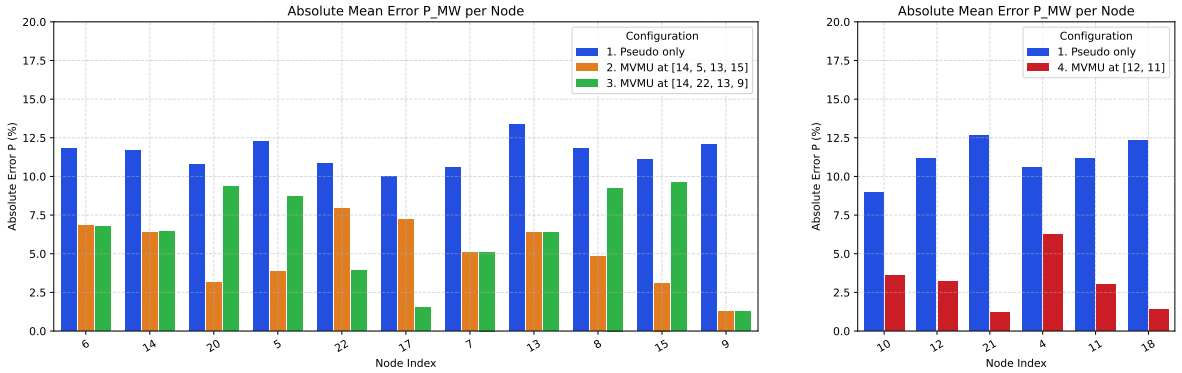

(a) Feeders of nodes 6 and 7.

(b) Feeders of nodes 10 and 4.

Figure 5.11: Influence of spacing between MVMUs for all feeders.

5.4.9. Case 9: Prevented Placement

DSOs might envision a scenario in which all LV sides of the MV network that can be measured are equipped with PIMs. However, in some cases, placing a PIM at a specific node may not be possible. It is essential to determine whether the number of installed measurements would still be sufficient for an adequate state estimator.

Figure 5.12 illustrates five configurations starting with the reference baseline applied to the radial feeder starting at node six. The second configuration examines the effect of removing one PIM. The third scenario further worsens the conditions by removing two PIMs. The fourth and fifth scenarios introduce an MVMU between the nodes where PIM placement was impossible, which was node 14 in this case, with each configuration testing a different placement position.

Examining the second and third configurations, it is clear that for each PIM lost in a feeder, the absolute mean error increases at all nodes without a PIM. Configurations four and five show that introducing an MVMU between the two unmeasurable nodes significantly improves accuracy for both unmeasured nodes. This effect is likely due to the MVMU effectively dividing the long radial feeder into two smaller sections, where the total power flow is known for each. As a result, only one unmeasurable node remains per section. Therefore, when more than two unmeasurable nodes are present in a feeder, placing an MVMU between them is advisable.

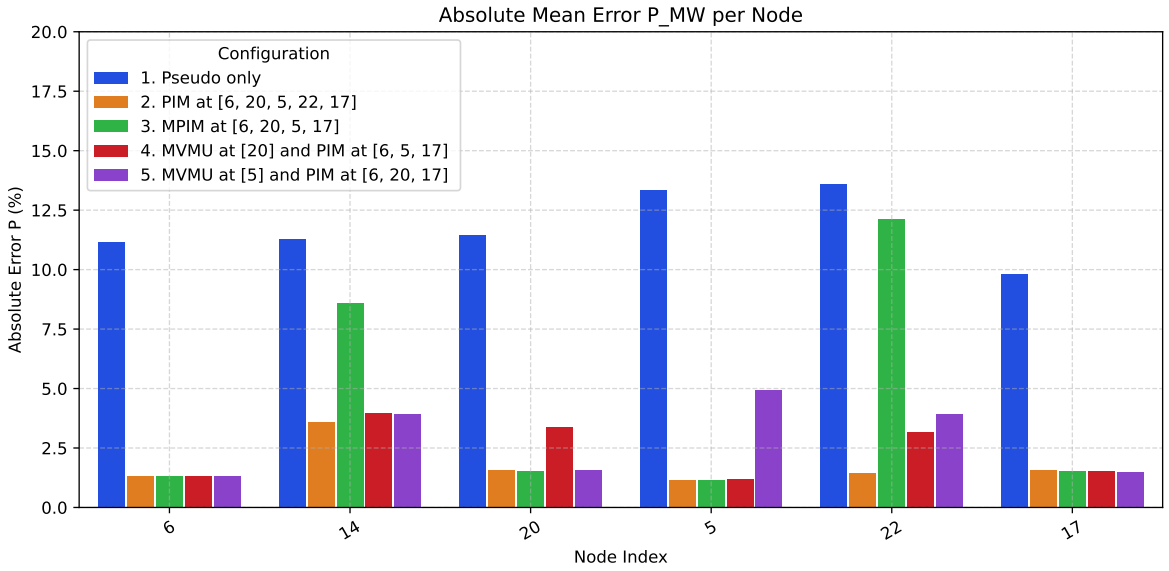

Figure 5.12: Possible configuration solutions in the case of prevented placement on certain nodes.

5.5. Results: Network 1

The case studies performed in section 5.4 provide information about the effect of pseudo measurements, PIMs and MVMUs on networks and, more specifically, within radial feeders. More significant inaccuracies were typically found at lower loads, i.e. the accuracy of a node was highly dependent on the load randomly generated for that node. That is why the resulting accuracies were not considered directly, but the effect shown when placing a measurement was analysed, making this part of the thesis a more heuristic approach. If a measurement placement is selected where the most significant inaccuracies are, the loads assigned to the nodes should mirror the real-life network. PIMs could be placed at all nodes using the method with randomised loads to acquire somewhat of the same improvement in accuracy. Actual network measurements are best placed at nodes with volatile behaviour, such as solar panel generation or industry nodes. In this way, only predictable loads remain, and the general maximum error of the pseudo measurements decreases, resulting in better overall state estimation.

However, some general results can be used to implement state estimation for DSOs. Firstly, pseudo measurements should always be placed on all nodes as a foundation. This will give better results than the minimum amount, as more reference points are provided for the state estimator to consider and will ensure observability. The exception is if a PIM is placed, then the pseudo measurement for that node should be deleted, or it will negatively affect the state estimation. This is not a problem for MVMU as it is a different type of measurement. As pseudo-measurements are relatively cheap to acquire for every node when enough data is available, this should not be a problem.

Secondly, placing measurements on a node only affects the state accuracies on the respective node's feeder. So, to decrease the inaccuracies of all nodes in the network, every radial feeder should have measurements. This is probably due to the number of measurements on the slack buses, which makes their states perfectly known, so uncertainties can only propagate within a feeder.

Thirdly, to get an adequate state estimation, a substantial number of the nodes on the radial feeders have to be covered with measurements and have a foundation of pseudo-measurements. Currently, with an accuracy of 50% for pseudo measurements, there can only be one node without an actual (MVMU/PIM) measurement between two MVMUs or on the whole feeder if there are only PIMs. Then, the state estimation's absolute mean error towards the 'perfect case' will be at its lowest while using the least amount of measurements possible within the accuracy standards. It is best to leave the node with the highest load unmeasured, as this results in the least error towards the 'perfect case' values for the nodes.

Lastly, a distinction between MVMUs and PIMs should be highlighted. PIMs are node-specific mea-

surements, which means they directly improve the accuracy of the targeted node. They also lead to a modest improvement in the accuracy of other nodes within the same feeder. This indirect benefit occurs because the total uncertainty across the feeder is slightly reduced. The change in accuracy is primarily positive but can be negative. MVMUs, as they are line measurements, have a good effect on the node it is placed around, but also impact the surrounding nodes. Especially when it singles out a node, for example, if the MVMU is placed on the second or second-to-last node of an unmeasured radial feeder, it will single out the first or last node, thereby measuring the power flow towards it. This property of MVMUs can also be used to divide a feeder into two parts, of which the total flow is measured. In this way, both sides can have one node without an actual measurement. It will still have a pseudo measurement. This is particularly handy if the placement of the measurement is prohibited due to physical building constraints.

These results have demonstrated how certain measurements can influence the state estimation accuracy of specific nodes or along a feeder. However, they do not yet provide a general solution to the problem. Therefore, a second case study will be conducted on Network 2 in Chapter 6 to reach a more general solution.

5.6. Discussion: Network 1

The results from chapter 5 are not very general for every case, as there are still many variables. This chapter describes what specific measurements do regarding accuracy and how they could be strategically implemented in certain conditions.

The main problem is the randomness of the loads and, thereby, the measurements and results. As the loads are randomly generated to represent the different situations that could occur in a network, the accuracy of the nodes is not stable. So, in this case, there were no specific nodes from which you could say that they were more accurate than others. This is simultaneously a problem with designing the network based on the accuracy of state estimation. To find the best locations for measurement placement, only one load scenario can be considered to see differences in the state estimation accuracy per node. However, this load scenario may not represent the network in real life, making the concluded measurement locations absolute.

The network also contains switches, which can change its whole topology. It is uncertain if topology changes significantly influence the network's accuracy. The topology of the used network is simple. Average MV distribution networks are more extensive and may have more complex topologies than radial designs. Some conclusions drawn from the results may be null and void when tested in these more comprehensive, complex networks, as different conditions may present themselves.

Networks often contain existing equipment that can be utilised for state estimation. However, in this study, such pre-installed measurements were deliberately excluded, as the focus was solely on evaluating the impact of strategically placed measurements. To ensure that the analysis was not influenced by existing infrastructure, a "clean slate" network model was used. In the actual design process for measurement placement, equipment that has already been installed should be considered to minimise costs and avoid unnecessary installations.

DSOs should also assess whether existing equipment can provide measurements, even if it is not currently used. Leveraging such capabilities can enhance the functionality of installed equipment without requiring additional investments. Additionally, DSOs must consider the feasibility of placing new measurements. Space limitations or other physical building constraints may restrict installation options. DSOs must either find alternative solutions or plan for necessary substation modifications.

The HV/MV transformer was included in the topology of this network, but measurements were only taken on the MV side. This approach was initially chosen to represent the complete network structure. However, aside from having the same external network, it did not fully achieve this goal. Since this level of modelling did not contribute meaningfully to the analysis, it will be excluded from future case studies.

6

Case Study: Network 2

This chapter will apply insights from the literature and chapter 5 to design measurement locations and types in a more extensive Stedin network. A generalised approach for measurement placement will be presented, considering key network design factors such as load magnitude, load volatility, and practical placement constraints. The significance of these factors will first be discussed, followed by an overview of their distribution within the network. A simple network graphic design is shown in Figure 6.1.

6.1. Workflow Related to Network 2

The general workflow shown in Figure 4.5 for analysing strategic measurement placement is adapted for use on network 2. The adaptations in the workflow are the following:

1. *Mapping Existing Network and Equipment*

   Initialising the network from the company files to a PandaPower network. All unnecessary components are removed from the network, leaving only MV components. Existing measurements are considered to simulate real-life conditions and decision-making for a DSO.

2. *Load Scenario*

   A single load scenario is used for most cases, representing a network snapshot at a specific moment. Load levels can influence the accuracy of certain nodes. At the end, the load scenario is changed to perform a sensitivity analysis and assess the robustness of the results.

5. *Location Configuration Selection*

   The measurement location will be chosen based on reasoning and accuracy factors. Certain network characteristics have presented more opportunities to test based on reason. When strategic points are determined, an effort will be made to fix the accuracy gap with placement targeting low-accuracy nodes to see if this is an effective strategy to tackle the problem.

7. *Assessment*

   Once all iterations are completed and the state estimation results are collected, they will be compared to each respective node's "perfect case" values. This case study focuses on the absolute values of all the results, looking not just at the mean but also the median, the outliers, and the error distribution, which are visualised in boxplots.

6.2. Network Design Factors

Current circumstances should influence the design process for measurement allocation. This section covers the most important factors that DSO and Stedin should consider when designing new measurement locations.

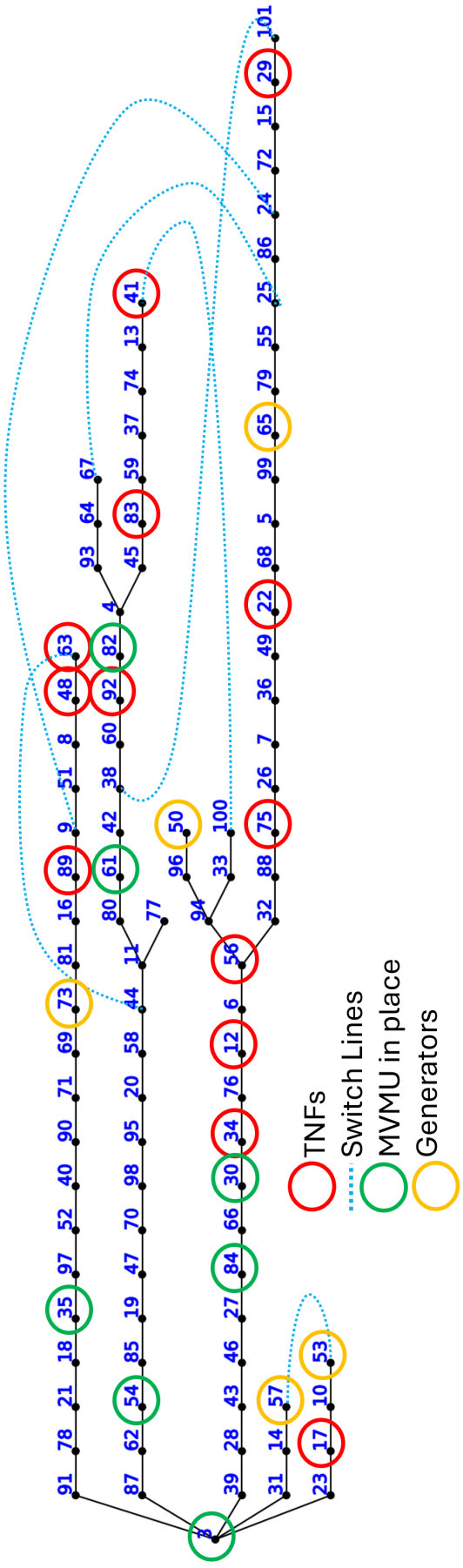

Figure 6.1: Existing network including all components.

6.2.1. Stedin's Vision

It is vital to consider Stedin's existing plans for their network to ensure that different policies do not conflict, allowing for a streamlined process within the company. In [74], Stedin Groep announced its plans to install 22.000 DA3 boxes as measurement equipment. These are primarily LV-side measurements but can also contribute to MV network observability. Given this, designing the network with power injection measurements may align best with Stedin's strategic goals.

6.2.2. Network Loads

Due to key aspects within the network, some locations are more likely to receive measurements. However, a measurement may not have the same effect in every location. Here are two examples of how the location or the load influence the effectiveness of the measurement.

When MVMUs are placed at the beginning of a feeder, it can result in higher errors in the power consumption of that node than placing it at the end of a feeder. This phenomenon occurs as the line measurements are relatively high towards the power consumption of that node. If, for example, an error occurs of just 0.5% in both line measurements in opposite directions that are 4.2 and 4 MW, the value chosen for power consumption by the state estimation will likely be around 0.241 MW instead of the exact value of 0.2 MW. So the 0.5% line power flow error introduces an error of 20.5% in the node's power consumption. Therefore, if MVMUs are placed at the beginning of feeders, the outgoing line to the load should also be measured.

This effect also occurs when using PIMs. Since the feeder's total load is known, the nodes' accumulation must be equal (minus losses). By accurately measuring smaller rather than larger loads, the possible error introduced in the summation remains smaller. The inaccurate measurements will be adjusted using state estimation to fit the total load of the feeder. However, this only works when all nodes except one have accurate measurements. When two or more nodes are not accurately measured, the error can still be introduced by one with a higher load than the actual load and the other with a lower load.

6.2.3. Network Details

Every Network has existing components and possible gaps in data. This test network was no exception; its details will be explained further to help you better understand the design choices.

Load Allotment

The test network is loaded from internal BM-GIS files and has predefined loads for most nodes. There are a few exceptions. According to the file, nodes 12 and 14 had a zero load, which is likely false, so it has to be changed. No node data was available for [10, 24, 28, 47, 74, 95]. This data was created by cross-checking in PowerFactory at a similar time on another day and comparing with one of the nodes next to the node with the most compatible information. In PowerFactory, no load existed for nodes 28 and 74, so their loads are set to 0.001 MW, so the state estimation keeps working as it can not process values too close to zero. According to PowerFactory, the power factor of the network is 0.98. This value is used in the simulations

Technically not Feasable

Real-life physical limitations can prevent the placement of measurement equipment in substations. Stedin experiences these TNF substations in around 15% of their MV substations [75]. For the test network, no data on TNFs was available. From the 98 substations, fifteen have been randomly selected to be such a TNF substation, resulting in prevented placement at substations [12, 17, 22, 29, 34, 41, 48, 56, 63, 75, 83, 89, 92, 97, 101].

Generation Measurements

In the Netherlands, all large energy producers on the MV network have to place metering devices and communicate this to their respective DSO under [76]. Following this, all places in the test network that have distribution according to their topology map will receive a PIM of the same accuracy explained in subsection 4.2.2.

Intellegent Fault Indicators

The existing intelligent fault detectors are assumed to function identically to the MVMUs discussed in subsection 4.2.1. Any MVMU placed within the network will be assigned the same accuracy as these

devices to maintain consistency.

Profile Accuracy
Pseudo measurements, also called profiles in Stedin terminology, can differ widely in accuracy. In subsection 4.2.3, it was discussed that 48% of the profiles fell in a ±10 margin [68]. Different levels of pseudo-measurement accuracy occur in a network, but which network elements are associated with the inaccurate profiles remains uncertain for untested networks. Therefore, they are generalised to all have the same maximum error.

6.2.4. Simulation Conditions

All measurements used for state estimation are generated in advance. One dataset includes all line and node power and voltage measurements with a maximum error of 5% and 0.5%, representing highly accurate measurements. Four additional datasets simulate different levels of pseudo-measurement accuracy, with maximum errors of 50%, 40%, 30%, and 20%. These datasets are generated for multiple load scenarios to capture varying network conditions.

Since the noise introduced in the measurement process is random, the accuracy of the state estimation will fluctuate per iteration. In Figure 6.2, the mean of the error is shown, and the results converge around 5000 iterations. Every configuration number can be multiplied by 1000 to get the number of iterations done, i.e. configuration 5 has the mean of 5000 iterations. Therefore, a Monte Carlo simulation with 5000 iterations will be conducted to account for this variability. This ensures that results are statistically robust and reflect various possible conditions. These generated measurement sets will be used to evaluate different metering placement configurations. All 5000 iterations will be processed through the state estimator, and the results will be compared against the 'perfect case' for accuracy assessment. To mitigate the influence of outliers, the median error across all iterations will be used as the primary metric for evaluating state estimation performance per node and line. Different cases are discussed, and the feeders are classified from 1 to 5. Table 6.1 shows which nodes belong to each feeder. For all cases, substations will again be referred to as nodes

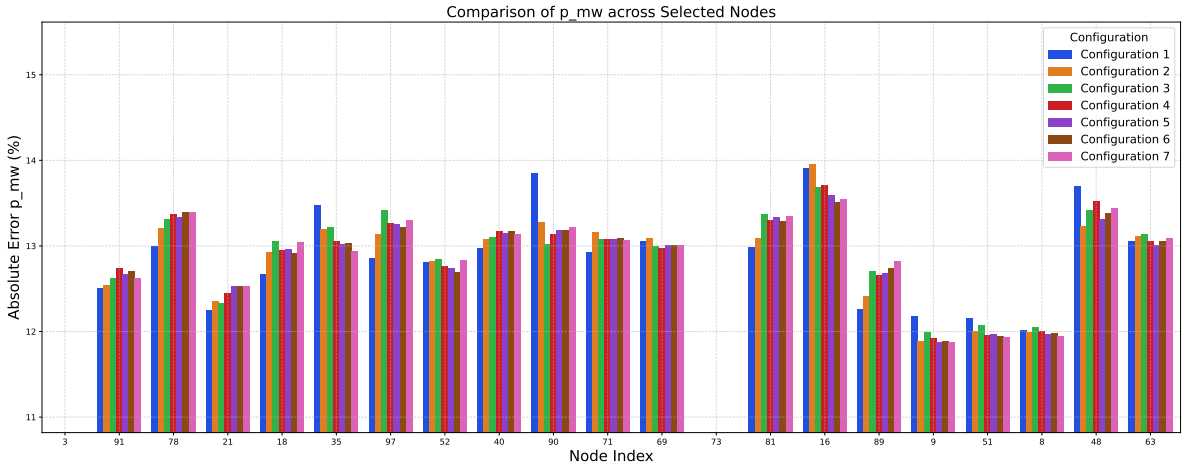

Figure 6.2: Convergence of result due to number of Monte Carlo iterations.

Feeder	Nodes
First	[91, 78, 21, 18, 35, 97, 52, 40, 90, 71, 69, 73, 81, 16, 89, 9, 51, 8, 48, 63]
Second	[87, 62, 54, 85, 19, 47, 70, 98, 95, 20, 58, 44, 11, 77, 80, 61, 42, 38, 60, 92, 82, 4, 93, 64, 67, 45, 83, 59, 37, 74, 13, 41]
Third part 1	[39, 28, 43, 46, 27, 84, 66, 30, 34, 76, 12, 6, 56, 94, 96, 50, 33, 100]
Third part 2	[32, 88, 75, 26, 7, 36, 49, 22, 68, 5, 99, 65, 79, 55, 25, 86, 24, 72, 15, 29, 101]
Fourth	[31, 14, 57]
Fifth	[23, 17, 10, 53]

Table 6.1: Feeder categorisation for further reference.

6.3. Case 1: Addition of MVMUs on feeder splitting nodes

In literature [35], nodes, where a feeder splits into multiple feeders, are identified as strategic locations for measurement placement. These locations offer higher cost-effectiveness than most nodes, as various measurements can be placed simultaneously. Additionally, placing an MVMU at these points provides the advantage of knowing the total power flow of each feeder, thereby reducing the total possible error for the nodes on each feeder. For these reasons, the measurement configuration of the standard network will be tested against one where MVMUs are placed at these feeder splitting points.

Looking at the results of the second feeder in Figure 6.3, starting with node 87, the effect of the MVMUs is noticeable, especially near the end of the feeder upward from node 82. The impact on node 77 is significant, as expected from the previous cases in the empty network. Node 11 does not seem to be impacted as much. This is likely due to the difference in magnitude of the node's power consumption towards the power going through the lines as explained in subsection 6.2.2.

The cost advantages and improvements in accuracy while strategically dividing the feeder into multiple known total loads, reducing the possible total error of the feeder part, make nodes with multiple outgoing feeders a strategic point. In further cases, MVMUs will be placed at the split points of feeders.

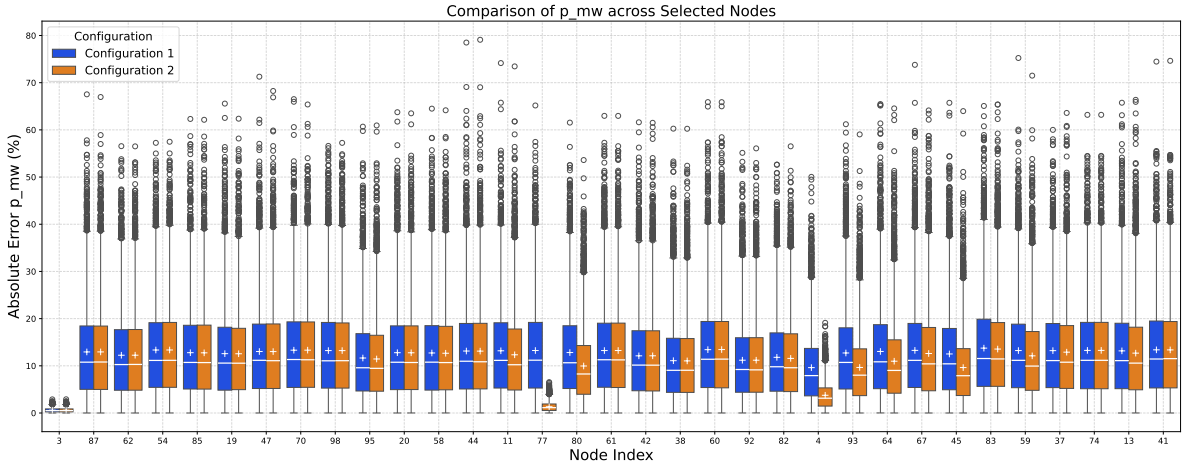

Figure 6.3: Improvement of adding measurements on splitting points for the second feeder.

6.4. Case 2: Improved Pseudo-Measurements

Pseudo-measurements are the backbone of the state estimator. They ensure observability at all times and are cheaper to fabricate. Their accuracy, however, is a problem. Good pseudo measurements are necessary if a DSO wants to use state estimation with a relatively small amount of actual measurements

while ensuring observability and adequate accuracy. This is because if there are two or more nodes in one feeder part of which the total power flow is known, their inaccuracy could theoretically cancel each other's error if their load is the same.

It is essential to assess whether, with improved measurements, the most significant errors shift to other nodes or if the nodes that initially exhibited the highest errors continue to experience the worst errors. Understanding this pattern is crucial for determining the optimal ratio and placement of actual and pseudo measurements within the system.

Furthermore, it is essential to consider whether design choices should be based on current circumstances or if future developments, such as improvements in pseudo-measurements, should also be incorporated into the decision-making process. This foresight can help avoid the need for a system redesign in the future, ultimately leading to cost savings while achieving the best possible accuracy.

Logically, the state estimation error decreases as the accuracy of the pseudo measurements improves, as shown in Figure 6.4. Configurations 1, 2, 3, and 4 have a pseudo measurement max error of 50%, 40%, 30% and 20%, respectively. The median declines almost linearly over a node with every 10% increase in accuracy. The nodes with the worst accuracy change through the pseudo-measurement configurations. To ensure proper meter placement, one can compare the worst errors in all nodes for all pseudo configurations. Starting with the node with the worst error for every configuration. If the node does not occur in every configuration's worst error node list, increase the list containing the worst error nodes with one node for all configurations. In Table C.1, the selection of nodes for placement resulting from this method is given.

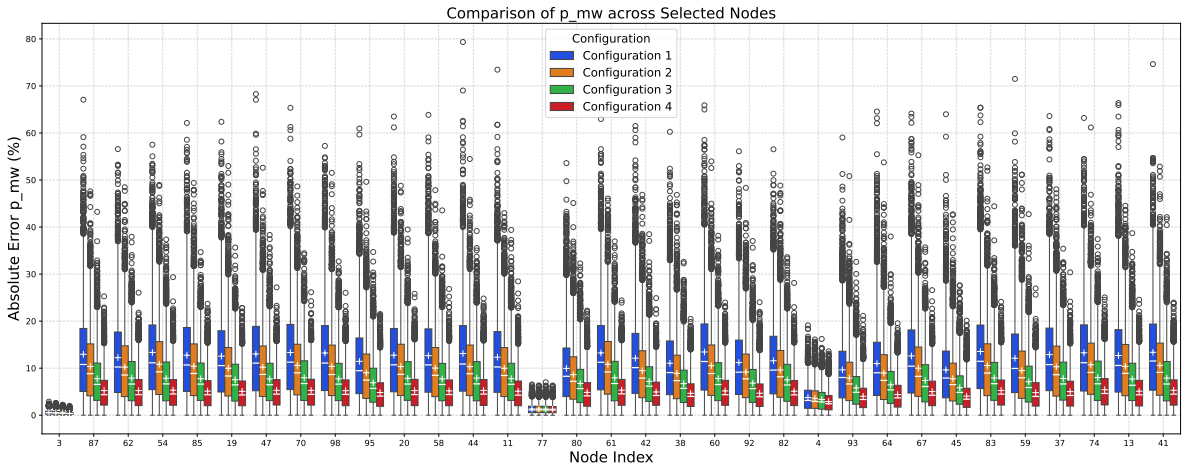

Figure 6.4: Difference between pseudo accuracy for the second feeder.

6.5. Case 3: PIM Placement Ratio

This case will illustrate a gradual introduction of additional measurements into the network. The placement of these measurements will be determined based on the accuracy of the state estimation in the initial configuration, where no extra measurements were placed. In practice, the characteristics of the consumers behind a node should also be considered, as they may be an even more critical factor than the accuracy of the specific node. This is because a node selected for measurement placement might serve a relatively insignificant load. Figure 6.5 to Figure 6.8 display the error in P of each node for different max error of the pseudo measurements, going from 50% to 20 % in steps of 10%. Configurations 1,2,3 and 4 display a difference in additional measurement coverage of 0%, 30%, 50% and 70%, respectively.

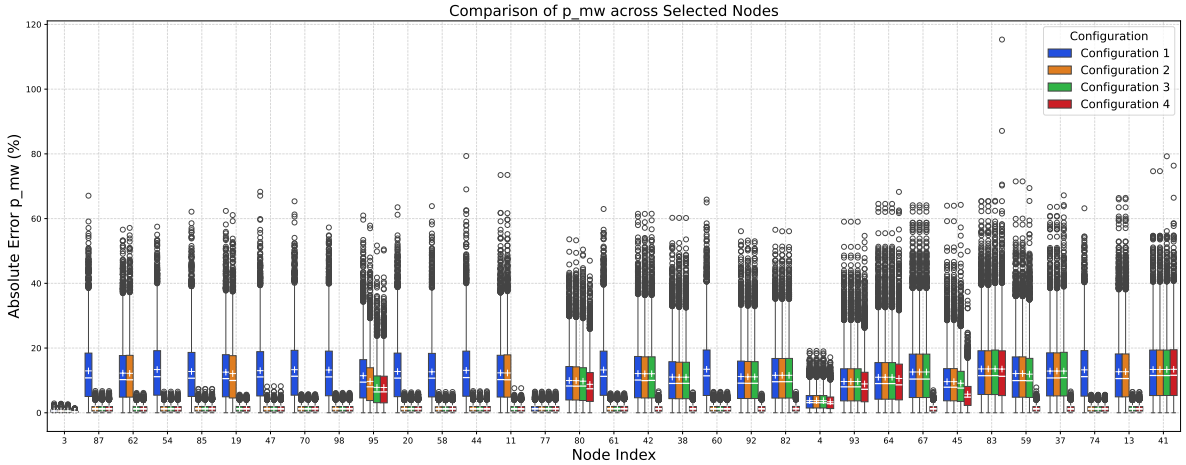

Figure 6.5: Errors in the nodes of the second line with a 50% max error for pseudo measurements.

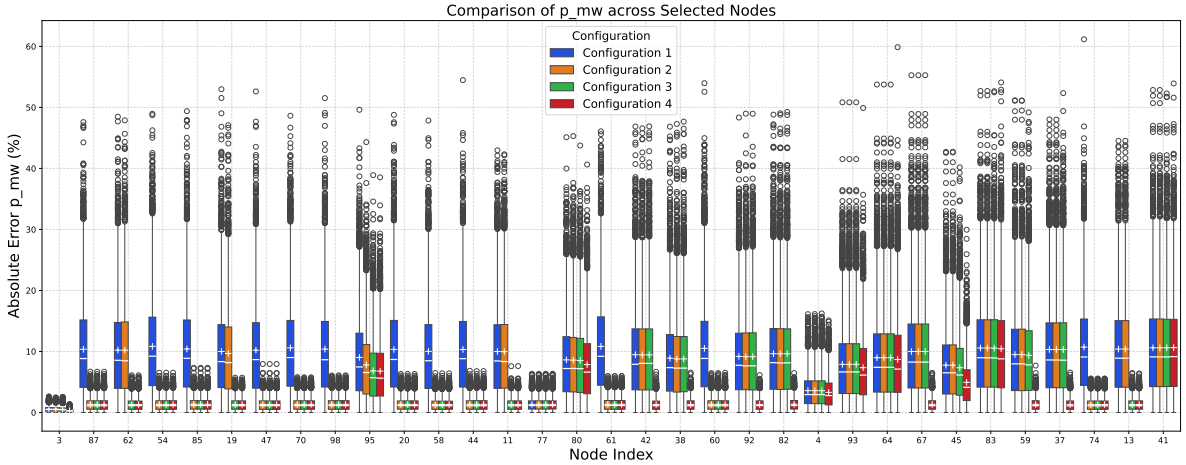

Figure 6.6: Errors in the nodes of the second line with a 40% max error for pseudo measurements.

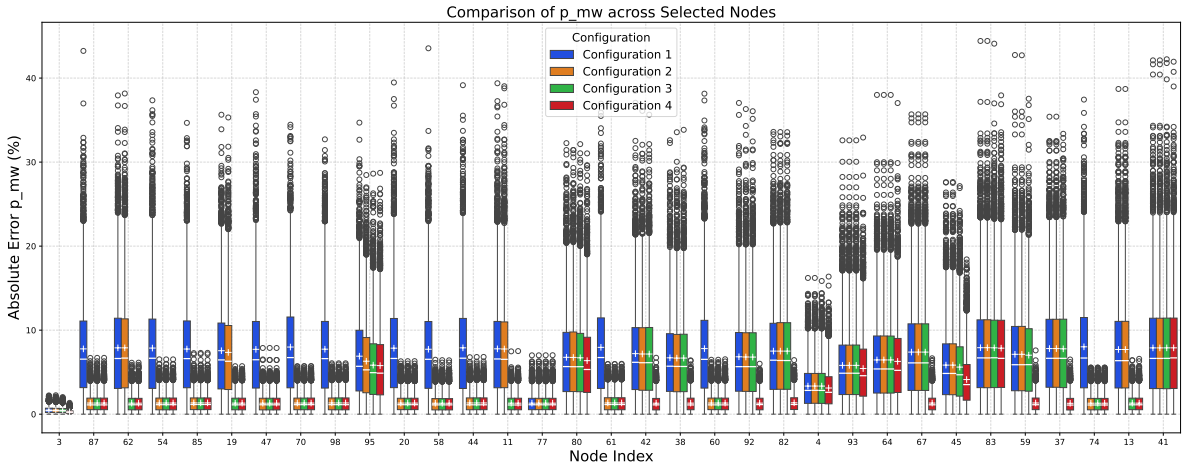

Figure 6.7: Errors in the nodes of the second line with a 30% max error for pseudo measurements.

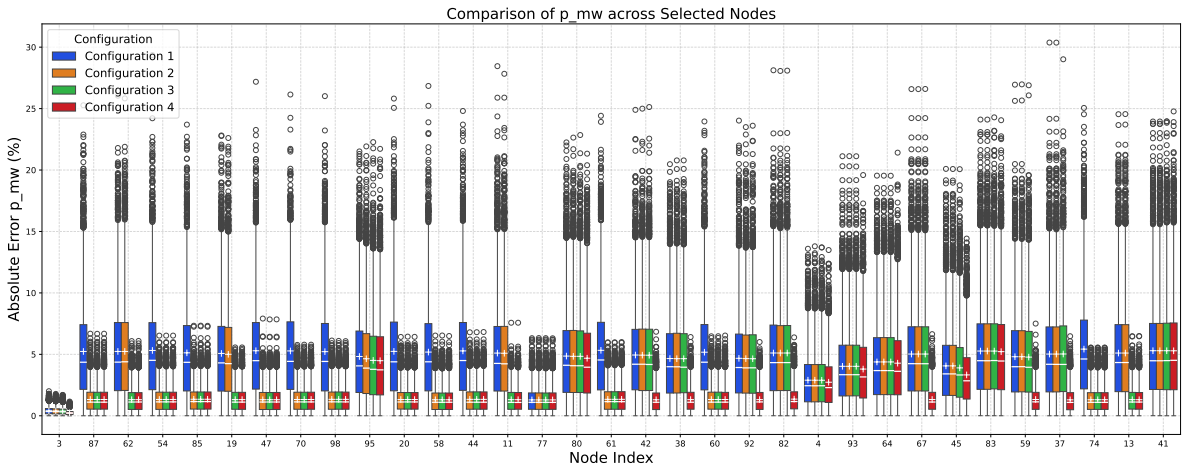

Figure 6.8: Errors in the nodes of the second line with a 20% max error for pseudo measurements.

The error in nodes that rely solely on pseudo-measurements either remains unchanged or decreases slightly, even with increased coverage of additional measurements, as shown in Table 6.2 for a 30% maximum error. This trend is observed across all levels of pseudo-measurement accuracy. Therefore, the pseudo-measurements' accuracy must be improved to nearly five times the desired level of an acceptable median to achieve adequate state estimation. Despite this, error outliers of up to 25% still occur in unmeasured nodes, even when pseudo-measurements have a maximum error of 20%. This discrepancy arises because, as discussed in subsection 4.5.4, a simplification was applied, meaning that the stated 20% maximum error does not represent a strict upper bound.

Nodes	0% Coverage			30% Coverage			50% Coverage			70% Coverage		
	Median	Mean	StD	Median	Mean	StD	Median	Mean	StD	Median	Mean	StD
3	0.42	0.49	0.37	0.41	0.48	0.36	0.40	0.46	0.34	0.23	0.27	0.21
87	6.55	7.77	5.90	1.11	1.33	1.00	1.10	1.33	1.00	1.11	1.33	1.00
62	6.63	7.89	5.98	6.68	7.89	5.95	1.12	1.31	0.99	1.12	1.31	0.99
54	6.66	7.87	6.06	1.13	1.33	1.01	1.13	1.33	1.01	1.13	1.33	1.01
85	6.61	7.75	5.81	1.15	1.34	1.01	1.15	1.34	1.01	1.15	1.34	1.01
19	6.46	7.55	5.66	6.30	7.35	5.48	1.11	1.32	0.99	1.11	1.32	0.99
47	6.48	7.72	5.91	1.12	1.31	0.99	1.11	1.31	1.00	1.11	1.31	1.00
70	6.74	7.99	6.02	1.13	1.33	1.00	1.13	1.33	1.00	1.13	1.33	1.00
98	6.61	7.74	5.80	1.13	1.34	1.02	1.14	1.34	1.02	1.13	1.34	1.02
95	5.70	6.90	5.29	5.28	6.30	4.78	4.94	5.83	4.43	4.88	5.78	4.40
20	6.63	7.86	5.93	1.13	1.32	0.99	1.13	1.32	0.99	1.13	1.32	0.99
58	6.53	7.73	5.89	1.11	1.30	0.99	1.11	1.30	1.00	1.11	1.30	1.00
44	6.66	7.90	5.96	1.12	1.34	1.02	1.11	1.34	1.02	1.12	1.34	1.02
11	6.57	7.78	5.89	6.53	7.73	5.87	1.10	1.31	0.99	1.09	1.31	0.99
77	1.12	1.31	0.98	1.12	1.31	0.98	1.12	1.31	0.98	1.12	1.31	0.98
80	5.66	6.77	5.19	5.65	6.76	5.17	5.65	6.76	5.17	5.32	6.37	4.83
61	6.74	7.95	6.06	1.15	1.34	1.00	1.15	1.34	1.00	1.15	1.34	1.00
42	6.17	7.21	5.40	6.12	7.16	5.37	6.13	7.16	5.37	1.11	1.31	1.00
38	5.71	6.71	5.08	5.68	6.67	5.05	5.68	6.67	5.05	1.10	1.31	1.00
60	6.53	7.81	6.05	1.11	1.33	1.00	1.11	1.33	1.00	1.11	1.33	1.00
92	5.66	6.83	5.25	5.66	6.80	5.24	5.66	6.80	5.24	1.14	1.32	0.99
82	6.43	7.51	5.66	6.39	7.51	5.66	6.38	7.51	5.66	1.16	1.36	1.01
4	2.83	3.35	2.54	2.84	3.35	2.54	2.83	3.35	2.54	2.60	3.11	2.38
93	4.88	5.81	4.46	4.88	5.81	4.46	4.87	5.81	4.46	4.58	5.43	4.19
64	5.38	6.46	4.93	5.38	6.46	4.93	5.38	6.46	4.93	5.22	6.28	4.78
67	6.10	7.39	5.70	6.10	7.39	5.70	6.10	7.39	5.70	1.12	1.32	1.00
45	4.85	5.84	4.54	4.85	5.84	4.54	4.69	5.60	4.36	3.52	4.18	3.02
83	6.70	7.91	6.01	6.70	7.91	6.01	6.71	7.90	6.01	6.64	7.85	5.94
59	5.89	7.13	5.49	5.89	7.13	5.49	5.90	7.02	5.39	1.13	1.33	1.01
74	6.68	8.02	6.09	1.09	1.31	0.99	1.09	1.31	0.99	1.09	1.31	0.99
13	6.37	7.70	5.86	6.37	7.70	5.86	1.12	1.31	0.98	1.12	1.31	0.98
41	6.64	7.89	6.02	6.64	7.89	6.02	6.65	7.89	6.03	6.70	7.89	6.02

Table 6.2: Median, mean and standard deviation of the absolute error in % for each coverage level for each node of feeder 2 while the maximum error of the pseudo measurements is 30%.

This research assumes that the accuracy of pseudo-measurements is uniform across all nodes. However, some nodes may be significantly more straightforward to predict than others. Prioritising nodes with the poorest pseudo-measurement accuracy, most likely those serving industrial loads or RES due to their volatility, has the most significant impact. This approach improves the accuracy of those specific nodes and enhances the accuracy of the pseudo-measurements overall across the network. This is confirmed in [68] where 48% of distribution transformer profiles fall within a 10% margin of the measured values. For further cases, it is assumed that with a coverage of 50%, a max error of 30% is achieved. The achieved results of 50% coverage and 30% pseudo measurement maximum error are displayed in Table 6.2.

6.6. Case 4: Placement in TNFs

Circumstances may arise when placing a measurement at the TNF location is the best option for overall improved accuracy. However, this could be costly, requiring a revision of the node. Alternative solutions may be utilised to work around the TNF node, which, while involving additional measurements, could prove to be more cost-effective. This case is designed to find the possible necessity for station revision or an alternative placement. As it is now considered that a 30% max pseudo-measurement error is achieved with 50% PIM coverage, the nodes for PIM placement will be selected on this 30% error with 0% coverage. Table 6.3 displays to selected nodes for PIM placement. For clarity, a split in the third feeder occurs between nodes 56 and 32. The numbers are shown in the order of their error, from largest to smallest. A comparison will be made between placement at TNF spots and avoiding them.

Feeder	**Nodes**
First	[90, 81, 16, 35, 18, 78, 48, 63, 21, 91, 97, 69]
Second	[61, 70, 83, 74, 44, 54, 37, 41, 20, 62, 85, 98, 11, 87, 58, 60, 47, 19]
Third part 1	[66, 43, 84, 34, 28, 46, 94, 76, 27, 56, 6]
Third part 2	[88, 68, 32, 55, 75, 86, 5, 15, 72, 49, 7, 29, 26]
Fourth and Fifth	[31, 17, 23]

Table 6.3: Selected PIM locations for 30% pseudo accuracy and 50% coverage.

There is no improvement in the overall state estimation, as shown in Figure 6.9 and Figure 6.10. Configuration 1 is the situation where TNFs can not be considered as nodes for measurement placement. In configuration 2, they are considered, resulting in different nodes with PIM. The only difference in configuration 2 is that the TNF nodes have become accurate, but the nodes where the PIMs were placed before now have become less accurate. The error has shifted to different nodes. Revising TNF nodes would cost a lot of money. It would not be worth it. Other options would be cheaper, like a specialised pseudo measurement for the specific TNFs, increasing accuracy or MVMU on nodes neighbouring the TNF. The MVMU option would only work towards the end of a feeder, considering the logic explained in subsection 6.2.2.

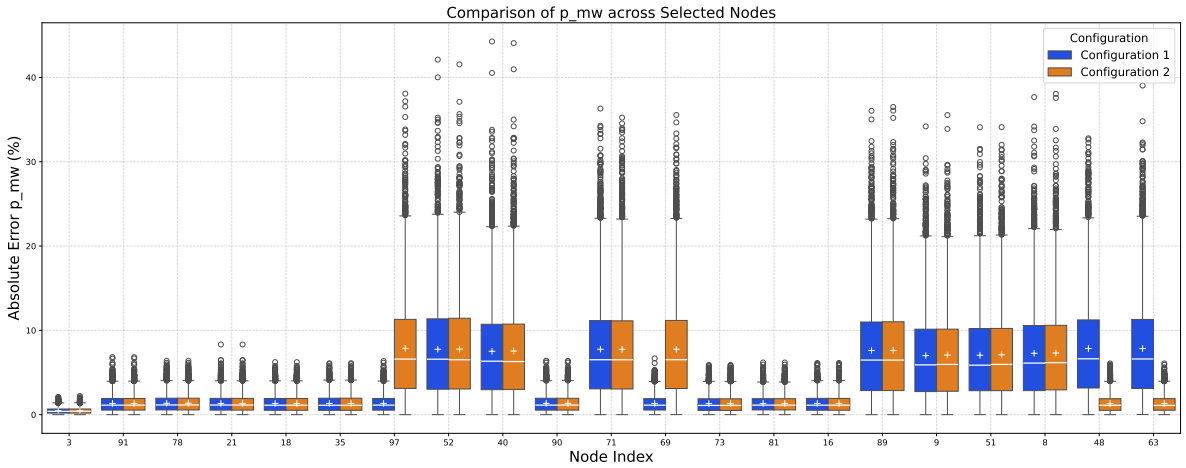

Figure 6.9: Active power error in nodes for whether or not TNF was taken into account for Line 1.

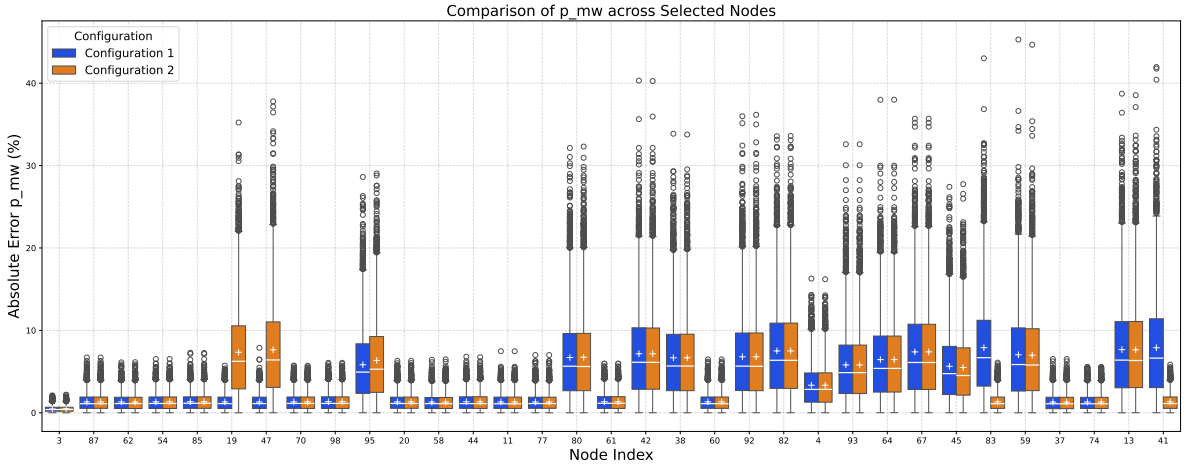

Figure 6.10: Active power error in nodes for whether or not TNF was taken into account for Line 2.

6.7. Sensitivity analysis

The selected measurement locations are based on a specific load scenario associated with the network. However, these choices may have been significantly different under an alternative load scenario. To assess the robustness of the designed network, the network with added measurements will be tested against more extreme load scenarios. This will help evaluate the impact of these changes and determine whether the state estimation remains accurate under varying conditions.

Given the growing role of RES in future distribution systems, one load scenario will focus on high renewable energy penetration. Additionally, since voltage magnitude estimation has shown high accuracy, another scenario will introduce high loads at the end of feeders to challenge voltage levels and assess whether the state estimation remains reliable under such conditions.

A comparison will be made between the network with 50% coverage and pseudo measurement with a maximum error of 30% and a network following Stedin's vision, i.e., all measurable nods will be measured. This network will also receive a pseudo measurement of 30% so a comparison can be made. In reality, the error might be lower due to the 85% foreseeable coverage of the Stedin network.

To highlight the differences in error across load scenarios, the error for the standard load scenario with 50% measurement coverage and 30% pseudo-measurement accuracy will be presented in Figure 6.11 for feeder 3.1, and in Figure 6.12 for feeder 2. The PIM placement of Table 6.3 without TNFs is used.

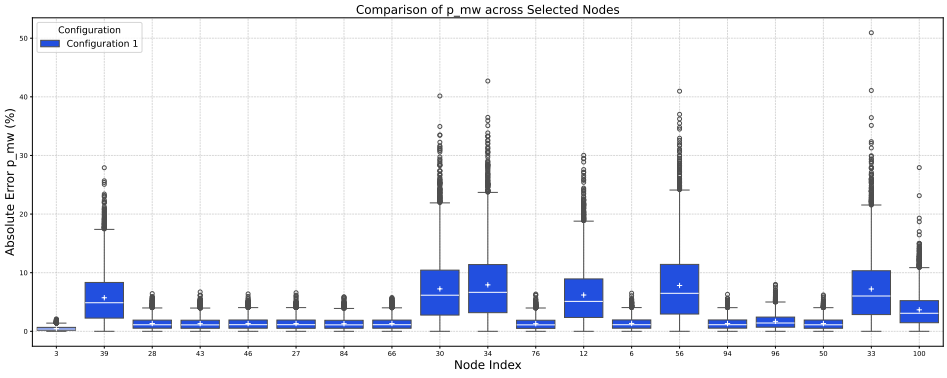

Figure 6.11: Errors for feeder 3.1 in a standard load scenario and PIM placement for 30% pseudo-measurement accuracy.

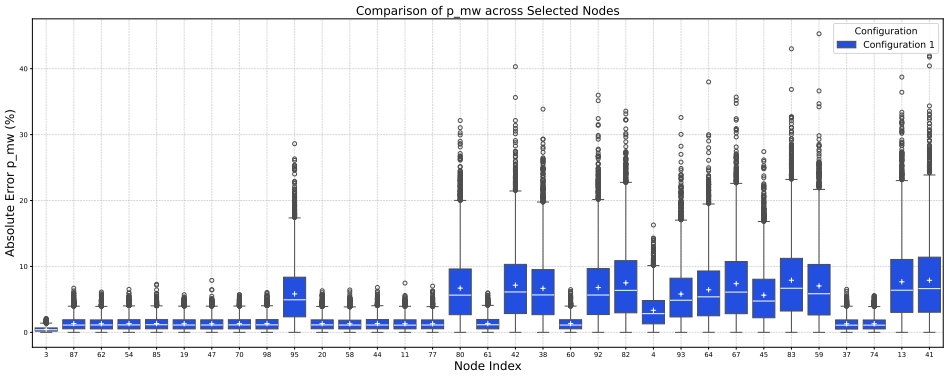

Figure 6.12: Errors for feeder 2 in a standard load scenario and PIM placement for 30% pseudo-measurement accuracy.

6.7.1. High Renewable Energy Peneration

This case focuses on introducing RES and bi-directional flow within the network. A generation of 0.75 MW is introduced on all nodes in Table 6.4. The designed network will be evaluated under these new conditions to see if accuracy is challenged.

Feeder	First	Second	Third part 1	Third part 2	Fourth and Fifth
Nodes	[78, 35, 73]	[62, 19, 42]	[46, 66, 56, 50]	[65]	[57, 53]

Table 6.4: Selected Nodes with RES.

The Figure 6.13 illustrates the absolute error in P for two different configurations. Configuration 1 has a 50% measurement coverage, while Configuration 2 aligns with Stedin's vision, where all possible points receive a PIM. The worst-performing node, indexed as 34, exhibits approximately the same median error of 6.7% in both configurations. However, due to the higher measurement coverage in Configuration 2, slightly improved accuracy can be observed across multiple nodes. This improvement is particularly noticeable at nodes with actual measurements absent in Configuration 1, which is expected given the accuracy difference. However, nodes measured in both configurations show slight accuracy gains in Configuration 2 due to the high coverage level.

In Figure 6.11, the errors are shown for a standard load scenario of the same feeder as in Figure 6.13. Surprisingly, the error in some nodes decreased when RES was introduced into the feeder. This is likely due to lower power flows in some parts of the feeder where MVMU placement makes the error in their estimates relatively lower. The opposite is happening around nodes 96 and 50. Due to the generation in 50, the power flow measured on the line between 94 and 96 will be relatively high compared to the load on 96.

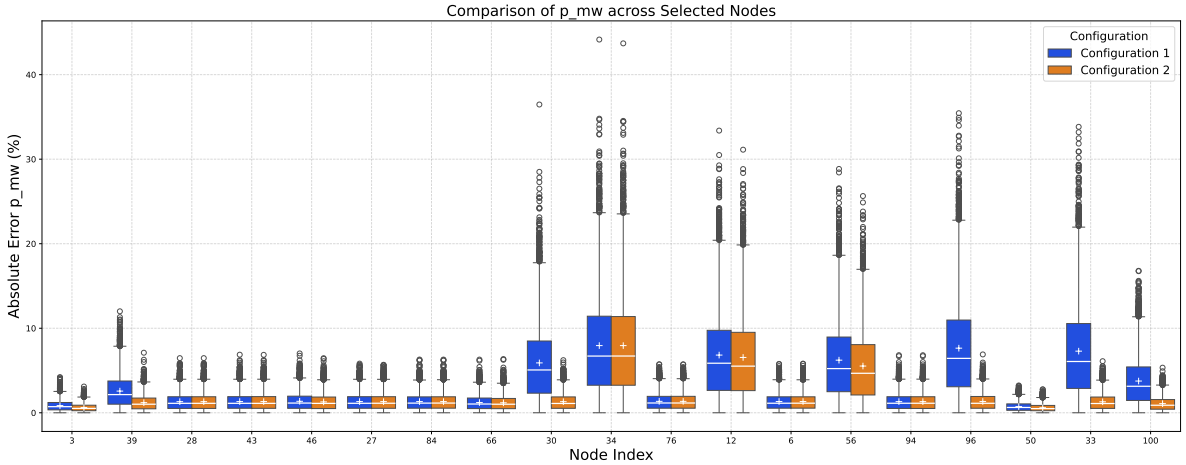

Figure 6.13: Error in estimated power with high RES penetration.

6.7.2. Heavy loads at the end of feeders

To challenge voltage levels in the network, all nodes given in Table 6.5 will have a load of 1 MW. Line 2 is shown in Figure 6.14 as it includes the most nodes where a heavy load was introduced.

Feeder	First	Second	Third part 1	Third part 2	Fourth and Fifth
Nodes	[8, 63]	[77, 93, 45, 74]	[33]	[55, 15]	[14, 10]

Table 6.5: Selected Nodes with a Heavy Load.

Again, the two configurations are comparable, with Stedin's vision configuration having slightly better state estimation accuracy due to higher measurement coverage. When compared with the standard load scenario from Figure 6.12, the statement in subsection 6.2.2 about that higher loads should be measured later than smaller loads is confirmed. The accuracy of the nodes that were given higher loads increased.

Again, the two configurations are comparable, with Stedin's vision configuration achieving slightly better state estimation accuracy due to higher measurement coverage. When compared to the standard load scenario from Figure 6.12, the statement in subsection 6.2.2 that smaller loads should be measured before high loads is confirmed. The accuracy of the nodes with higher assigned loads in the heavy load scenario improved while the measurement locations remained the same.

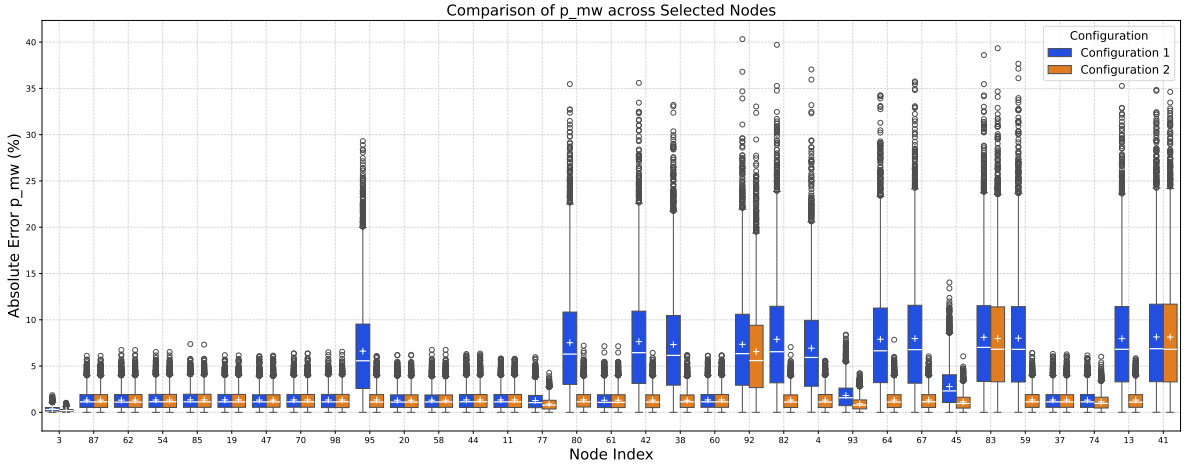

Figure 6.14: Error in estimated power with the introduction of heavy loads for line 2.

6.8. Reflection on State Estimation

The consensus is to lower all pseudo measurements by placing actual measurements where pseudo measurements tend to be poor. But if all pseudo-measurements suddenly fall within the set requirements for accuracy, can a state estimator still add value to the results? To showcase this, the measurements with noise will be compared with the states after the state estimation for nodes 34 and 39 picked from Figure 6.11, with the standard load scenario and PIM locations based on the measurement error. The exact locations of the PIMs can be found in Table 6.3.

Figure 6.15 and Figure 6.16 display the bell curves for nodes 34 and 39. In each figure, part (a) illustrates the noise introduced using a normal distribution with a maximum error of 30%. Part (b) shows the results at the respective nodes after state estimation. It is evident that state estimation significantly improves the accuracy for some nodes, while the effect is minimal for others. Beyond improving data accuracy, state estimation can also be employed for bad data detection, further reinforcing its value in distribution networks.

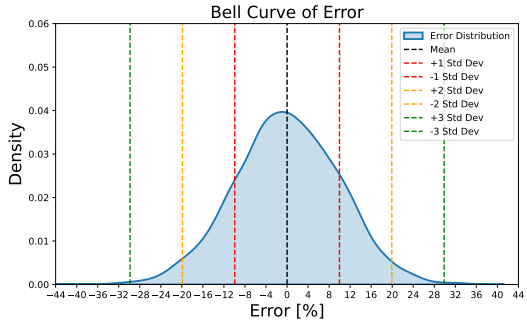

(a) Bell curve of the error of the noise added.

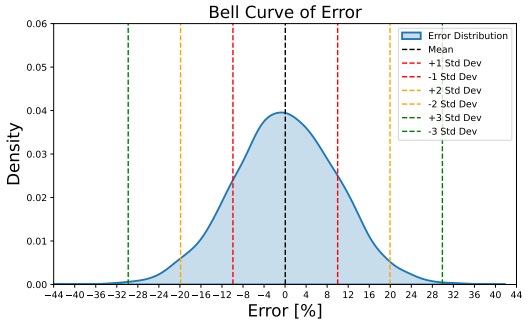

(b) Bell curve of the error of the state estimation.

Figure 6.15: Bell curves of Node 34.

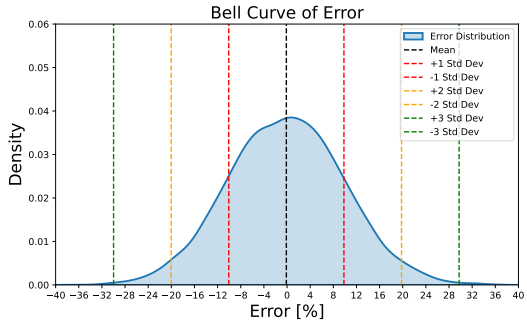

(a) Bell curve of the error of the noise added.

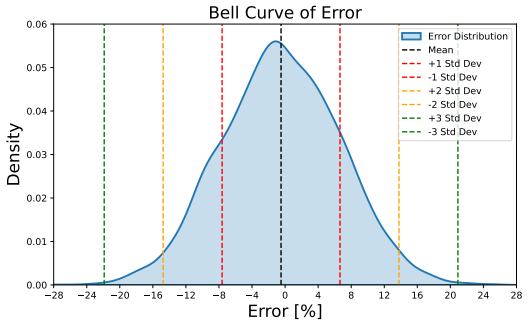

(b) Bell curve of the error of the state estimation.

Figure 6.16: Bell curves of Node 39.

6.9. Results: Network 2

This chapter explores various cases to identify the most effective workflow for developing a reliable state estimator for a DSO. The emphasis is on entirely using existing measurement equipment within the network. Any installed devices with measuring capabilities should be assessed and, if currently under-utilised, updated or reconfigured to contribute to the estimation process. Once all existing equipment is optimally employed, additional measurements can be considered.

One specific type of substation stands out. If a substation has multiple outgoing feeders (not considering the load), it is one of the most efficient spots in the network for measurement placement. While only working in one station, multiple measurements can be placed simultaneously, saving time and cost. Next to the slack bus, these stations have the highest possible measurement density in the system. In

addition to the cost efficiency of selecting these stations for measurements, they are also in strategic locations for information flow. The MVMUs at these stations measure the power flow into the separate feeders. In this way, the feeder is split into all single-line feeders, the total power flow of which is known.

From a finance perspective, the least amount of measurements would be best. Pseudo-measurement expenses are relatively low compared to actual measurements and, keeping costs in mind, will contribute a large part to the results. Improving these measurements should be one of the key points for a DSO and can roughly be done in two ways. Improving the algorithms behind making the pseudo measurements or placing actual measurements at substations with bad pseudo measurements. The second consequence is that the overall pseudo-measurement accuracy will improve, and so will the state estimation. Finding the substations with these poor pseudo-measurements is a challenge on its own and out of the scope of this research.

The stations classified as TNFs do not have to be revised. The results of placing measurements on these substations did not influence the overall outcome. The costs are too high for the achieved results. The combination of actual measurement and good pseudo-measurement can ensure a good enough state estimation. A problem can, however, arise when the poor pseudo measurements are all at the TNF substations.

The sensitivity analysis demonstrated that good results can be achieved even when more extreme load scenarios arise. The substation median error remained approximately consistent with the standard load scenario. Additionally, the analysis confirmed two suspicions: that the MVMU, if placed at a substation with high line power flow, will not ensure accurate load measurements on the substations it is placed at or that it singles out and that measuring substations with low loads is better than measuring higher substations.

The reactive power results were comparable to the active power in terms of error. The median errors for voltage magnitude and phase estimates were below 0.1% and 1%, respectively. Consequently, no further research was conducted on placing additional voltage measurements or PMUs. These results will be shown in Appendix B.

The state estimation process generally positively impacted noisy measurements, improving overall accuracy. This improvement was reflected in bell curves, where a reduced standard deviation for substation 39 indicates more precise estimations. For substation 34, the effect was negligible.

6.10. Discussion: Network 2

The Role and Limits of State Estimation
State estimation can be a valuable tool to enhance measurement accuracy, but it is not a panacea. A solid foundation of measurements, both actual and pseudo, is essential. The lowest accuracy among these measurements will still determine the worst estimation performance, mainly when only an economically feasible number of actual measurements is deployed. Its additional functionalities, such as bad data detection, should also be utilised to fully leverage the potential of state estimation. Incorporating these capabilities can better justify the computational demands associated with state estimation.

The Impact of Pseudo Measurements
The most significant improvement in state estimation accuracy was achieved by enhancing the quality of the pseudo-measurements. As shown in Table 6.2, increasing the measurement coverage had little to no impact on substations relying solely on pseudo-measurements. The most inaccurate substation continued exhibiting an error of 7.89% with a standard deviation of 6.02. Operating under these conditions does not allow a reliable view of the system states. However, the assumed 30% maximum error for pseudo-measurements was chosen conservatively, meaning the state estimator would likely perform better in practice.

Building on this, it becomes clear that improving pseudo-measurements is a priority. However, the process of doing so remains complex. The substations associated with significant errors must first be identified to enhance their accuracy. These inaccuracies often originate from imperfect data. Yet, this creates a paradox: how can inaccurate locations be identified using flawed data? Since DSOs typically do not know which data is unreliable, pinpointing the source of error becomes challenging. As a result,

what appears to be a potential solution in this thesis ultimately presents another complex problem for DSOs.

Active Measurements
The locations identified for existing measurements only considered SCADA data. However, direct MV customers also have measurements, although these occur less frequently. If state estimation is used to enhance historical data, these customer measurements can be incorporated as well. Still, because they are actual measurements, they do not contribute to improving the accuracy of pseudo-measurements. The unmeasured outgoing LV fields introduce the largest inaccuracies. Following Stedins' research, a 50% increase in measurements at currently unmonitored LV stations is necessary to address this.

Location Selection
The thesis's method for selecting measurement locations is based on each substation's current error, not the system's total. However, the best progression can be made by reducing the worst errors affecting the most substations. Selectively targeting errors can be helpful if the system performs well overall but has a few outliers.

The simulations and reasoning show that larger errors are more likely to occur at substations with smaller loads, as any absolute error in the total load is relatively significant compared to the size of the small load. This effect of placing measurements at low loads is compounded by the fact that when most small-load substations in a feeder are measured, the accuracy of larger-load substations also tends to improve. This occurs because the total feeder power flow acts as a constraint, limiting the possible estimation error at those larger substations. Consequently, prioritising the measurement of smaller-load substations is generally advantageous for improving overall accuracy.

However, this strategy comes with a trade-off. Errors at high-load substations can have more severe operational consequences, such as transformer overloading, mainly if the estimated load is significantly lower than the actual value and the state estimation is used for active system control. Therefore, a DSO must decide between optimising overall estimation accuracy or safeguarding critical substations. If state estimation is not intended for real-time control, prioritising overall accuracy is preferred.

Topology Changes
The strategy regarding split points has only identified active split points as strategic locations for MVMU placement. However, the network contains numerous switches that, if activated, could create additional split points within the feeders. To ensure the network remains adaptable to potential topology changes, all substations adjacent to a switch that could turn a substation into a splitting point should also be measured. This proactive approach would ensure readiness for topology changes.

The solution given is general, and if applied to all networks, topology changes should not influence the state estimation accuracy. All the worst measurements are replaced with actual, accurate measurements, creating a threshold over all networks. There were no indications in the studied networks that certain topological formations could impact this accuracy.

Feeder Length and Load Variability
The length of the feeder can influence the effectiveness of measurement placement strategies. For shorter feeders, it was confirmed that if only one substation lacks an accurate measurement, it is strongly influenced by the accuracy of the other substations. However, it is unclear if the same effect occurs in longer feeders where the line power flow is only measured at the start of the feeder. The law of large numbers could come into effect,i.e., the number of substations with positive and negative deviations might balance out if all loads were identical. This is not the case in reality, where load sizes vary. The smaller proportion of high-load substations increases the chance that several fall on the same side of the deviation, leading to higher total feeder flow errors and adaptations in the states. This effect is more random in shorter feeders, and the law of large numbers does not apply.

Noise Distribution
The nature of the noise introduced in the "perfect case" can play an active role in the results. The noise introduced in this study is assumed to follow a normal distribution. However, whether the actual measurement equipment follows this same distribution is uncertain. This discrepancy could potentially affect the overall state estimation. If the measurement noise distribution is non-normal and, for example, heavy-tailed, so closer to the true values most of the time, the state estimation will likely become more

accurate, with more outliers. In this case, reducing the required measurements might be possible if the outliers are ignored. On the other hand, if the distribution is more uniform, meaning there is more variability in the noise of the measurements, more measurements would be needed to reduce the maximum error and improve the accuracy of the state estimation.

Data Reliability
Despite the limitations discussed, the data used in this research is considered reliable for drawing conclusions. The perfect case, constructed as a reference, can be adjusted as needed. It is up to the user to define load scenarios that represent the network's daily operation. Some simplifications were made when calculating the standard deviation, where the maximum error was assumed to be three standard deviations. Following a normal distribution, the maximum error can exceed three standard deviations, which explains why outlier errors in the state estimation sometimes exceed the measurement's maximum error. The randomness introduced by the noise in the perfect case was filtered out using a Monte Carlo Simulation with 5000 iterations. This number could be increased, as variations between 5000 and 7000 iterations were still visible, as shown in Figure 6.2. Improved computational power would be necessary to store and process all the information, as the equipment used during this research was pushed to its limits. While the PandaPower state estimator is reliable, better versions may offer greater precision. However, PandaPower was sufficiently accurate for this research, as the conclusions drawn are more general and do not require the highest level of precision.

6.11. Future Research

The workflow proposed in this thesis has identified a problem surrounding adequate state estimation, but it does not provide a complete solution. Reducing the worst measurements, particularly the maximum error in pseudo measurements, is crucial for success. However, it remains uncertain which specific substations contribute to poor-performing pseudo measurements. Previous research by Stedin employed temporary measurements or accumulated data to assess their profiles. While this approach might offer valuable insights, it is not feasible for all existing MV networks due to the extensive time and equipment requirements. To reduce the overall maximum error in pseudo measurements, it is essential to identify the substations responsible for the significant errors and understand the underlying causes of these errors. Suppose the issue concerns flawed data allocation from existing equipment, such as topology errors in LV networks. In that case, addressing these errors may be a more straightforward solution than pinpointing the exact substations with substantial errors for accurate measurement placement.

The proposed method has been limited to radial networks, the most common configuration for MV networks. However, there may be instances where ring or meshed topologies are used instead. It is necessary to evaluate whether the measurement placement strategy employed in this thesis would remain effective under these alternative network conditions. These different topologies may require additional measurements or more advanced equipment, such as PMUs, to ensure accurate state estimation and network observability.

7

Conclusion

This thesis presents a general workflow for DSOs to prepare radial networks for state estimation, focusing on ensuring both observability and accuracy. The conclusions are drawn from research into the effects of measurement placement on individual substations and the overall network section. To explore these effects, two networks were modelled, enabling simulations across different load scenarios and measurement configurations. This approach provided a comprehensive understanding of how different measurements impact system behaviour. The resulting workflow offers guidance on identifying problematic measurement configurations across different topologies and load conditions, providing a general solution that can be applied under various circumstances.

Research Question 1: *What are the minimum conditions to create an observable network?*

The minimum conditions for an observable network are straightforward. A minimum of $2n - 1$ measurements is required, where n represents the number of network substations. The number $4n$ is usually considered to perform well for practical purposes. These measurements must be distributed across the network in a way that allows the formation of a spanning tree. However, relying solely on this minimum number of measurements has a significant drawback: the state estimator lacks redundancy, meaning it cannot cross-verify measurements. Instead, it must assume the provided measurements are valid values and will not change them. Additionally, the choice between pseudo-measurements, PIMs or MVMUs used to achieve minimum observability is generally flexible, as long as at least one voltage measurement is included.

Research Question 2: *What is the effect of placing more than the minimum amount of measurements?*

The most significant difference is that the state estimation process begins to function as intended, balancing the network based on the available measurements while accounting for their accuracy. However, this can only be achieved if sufficient measurements are available for comparison. The larger the number of measurement units, the more comparisons can be made, improving state estimation results. Additionally, selecting measurements with higher accuracy, such as going from pseudo-measurements to PIMs, has a considerable impact on the node accuracy of the state estimation. It improves the mean error from approximately $\pm 12.5\%$ to around $\pm 1.3\%$. When a sufficient number of measurements are strategically placed, less accurate substations can benefit from the accuracy of their surrounding substations, ultimately enhancing their accuracy.

Research Question 3: *Is the type of measurement taken of great importance to the accuracy of the system's states?*

PIMs generally have the most significant impact on substation accuracy, as they directly measure the parameter of interest. Introducing distributed generation within a feeder can also lead to high inaccuracies, particularly at the tipping point in a cable when the generation offsets the loads at the end of the feeder. This creates a zero point in the cable where state estimation inaccuracies given in (%) can become high for line power flows. Node power injections remain accurate. MVMUs can be used to measure this tipping point; the challenge lies in their dynamic

nature, which constantly shifts depending on generation and consumption patterns, making it difficult to assign a fixed measurement location. However, MVMUs can effectively 'split' feeders into multiple known segments, improving state estimation accuracy. This approach is particularly beneficial when a single substation within the segmented feeder has poor measurement accuracy. This method is most effective when line power flows are relatively low compared to the load in the poorly measured substation. PMUs are not necessary for MV networks like the one tested, as the voltage phase was estimated with a median accuracy below 1%.

Research Question 4: *Which strategic substations would benefit the most from the placement of a measurement?*

Distinct types of strategic substations can be identified. The first strategic location is any substation situated at a feeder splitting point. Placing an MVMU at such a station is the most cost-efficient approach. It also allows a large feeder to be divided into distinct radial single-line feeders, each with a known total load. Other strategic substations contribute more generally to improving state estimation accuracy. Substations with known poor pseudo-measurements should be prioritised for measurement, as this enhances the overall accuracy of pseudo-measurements and, consequently, the state estimation. This is the only scenario in which revising a TNF-labelled substation would be justified. In other cases, the cost would not be worthwhile. Additionally, MVMUs have a negligible effect if the power flow in the line is too high relative to the load of the substation at which they are placed. When selecting measurement locations, prioritising substations with smaller loads over larger ones generally benefits state estimation. However, this decision should be based on an average assessment since load distribution can shift over time.

7.1. Recommendations

This research has led to a few key recommendations. While these are tailored to Stedin's specific conditions and assumptions, other DSOs may also benefit from applying them to improve their state estimation.

1. MVMU should be placed at substations where feeders split into two or more sections.

   Placing measurements at these points is economically the most logical point, as the possible measurement density is at its highest at these points. It also cuts the feeder into smaller sections, for which the total power flow is known, increasing accuracy.

2. Place PIMs at the most inaccurate pseudo measurements.

   To lower the error in the state estimation, the nodes with the worst pseudo measurements need to be measured, or almost everything else has to be measured. The first is financially more responsible, but comes with a new problem.

3. Find out which network elements have inaccurate pseudo measurements.

   DSO must know which pseudo measurements are bad without measuring all nodes currently relying on pseudo measurements, as this would consume too much time and money. A few tests could indicate similarities that nodes with bad pseudo measurements share and choose to place measurements based on that knowledge, but this would not ensure accurate placement.

4. Ensure reliable data coupled to the right locations, as reliance on pseudo measurements acquired from this data is considerable.

   Accurate pseudo measurements are based on accurate historic data to create a proper profile. If data is coupled to the wrong locations, it interferes with creating accurate profiles. Therefore, accurate data acquisition is of high importance.

5. Do not revise TNFs substations except if it is done to improve overall pseudo measurement accuracy.

   The revision of a substation is expensive, so it should be avoided at all times if not necessary. The only trade-off worth it is if a TNF substation experiences the worst accuracy among the nodes.

6. Place measurements if stations are built or revised.

   If a station is already undergoing work, it presents an ideal opportunity to install measurements at a low additional cost, as the supplementary expense of placing them is minimal. The increase in measurements will eventually lead to a better state estimation.

References

[1] Sanne Akerboom et al. "Meeting goals of sustainability policy: CO2 emission reduction, cost-effectiveness and societal acceptance. An analysis of the proposal to phase-out coal in the Netherlands". In: *Energy Policy* 138 (Jan. 2020), pp. 111210–111210. DOI: https://doi.org/10.1016/j.enpol.2019.111210.

[2] Parlement of the Netherlands. 2019. URL: https://www.klimaatakkoord.nl/documenten/publicaties/2019/06/28/national-climate-agreement-the-netherlands.

[3] Europese Commissie and Directoraat-generaal Klimaat. *Op weg naar een klimaatneutraal Europa in 2050 : een strategische langetermijnvisie voor een welvarende, moderne, concurrerende en klimaatneutrale EU-economie*. Publications Office, 2019. DOI: doi/10.2834/76194.

[4] Eric Martinot, Lorenzo Kristov, and J. David Erickson. "Distribution System Planning and Innovation for Distributed Energy Futures". In: *Current Sustainable/Renewable Energy Reports* 2.2 (Apr. 2015), pp. 47–54. DOI: 10.1007/s40518-015-0027-8.

[5] G. T. Heydt. "The Next Generation of Power Distribution Systems". In: *IEEE Transactions on Smart Grid* 1.3 (Dec. 2010), pp. 225–235. DOI: 10.1109/tsg.2010.2080328.

[6] M. Gandomkar, M. Vakilian, and M. Ehsan. "Optimal distributed generation allocation in distribution network using Hereford Ranch algorithm". In: *2005 International Conference on Electrical Machines and Systems*. Vol. 2. 2005, 916–918 Vol. 2. DOI: 10.1109/ICEMS.2005.202678.

[7] T. Adefarati and R.C. Bansal. "Integration of renewable distributed generators into the distribution system: a review". In: *IET Renewable Power Generation* 10.7 (Aug. 2016), pp. 873–884. DOI: 10.1049/iet-rpg.2015.0378.

[8] Nikita Gupta and Seethalekshmi K. "A review on Key Issues and Challenges in Integration of Distributed Generation System". In: *2018 5th IEEE Uttar Pradesh Section International Conference on Electrical, Electronics and Computer Engineering (UPCON)*. 2018, pp. 1–7. DOI: 10.1109/UPCON.2018.8597014.

[9] Martin Scheepers et al. "Towards a climate-neutral energy system in the Netherlands". In: *Renewable and Sustainable Energy Reviews* 158 (Jan. 2022), pp. 112097–112097. DOI: https://doi.org/10.1016/j.rser.2022.112097.

[10] M. Ourahou et al. "Review on smart grid control and reliability in presence of renewable energies: Challenges and prospects". In: *Mathematics and Computers in Simulation* 167 (Nov. 2018), pp. 19–31. DOI: https://doi.org/10.1016/j.matcom.2018.11.009.

[11] Fred C. Schweppe and J. Wildes. "Power System Static-State Estimation, Part I: Exact Model". In: *IEEE Transactions on Power Apparatus and Systems* PAS-89.1 (1970), pp. 120–125. DOI: 10.1109/TPAS.1970.292678.

[12] Fred C. Schweppe and Douglas B. Rom. "Power System Static-State Estimation, Part II: Approximate Model". In: *IEEE Transactions on Power Apparatus and Systems* PAS-89.1 (1970), pp. 125–130. DOI: 10.1109/TPAS.1970.292679.

[13] Fred C. Schweppe. "Power System Static-State Estimation, Part III: Implementation". In: *IEEE Transactions on Power Apparatus and Systems* PAS-89.1 (1970), pp. 130–135. DOI: 10.1109/TPAS.1970.292680.

[14] Phase to Phase - Technolution. 2024. URL: https://www.phasetophase.nl/boek/boek_1_2.html.

[15] Tim Huang and Anil Kumar. 2023. URL: https://www.netbeheernederland.nl/publicatie/rapport-spanningskwaliteit-nederland-2023.

[16] Tim Huang and Anil Kumar. 2023. URL: https://www.netbeheernederland.nl/publicatie/achtergronddocument-spanningskwaliteit-nederland-2023.

[17] E. Lakervi and E. J. Holmes. *Electricity Distribution Network Design*. Institution of Engineering and Technology, Jan. 2003. ISBN: 9780863413094. DOI: https://doi.org/10.1049/pbpo021e.

[18] Dirk Kuiken and Heyd F Más. "Integrating demand side management into EU electricity distribution system operation: A Dutch example". In: *Energy Policy* 129 (Feb. 2019), pp. 153–160. DOI: https://doi.org/10.1016/j.enpol.2019.01.066.

[19] Ali Abur and Antonio Gómez Expósito. *Power System State Estimation*. Informa, Mar. 2004. DOI: https://doi.org/10.1201/9780203913673.

[20] Milton Brown. "Power System State Estimation and Forecasting". In: *SpringerLink* (2024). DOI: https://doi.org/10.1007-978-3-031-63288-4.

[21] A. Monticelli. *State Estimation in Electric Power Systems*. Boston, MA: Springer US, Jan. 1999. DOI: 10.1007/978-1-4615-4999-4.

[22] Seyed Morteza Alizadeh, Cagil Ozansoy, and Tansu Alpcan. "The impact of X/R ratio on voltage stability in a distribution network penetrated by wind farms". In: *2016 Australasian Universities Power Engineering Conference (AUPEC)*. 2016, pp. 1–6. DOI: 10.1109/AUPEC.2016.7749289.

[23] A. Keane et al. "Planning and operating non-firm distributed generation". In: *IET Renewable Power Generation* 3.4 (Jan. 2009), p. 455. DOI: 10.1049/iet-rpg.2008.0058.

[24] 2016. URL: https://pandapower.readthedocs.io/en/latest/estimation.html.

[25] B. Gou and A. Abur. "A direct numerical method for observability analysis". In: *IEEE Transactions on Power Systems* 15.2 (2000), pp. 625–630. DOI: 10.1109/59.867151.

[26] A. Monticelli and Felix F. Wu. "Network Observability: Identification of Observable Islands and Measurement Placement". In: *IEEE Transactions on Power Apparatus and Systems* PAS-104.5 (1985), pp. 1035–1041. DOI: 10.1109/TPAS.1985.323453.

[27] Madson Almeida, Eduardo Asada, and Ariovaldo Garcia. "Power system observability analysis based on gram matrix and minimum norm solution". In: *2009 IEEE Power & Energy Society General Meeting*. 2009, pp. 1–1. DOI: 10.1109/PES.2009.5275188.

[28] G. R. Krumpholz, K. A. Clements, and P. W. Davis. "Power System Observability: A Practical Algorithm Using Network Topology". In: *IEEE Transactions on Power Apparatus and Systems* PAS-99.4 (1980), pp. 1534–1542. DOI: 10.1109/TPAS.1980.319578.

[29] R.R. Nucera and M.L. Gilles. "Observability analysis: a new topological algorithm". In: *IEEE Transactions on Power Systems* 6.2 (1991), pp. 466–475. DOI: 10.1109/59.76688.

[30] Haibo Zhang and Kexin Han. "A Hybrid Observability Analysis Method for Power System State Estimation". In: *IEEE Access* 8 (2020), pp. 73388–73397. DOI: 10.1109/ACCESS.2020.2987358.

[31] G.N. Korres and P.J. Katsikas. "A hybrid method for observability analysis using a reduced network graph theory". In: *IEEE Transactions on Power Systems* 18.1 (2003), pp. 295–304. DOI: 10.1109/TPWRS.2002.807072.

[32] G.N. Korres et al. "Numerical observability analysis based on network graph theory". In: *IEEE Transactions on Power Systems* 18.3 (2003), pp. 1035–1045. DOI: 10.1109/TPWRS.2003.814882.

[33] L. Thurner et al. "pandapower — An Open-Source Python Tool for Convenient Modeling, Analysis, and Optimization of Electric Power Systems". In: *IEEE Transactions on Power Systems* 33.6 (Nov. 2018), pp. 6510–6521. ISSN: 0885-8950. DOI: 10.1109/TPWRS.2018.2829021.

[34] M.E. Baran, Jinxiang Zhu, and A.W. Kelley. "Meter placement for real-time monitoring of distribution feeders". In: *IEEE Transactions on Power Systems* 11.1 (1996), pp. 332–337. DOI: 10.1109/59.486114.

[35] Yu Xiang, Paulo F. Ribeiro, and Joseph F. G. Cobben. "Optimization of State-Estimator-Based Operation Framework Including Measurement Placement for Medium Voltage Distribution Grid". In: *IEEE Transactions on Smart Grid* 5.6 (2014), pp. 2929–2937. DOI: 10.1109/TSG.2014.2343672.

[36] Bernd Brinkmann and Michael Negnevitsky. "A Probabilistic Approach to Observability of Distribution Networks". In: *IEEE Transactions on Power Systems* 32.2 (2017), pp. 1169–1178. DOI: 10.1109/TPWRS.2016.2583479.

[37] Basanta Raj Pokhrel, Birgitte Bak-Jensen, and Jayakrishnan R. Pillai. "Integrated Approach for Network Observability and State Estimation in Active Distribution Grid". In: *Energies* 12.12 (June 2019), p. 2230. DOI: 10.3390/en12122230.

[38] Pierre Janssen, Tevfik Sezi, and Jean-Claude Maun. "Meter placement impact on distribution system state estimation". In: *22nd International Conference and Exhibition on Electricity Distribution (CIRED 2013)*. 2013, pp. 1–4. DOI: 10.1049/cp.2013.0847.

[39] Vincent Thornley, Nick Jenkins, and Sara White. "State estimation applied to active distribution networks with minimal measurements". In: (2005).

[40] Basanta Raj Pokhrel et al. "An Intelligent Approach to Observability of Distribution Networks". In: *2018 IEEE Power & Energy Society General Meeting (PESGM)*. 2018, pp. 1–5. DOI: 10.1109/PESGM.2018.8585752.

[41] Marco António do R. S. Cruz and Hélder R. de O. Rocha. "Planning Metering for Power Distribution Systems Monitoring with Topological Reconfiguration". In: *Journal of Control, Automation and Electrical Systems* 28.1 (Sept. 2016), pp. 135–146. DOI: 10.1007/s40313-016-0279-6.

[42] Robin J. Wilson. *Introduction to Graph Theory*. Pearson Education India, 1970.

[43] N. Nusrat, M. Irving, and G. Taylor. "Novel meter placement algorithm for enhanced accuracy of distribution system state estimation". In: *2012 IEEE Power and Energy Society General Meeting*. 2012, pp. 1–8. DOI: 10.1109/PESGM.2012.6344931.

[44] A Ketabi and SA Hosseini. "A new method for optimal harmonic meter placement". In: *American journal of applied sciences* 5.11 (2008), pp. 1499–1505.

[45] Xiaoshuang Chen et al. "Optimal Meter Placement for Distribution Network State Estimation: A Circuit Representation Based MILP Approach". In: *IEEE Transactions on Power Systems* 31.6 (2016), pp. 4357–4370. DOI: 10.1109/TPWRS.2015.2513429.

[46] Diogo M.V.P. Ferreira, Pedro M.S. Carvalho, and Luís A.F.M. Ferreira. "Optimal Meter Placement in Low Observability Distribution Networks with DER". In: *Electric Power Systems Research* 189 (Dec. 2020), p. 106707. DOI: 10.1016/j.epsr.2020.106707.

[47] Jamshid Aghaei et al. "Probabilistic PMU Placement in Electric Power Networks: An MILP-Based Multiobjective Model". In: *IEEE Transactions on Industrial Informatics* 11.2 (2015), pp. 332–341. DOI: 10.1109/TII.2015.2389613.

[48] Themistoklis C. Xygkis and George N. Korres. "Optimized Measurement Allocation for Power Distribution Systems Using Mixed Integer SDP". In: *IEEE Transactions on Instrumentation and Measurement* 66.11 (2017), pp. 2967–2976. DOI: 10.1109/TIM.2017.2731019.

[49] Themistoklis C. Xygkis, George N. Korres, and Nikolaos M. Manousakis. "Fisher Information-Based Meter Placement in Distribution Grids via the D-Optimal Experimental Design". In: *IEEE Transactions on Smart Grid* 9.2 (2018), pp. 1452–1461. DOI: 10.1109/TSG.2016.2592102.

[50] Yiyun Yao, Xuan Liu, and Zuyi Li. "Robust Measurement Placement for Distribution System State Estimation". In: *IEEE Transactions on Sustainable Energy* 10.1 (2019), pp. 364–374. DOI: 10.1109/TSTE.2017.2775862.

[51] Antonio A.M. Raposo, Anselmo B. Rodrigues, and Maria da Guia da Silva. "Optimal meter placement algorithm for state estimation in power distribution networks". In: *Electric Power Systems Research* 147 (June 2017), pp. 22–30. DOI: 10.1016/j.epsr.2017.02.015.

[52] M. Armendariz et al. "A method to place meters in active low voltage distribution networks using BPSO algorithm". In: *2016 Power Systems Computation Conference (PSCC)*. 2016, pp. 1–7. DOI: 10.1109/PSCC.2016.7540873.

[53] T.L. Baldwin et al. "Power system observability with minimal phasor measurement placement". In: *IEEE Transactions on Power Systems* 8.2 (1993), pp. 707–715. DOI: 10.1109/59.260810.

[54] R.F. Nuqui and A.G. Phadke. "Phasor measurement unit placement techniques for complete and incomplete observability". In: *IEEE Transactions on Power Delivery* 20.4 (2005), pp. 2381–2388. DOI: 10.1109/TPWRD.2005.855457.

[55] A.B. Antonio, J.R.A. Torreao, and M.B. Do Coutto Filho. "Meter placement for power system state estimation using simulated annealing". In: *2001 IEEE Porto Power Tech Proceedings (Cat. No.01EX502)*. Vol. 3. 2001, 5–pp. DOI: 10.1109/PTC.2001.964910.

[56] R. Steppan, A. Pfendler, and J. Hanson. "Meter placement algorithm for reliable distribution system state estimation". In: *27th International Conference on Electricity Distribution (CIRED 2023)*. Vol. 2023. 2023, pp. 3430–3434. DOI: 10.1049/icp.2023.0830.

[57] J.C.S. de Souza et al. "Optimal metering systems for monitoring power networks under multiple topological scenarios". In: *IEEE Transactions on Power Systems* 20.4 (2005), pp. 1700–1708. DOI: 10.1109/TPWRS.2005.857941.

[58] Amany El-Zonkoly. "Optimal meter placement using genetic algorithm to maintain network observability". In: *Expert Systems with Applications* 31.1 (2006), pp. 193–198. ISSN: 0957-4174. DOI: https://doi.org/10.1016/j.eswa.2005.09.016.

[59] Junqi Liu et al. "Trade-Offs in PMU Deployment for State Estimation in Active Distribution Grids". In: *IEEE Transactions on Smart Grid* 3.2 (2012), pp. 915–924. DOI: 10.1109/TSG.2012.2191578.

[60] Junqi Liu et al. "Optimal Meter Placement for Robust Measurement Systems in Active Distribution Grids". In: *IEEE Transactions on Instrumentation and Measurement* 63.5 (2014), pp. 1096–1105. DOI: 10.1109/TIM.2013.2295657.

[61] Jiangnan Peng, Yuanzhang Sun, and H.F. Wang. "Optimal PMU placement for full network observability using Tabu search algorithm". In: *International Journal of Electrical Power & Energy Systems* 28.4 (May 2006), pp. 223–231. DOI: 10.1016/j.ijepes.2005.05.005.

[62] H. Mori and Y. Sone. "Tabu search based meter placement for topological observability in power system state estimation". In: *1999 IEEE Transmission and Distribution Conference (Cat. No. 99CH36333)*. Vol. 1. 1999, 172–177 vol.1. DOI: 10.1109/TDC.1999.755335.

[63] Mohammad Ghasemi Damavandi, Vikram Krishnamurthy, and José R. Martí. "Robust Meter Placement for State Estimation in Active Distribution Systems". In: *IEEE Transactions on Smart Grid* 6.4 (2015), pp. 1972–1982. DOI: 10.1109/TSG.2015.2394361.

[64] Bhuvana Ramachandran and G. Thomas Bellarmine. "Improving observability using optimal placement of phasor measurement units". In: *International Journal of Electrical Power & Energy Systems* 56 (Mar. 2014), pp. 55–63. DOI: 10.1016/j.ijepes.2013.10.005.

[65] Horstmann Germany. 2025. URL: https://www.horstmanngmbh.com/en/products/short-circuit-and-earth-fault-indicators/product-finder?tx_pxaproductmanager_pi1%5Baction%5D=show&tx_pxaproductmanager_pi1%5Bcategory_0%5D=4&tx_pxaproductmanager_pi1%5Bcategory_1%5D=7&tx_pxaproductmanager_pi1%5Bcontroller%5D=Product&tx_pxaproductmanager_pi1%5Bproduct%5D=8&cHash=7268f0bc2f06a9038ae56418d6515c4d.

[66] Mikronika. *User Manuel Mikronika MEM-102*. Version DK.DF.MEM102.0424.02. mikronika.

[67] Gijs Henstra. *Expert Opinion on Stedin Grid Calculations*. Personal communication. 2025.

[68] Stedin. *Profielen Brochure*. Tech. rep. Internal documentation, not publicly accessible. Stedin Research, 2024.

[69] Ravindra Singh, Bikash Pal, and Richard Vinter. "Measurement placement in distribution system state estimation". In: *2009 IEEE Power & Energy Society General Meeting*. 2009, pp. 1–1. DOI: 10.1109/PES.2009.5275899.

[70] 2024. URL: https://en.wikipedia.org/wiki/Normal_distribution.

[71] Bart Bikker. *Expert Opinion on Stedin Networks*. Personal communication. 2025.

[72] Jos van Gelderen. *Expert Opinion on Stedin Networks*. Personal communication. 2025.

[73] Pieter Minnaar. *Expert Opinion on Stedin Networks*. Personal communication. 2025.

[74] Stedin Groep. *Verder versnellen*. 2023. URL: https://jaarverslag.stedingroep.nl/2023.

[75] Bart Kers. *Expert Opinion on Stedin Networks*. Personal communication. 2025.

[76] Nederlands Overheid. *Meetcode elektriciteit*. 2025. URL: https://wetten.overheid.nl/BWBR0037946/2024-08-27/#Hoofdstuk4_Paragraaf4.3_Sub-paragraaf4.3.3.

A

Derivatives Power Flow Equations

All these equations are obtained from [20].

Active Power Flows

$$\frac{\partial \boldsymbol{P}_{i-k}}{\partial \boldsymbol{\theta}_i} = |\boldsymbol{V}_i||\boldsymbol{V}_k|(g_{i-k}\sin\boldsymbol{\theta}_{ik} - b_{i-k}\cos\boldsymbol{\theta}_{ik}) \tag{A.1a}$$

$$\frac{\partial \boldsymbol{P}_{i-k}}{\partial \boldsymbol{\theta}_k} = -|\boldsymbol{V}_i||\boldsymbol{V}_k|(g_{i-k}\sin\boldsymbol{\theta}_{ik} - b_{i-k}\cos\boldsymbol{\theta}_{ik}) \tag{A.1b}$$

$$\frac{\partial \boldsymbol{P}_{i-k}}{\partial |\boldsymbol{V}_i|} = -2|\boldsymbol{V}_i|(g_{i-k} + g_i^{sh}) - |\boldsymbol{V}_k|(g_{i-k}\cos\boldsymbol{\theta}_{ik} + b_{i-k}\sin\boldsymbol{\theta}_{ik}) \tag{A.1c}$$

$$\frac{\partial \boldsymbol{P}_{i-k}}{\partial |\boldsymbol{V}_k|} = -|\boldsymbol{V}_i|(g_{i-k}\cos\boldsymbol{\theta}_{ik} + b_{i-k}\sin\boldsymbol{\theta}_{ik}) \tag{A.1d}$$

Reactive Power Flows

$$\frac{\partial \boldsymbol{Q}_{i-k}}{\partial \boldsymbol{\theta}_i} = -|\boldsymbol{V}_i||\boldsymbol{V}_k|(g_{i-k}\cos\boldsymbol{\theta}_{ik} + b_{i-k}\sin\boldsymbol{\theta}_{ik}) \tag{A.2a}$$

$$\frac{\partial \boldsymbol{Q}_{i-k}}{\partial \boldsymbol{\theta}_k} = |\boldsymbol{V}_i||\boldsymbol{V}_k|(g_{i-k}\cos\boldsymbol{\theta}_{ik} + b_{i-k}\sin\boldsymbol{\theta}_{ik}) \tag{A.2b}$$

$$\frac{\partial \boldsymbol{Q}_{i-k}}{\partial |\boldsymbol{V}_i|} = -2|\boldsymbol{V}_i|(b_{i-k} + b_i^{sh}) - |\boldsymbol{V}_k|(g_{i-k}\sin\boldsymbol{\theta}_{ik} - b_{i-k}\cos\boldsymbol{\theta}_{ik}) \tag{A.2c}$$

$$\frac{\partial \boldsymbol{Q}_{i-k}}{\partial |\boldsymbol{V}_k|} = -|\boldsymbol{V}_i|(g_{i-k}\sin\boldsymbol{\theta}_{ik} + b_{i-k}\cos\boldsymbol{\theta}_{ik}) \tag{A.2d}$$

Active Power Injections

$$\frac{\partial \boldsymbol{P}_i}{\partial \boldsymbol{\theta}_i} = |\boldsymbol{V}_i|\sum_{\substack{l=1\\l\neq i}}^{n}|\boldsymbol{V}_l|(-G_{il}\sin\boldsymbol{\theta}_{il} + B_{il}\cos\boldsymbol{\theta}_{il}) \tag{A.3a}$$

$$\frac{\partial \boldsymbol{P}_i}{\partial \boldsymbol{\theta}_k} = |\boldsymbol{V}_i||\boldsymbol{V}_k|(G_{ik}\sin\boldsymbol{\theta}_{ik} - B_{ik}\cos\boldsymbol{\theta}_{ik}) \tag{A.3b}$$

$$\frac{\partial \boldsymbol{P}_i}{\partial |\boldsymbol{V}_i|} = 2|\boldsymbol{V}_i|G_{ii} + \sum_{\substack{l=1\\l\neq i}}^{n}|\boldsymbol{V}_l|(G_{il}\cos\boldsymbol{\theta}_{il} + B_{il}\sin\boldsymbol{\theta}_{il}) \tag{A.3c}$$

$$\frac{\partial \boldsymbol{P}_i}{\partial |\boldsymbol{V}_k|} = |\boldsymbol{V}_i|(G_{ik}\cos\boldsymbol{\theta}_{ik} + B_{ik}\sin\boldsymbol{\theta}_{ik}) \tag{A.3d}$$

Reactive Power Injections

$$\frac{\partial \boldsymbol{Q}_i}{\partial \boldsymbol{\theta}_i} = |\boldsymbol{V}_i| \sum_{\substack{l=1 \\ l \neq i}}^{n} |\boldsymbol{V}_l|(G_{il} \cos \boldsymbol{\theta}_{il} + B_{il} \sin \boldsymbol{\theta}_{il}) \tag{A.4a}$$

$$\frac{\partial \boldsymbol{Q}_i}{\partial \boldsymbol{\theta}_k} = |\boldsymbol{V}_i||\boldsymbol{V}_k|(-G_{ik} \cos \boldsymbol{\theta}_{ik} - B_{ik} \sin \boldsymbol{\theta}_{ik}) \tag{A.4b}$$

$$\frac{\partial \boldsymbol{Q}_i}{\partial |\boldsymbol{V}_i|} = -2|\boldsymbol{V}_i|B_{ii} + \sum_{\substack{l=1 \\ l \neq i}}^{n} |\boldsymbol{V}_l|(G_{il} \sin \boldsymbol{\theta}_{il} - B_{il} \cos \boldsymbol{\theta}_{il}) \tag{A.4c}$$

$$\frac{\partial \boldsymbol{Q}_i}{\partial |\boldsymbol{V}_k|} = |\boldsymbol{V}_i|(G_{ik} \sin \boldsymbol{\theta}_{ik} - B_{ik} \cos \boldsymbol{\theta}_{ik}) \tag{A.4d}$$

Voltage magnitude

$$\frac{\partial |\boldsymbol{V}_i|}{\partial \boldsymbol{\theta}_j} = 0 \qquad \ldots \forall j \tag{A.5a}$$

$$\frac{\partial |\boldsymbol{V}_i|}{\partial \boldsymbol{V}_j} = 0 \qquad \ldots j \neq i \tag{A.5b}$$

$$\frac{\partial |\boldsymbol{V}_i|}{\partial \boldsymbol{V}_j} = 1 \qquad \ldots j = i \tag{A.5c}$$

B

Other Network States Results

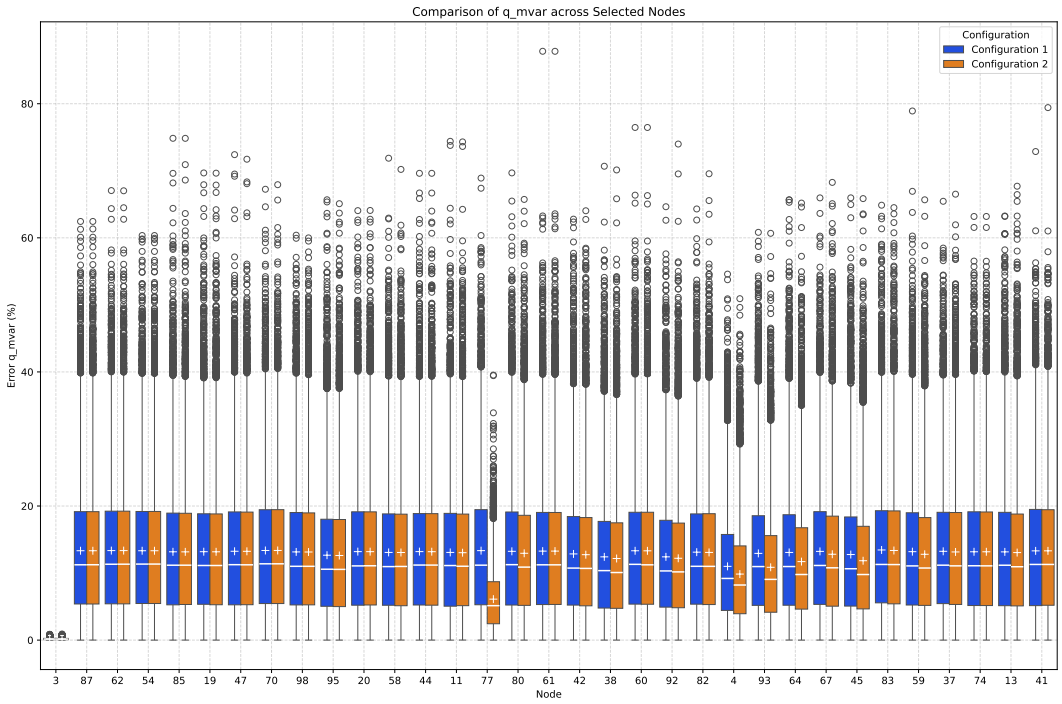

Figure B.1: Reactive power absolute error of Feeder 2 without an with the addition of MVMUs at the split points of the Feeder.

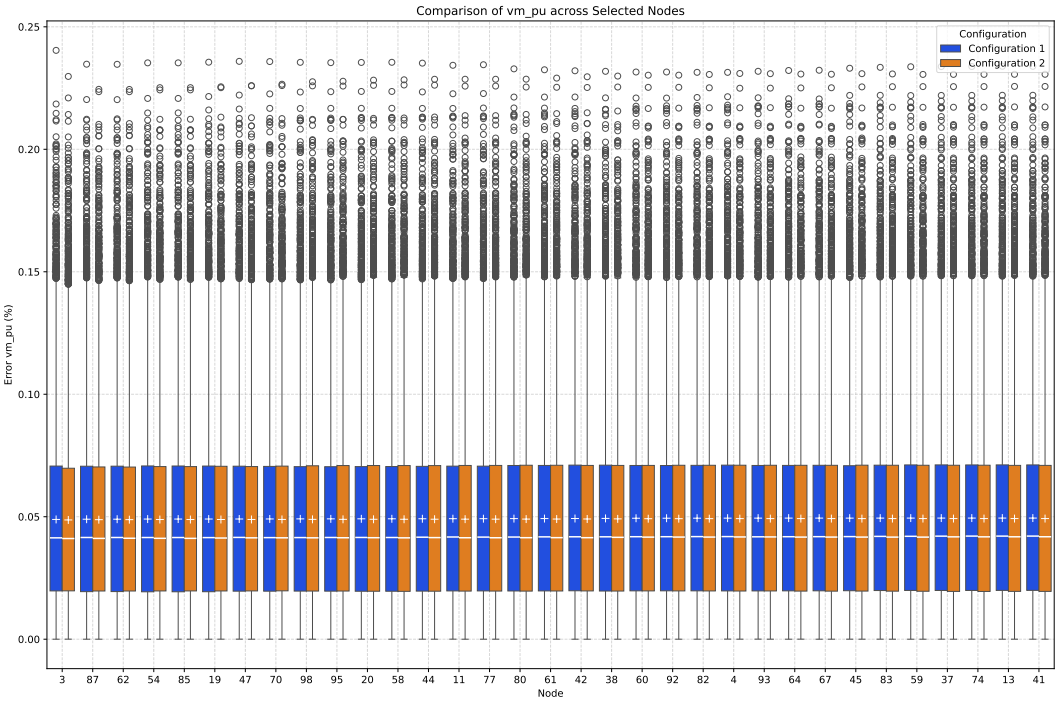

Figure B.2: Voltage magnitude absolute error of Feeder 2 without an with the addition of MVMUs at the split points of the Feeder.

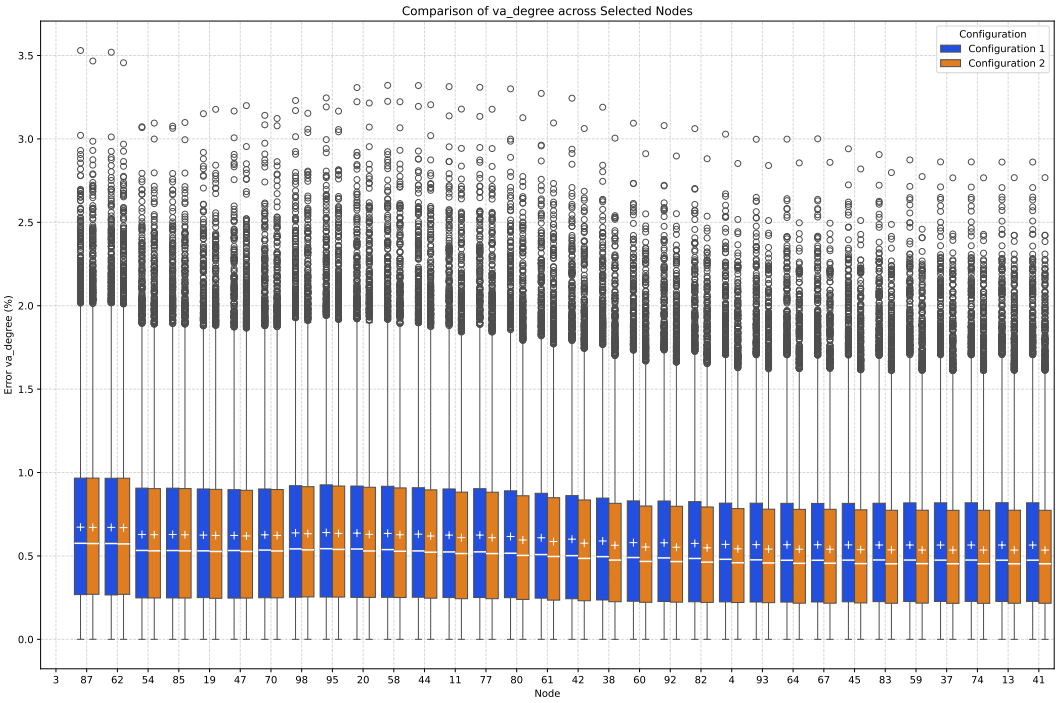

Figure B.3: Voltage phase absolute error of Feeder 2 without an with the addition of MVMUs at the split points of the Feeder.

C

Selected Nodes for Placement

Amount Feeder Measured	Nodes
30%	50, 53, 57, 65, 73, 16, 78, 90, 35, 18, 69, 52, 47, 85, 58, 20, 44, 87, 98, 54, 74, 61, 70, 60, 66, 43, 84, 27, 46, 94, 86, 49, 88, 26, 68, 72, 5, 31, 23
50%	50, 53, 57, 65, 73, 16, 78, 90, 97, 81, 35, 18, 69, 52, 91, 62, 11, 19, 13, 85, 58, 20, 87, 44, 47, 98, 54, 74, 61, 70, 60, 66, 43, 84, 27, 46, 94, 76, 28, 6, 33, 88, 5, 24, 26, 7, 72, 55, 15, 86, 68, 49, 31, 14, 23, 10
70%	50, 53, 57, 65, 73, 16, 69, 21, 91, 52, 18, 78, 40, 35, 71, 81, 97, 90, 8, 38, 92, 82, 59, 42, 62, 11, 67, 19, 13, 85, 58, 20, 37, 87, 44, 47, 98, 54, 74, 61, 70, 60, 66, 43, 84, 27, 46, 94, 76, 28, 6, 33, 30, 12, 39, 29, 68, 32, 56, 24, 36, 49, 88, 86, 15, 55, 72, 7, 26, 5, 31, 14, 23, 10

Table C.1: Selected PIM Locations for Different Pseudo Accuracy